University of Southampton

FACULTY OF ENGINEERING AND THE ENVIRONMENT
AERONAUTICS & ASTRONAUTICS

Assessing the use of network theory as a method for developing a targeted approach to Active Debris Removal

Rebecca Jane Newland

A thesis submitted for the qualification of
Doctor of Philosophy

NOVEMBER, 2012

UNIVERSITY OF SOUTHAMPTON

ABSTRACT

FACULTY OF ENGINEERING AND THE ENVIRONMENT
AERONAUTICS & ASTRONAUTICS

Doctor of Philosophy

ASSESSING THE USE OF NETWORK THEORY AS A METHOD FOR DEVELOPING A TARGETED APPROACH TO ACTIVE DEBRIS REMOVAL

by Rebecca Jane Newland

This thesis reports on the application of network theory to data representing space debris in Low Earth Orbit. The research was designed with a view to developing a targeted approach to Active Debris Removal (ADR). The need for remediation, via ADR, of the space debris environment is regarded as the only means by which we can control the growth of the future debris population to maintain use of Earth orbit.

A targeted approach to ADR is required to remove the objects that pose the greatest risk in terms of the creation of further debris by explosions or collisions in the future. Methods of determining target criteria are debated in the literature. Network theory is introduced here as an alternative method that, unlike other methods, does not treat debris-producing events in isolation and examines the role of objects in series of conjunctions.

The research involved using networks to represent various aspects of the space debris environment. Network theory analysis was carried out on the datasets to determine specific characteristics such as the presence of clustering and the extent of disassortative mixing. Once general characteristics of the 'space debris networks' were determined, two case studies were used as preliminary investigations to assess the use of network theory for targeting objects for removal.

The research shows that network theory can be used to determine that 'space debris networks' are robust and disassortative. Although there are limitations due to the uncertainties in the data used to create the networks, the findings suggest that careful development and application of target criteria would result in successful ADR.

Contents

List of Tables viii

List of Figures viii

Acknowledgements xix

Nomenclature xx

Acronyms xxii

1 INTRODUCTION 1

1.1 Problem Statement 1

1.1.1 Classification and sources 2

1.1.2 Historical growth 4

1.1.3 Instability and future predictions 8

1.1.4 Mitigation 12

1.1.5 Remediation 15

1.2 Measuring effectiveness 20

1.3 Literature review 22

1.4 Contributions and aims 28

2 NETWORK THEORY 33

2.1 Network types 33

2.2 Network and vertex measures 39

2.2.1 Degree centrality 39

2.2.2 Assortativity 42

2.2.3 Closeness centrality 44

2.2.4 Betweenness centrality 46

2.2.5 Clustering 49
2.2.6 Complexity 50
2.2.7 Network robustness 51

3 SPACE DEBRIS NETWORKS 55
3.1 DAMAGE networks 55
3.1.1 Modelling process 55
3.1.2 Reliability of DAMAGE 60
3.1.3 DAMAGE networks 66
3.2 SOCRATES networks 77
3.2.1 Conjunction assessment process 77
3.2.2 Reliability of SOCRATES 78
3.2.3 SOCRATES networks 82

4 CASE STUDIES 99
4.1 CASE STUDY 1: Removals based on weighted measures 100
4.1.1 Method 100
4.1.2 Results 101
4.2 CASE STUDY 2: Removals based on centrality measures 105
4.2.1 Method 105
4.2.2 Results 106
4.2.3 Applying ADR to a DAMAGE simulation 109

5 DISCUSSION 115
5.1 Using networks to represent various aspects of the SDE 115
5.2 Analysing space debris networks to determine their characteristics 116
5.3 Assessing the use of network theory for determining ADR target criteria 119
5.3.1 Advantages 119
5.3.2 Disadvantages 121
5.4 Other issues 123
5.4.1 Technology 124
5.4.2 Finance 125
5.4.3 International cooperation 126

6 CONCLUSIONS 129

Bibliography **133**

A Appendix **161**

A.1 Initial code 161

A.1.1 rjnNetworkAnalysis 161

A.1.2 BFS_FIFOQueue.cpp 187

List of Tables

3.1 Centrality and clustering statistics on the five vertices selected from the 52 vertices in the network in Figure 3.6 66
3.2 Statistics for the selected vertices in Figure 3.8 71
3.3 Network statistics for SOCRATES data on 12th July 2010. 83
3.4 Vertex measures for the selected vertices in Figure 3.20. 87
3.5 Network statistics for SOCRATES data on 1st January 2006 and 12th July 2010. 90
3.6 Network measures for networks built using satellite catalogue numbers and satellite names. 95

4.1 Effectiveness measures for the four ADR scenarios. 103
4.2 Network measures for scenarios 1–5. 108
4.3 Network measure rankings of Iridium-33 and Cosmos-2251. 109
4.4 Effectiveness measures three ADR scenarios removing five, ten, or 20 objects per year. 111

List of Figures

1.1 Monthly number of catalogued objects in Earth orbit 4
1.2 Contribution of recent breakup fragments to SOCRATES close approaches 7
1.3 Spatial density of objects $\geq$ 10 cm in LEO on 5 June 2009 7
1.4 From stability to collisional cascading 8
1.5 Two NFL scenarios 11
1.6 Cumulative number of collisions predicted in NFL and BAU scenarios 12
1.7 The percentage of debris remaining in a circular orbit at different altitudes 15
1.8 The survival probability of a single 2 mm tether, a net, and a braided tether 19
1.9 Comparing a non-remediation scenario to one in which 24 rocket bodies are removed per year 23
1.10 Results from ADR and non-ADR scenarios in a LEODEEM study 25
1.11 LEGEND ADR study in which five, ten and 20 objects are removed and compared to a non-mitigation scenario 28

2.1 A multigraph with multi-edges. 34
2.2 Network types. 36
(a) Uni-relational 36
(b) Multi-relational 36
(c) Directed 36
(d) Weighted 36
2.3 Vertices and edges on a space debris network. 38
2.4 Network types. 41
(a) Binomial degree distribution. 41
(b) US road network 41

(c) Power law degree distribution. 41
(d) US airline network 41
2.5 Comparing accidental failure and deliberate attack on assortative and disassortative networks 45
(a) Assortative network, accidental failure. 45
(b) Disassortative network, accidental failure 45
(c) Disassortative network, deliberate attack. 45
2.6 Calculating betweenness centrality 46
2.7 Breadth first search between pairs 47
2.8 Accumulation phase, stage 1 48
2.9 Accumulation phase, stage 2 48
2.10 Accumulation phase, stage 3 48

3.1 The distribution of number of fragments of different masses generated by the NASA break-up model in DAMAGE. 59
3.2 Comparison of DAMAGE historical evolution with historical catalogue data (data: NASA) 61
3.3 50 MC runs in DAMAGE "Collisions" study 63
3.4 First 50 MC runs 64
3.5 Average of all 150 MC runs 65
3.6 Uni-relational network formed from two MC runs 67
3.7 Multi-relational network vertices and edges. 69
3.8 Multi-relational network formed from one MC run 70
3.9 Vertices "A" and "E" are removed from the network in Figure 3.8. 73
3.10 Seven smaller networks remain when vertices "B", "C", and "D" are removed from the network in Figure 3.8. 74
3.11 The network formed from one MC run (Lewis et al., 2010). 75
3.12 The network formed from two combined MC runs (Lewis et al., 2010). 75
3.13 The network formed from three combined MC runs (Lewis et al., 2010). 76
3.14 The network formed from four combined MC runs (Lewis et al., 2010). 76
3.15 The age of TLE data as a function of number of conjunctions in SOCRATES conjunction assessments in August 2009 79

3.16 SOCRATES maximum probability and minimum distance predictions prior to the collision between Iridium-33 and Cosmos-2251. 80
3.17 Comparison of the Iridium-33/Cosmos-2251 conjunction to all other conjunctions (Kelso, 2009b). 81
3.18 Age of the TLE data used in the Iridium-33/Cosmos-2251 conjunction assessments. 81
3.19 120710 SOCRATES network. 84
3.20 120710 SOCRATES network close-ups. 85
(a) Close-up "28210" and "03510" 85
(b) Close-up "22012" 85
(c) Close-up "26829" and "08151" 85
(d) Close-up "11962" 85
3.21 Degree distribution of SOCRATES data on 12th July 2010. 86
3.22 Network of the conjunctions reported by SOCRATES on 1st January 2006. 89
3.23 Comparison of degree distributions between SOCRATES reports on 1st January 2006 and 12th July 2010. 92
3.24 Network of generated from SOCRATES report 291009(1244) based on satellite names. 93
3.25 Network generated from SOCRATES report 291009(1244) based on satellite catalogue numbers. 94

4.1 DAMAGE-simulated LEO debris populations between 2009 and 2030 for the 'No collisions' and 'Collisions' benchmark scenarios. There is no ADR in either scenario. 102
4.2 Effective number of objects in the 'Collisions' and the ADR scenario simulations 103
4.3 Effective Reduction Factor (ERF) between 2009 and 2030 for the four ADR scenarios. 104
4.4 Normalised Effective Reduction Factor (NERF) between 2009 and 2030 for the four ADR scenarios. 104
4.5 LEO debris populations between 2009 and 2059 for benchmark scenarios. 110
4.6 Effective number of objects in the 'Collisions' and ADR scenario simulations. 111

4.7 Effective Reduction Factor (ERF) between 2009 and 2059 for the three ADR scenarios. 113
4.8 Normalised Effective Reduction Factor (NERF) between 2009 and 2059 for the three ADR scenarios. 113

Declaration of authorship

I, *REBECCA JANE NEWLAND*, declare that the thesis entitled *ASSESSING THE USE OF NETWORK THEORY AS A METHOD FOR DEVELOPING A TARGETED APPROACH TO ACTIVE DEBRIS REMOVAL* and the work presented in the thesis are both my own, and have been generated by me as the result of my own original research. I confirm that:

- this work was done wholly or mainly while in candidature for a research degree at this University;
- where any part of this thesis has previously been submitted for a degree or any other qualification at this University or any other institution, this has been clearly stated;
- where I have consulted the published work of others, this is always clearly attributed;
- where I have quoted from the work of others, the source is always given. With the exception of such quotations, this thesis is entirely my own work;
- I have acknowledged all main sources of help;
- where the thesis is based on work done by myself jointly with others, I have made clear exactly what was done by others and what I have contributed myself;
- parts of this work have been published as:

  Lewis, H.G., Newland, R.J., Swinerd, G.G., and Saunders, A. (2010) A New Analysis of Debris Mitigation and Removal Using Networks. *Acta Astronautica*, **66**, (1-2), 257-268.

  Newland, R.J., Lewis, H.G., and Swinerd, G.G. (2009) Supporting the Development of Active Debris Removal Using Weighted Networks. At *5th European Conference on Space Debris, Darmstadt, Germany, 30 March - 2 April 2009.*

  Lewis, H.G., Swinerd, G.G., Newland, R.J., and Saunders, A. (2009) Active Removal Study for On-Orbit Debris Using DAMAGE, At *5th European Conference on Space Debris, Darmstadt, Germany, 30th March - 2nd April 2009.*

Signed:
Date:

This thesis is dedicated to Aunty Barbara

The strength you have shown through such difficult times and the courage that you've faced every situation with is inspirational.
Stay strong.
With love, from Rebecca

Acknowledgements

This thesis would not have been possible if it had not been for the help, support, and friendship of so many people.

Hugh and Graham, thank-you for your advice, encouragement, and for always having confidence in me.

Thank-you to Dr T S Kelso at the Center for Space Standards and Innovation for kindly giving me access to historical SOCRATES data (from 1st January 2006 to 31st August 2009).

François, thank-you for your patience and teaching me how to program. Thank-you for rewriting my basic code into something more sophisticated that I was able to use to process data for large networks.

To my parents, John and Jane, and my sister, Amy, thank-you for always being there for me.

Thank-you to my wonderful friends all over the world, without whom life would be empty: Viorica, Zuzana, Rūta, Yiorgios, Asti, Sarah S, Sam F, Lisa, Tadashi, Arrun, François, Piers, John, Nick L, Nick B, Su, Warin, Jenny, Jaye, Matti, Rich, Felicity, Teodor, and Oli. Special thanks go to Charlotte and Thomas; *tusind tak* for your friendship and your support, you helped me through when I thought I was never going to make it.

Nomenclature

β	beta index
γ	constant exponent
ρ	atmospheric density
σ	combined cross-sectional area
A	adjacency matrix
a_{ij}	adjacency matrix element
$\bar{B}$	network betweenness
B_i	betweenness centrality of vertex i
b_i^s	variable for calculating betweenness centrality of vertex i
$\bar{C}$	network clustering
C_D	drag coefficient
c_i	clustering coefficient of vertex i
$CN_R(t)$	cumulative number of objects removed in an ADR scenario
$\bar{D}$	network closeness
D_i	closeness centrality of vertex i
d_{ij}	shortest path distance between vertices i and j
dU	cube volume
F_D	atmospheric drag force
i	vertex in an breadth first search
i_e	degree of vertex i adjoined to vertex, j by edge, e
j_e	degree of vertex j adjoined to vertex, i by edge, e
k_i	degree of vertex i
$\bar{K}$	network degree
$\hat{l}$	normalised length of an impact projectile
l_c	characteristic length
l_x	largest shadow dimension
l_y	second largest shadow dimension
l_z	third largest shadow dimension
$\hat{m}$	normalised mass of an impact projectile
m	size of a network (number of edges)
m_p	mass of an impact projectile

n	order of a network (number of vertices)
N_f	number of fragments
$N(t)$	effective number of objects in a 'Collisions' scenario
$N_S(t)$	effective number of objects in an ADR scenario
$N_T(t)$	number of target objects in an ADR scenario
p	portion of a network
pc	critical portion of a network
$P_{i,j}$	collision probability
$P(k)$	probability that a vertex has degree, k
R	network assortativity
R_i	ranking value for ADR target objects
i	source vertex in an breadth first search
S	orbiting object reference area
s_i	strength of vertex i
s_j	residential probability of an object
V_{imp}	relative velocity
V_r	velocity
w_{ij}	weighted adjacency matrix element

Acronyms

ADR	Active Debris Removal
AMR	Area-to-Mass Ratio
ASAT	Anti-satellite
BAU	Business As Usual
CA	Conjunction Assessment
CIRA	COSPAR International Reference Atmosphere
COSPAR	Committee on Space Research
CSSI	Center for Space Standards and Innovation
DAMAGE	Debris Analysis and Modelling Architecture for the Geosynchronous Environment
DELTA	Debris Environment Long Term Analysis
DISCOS	Database and Information System Characterising Objects in Space
EDDE	Electrodynamic Debris Eliminator
EOL	End Of Life
ERF	Effective Reduction Factor
ESA	European Space Agency
FADE	Fast Debris Evolution
FY	Financial Year
GEO	Geostationary Earth Orbit
GOLD	Gossamer Orbit Lowering Device
GRASP	Grapple, Retrieve, and Secure Payload
IAA	International Academy of Astronautics
IADC	Inter-Agency Space Debris Coordination Committee
IDEAS	Innovative Deorbiting Aerobrake System
iDoD	Inflatable De-orbit Device
IMO	International Maritime Organization
LDEF	Long Duration Exposure Facility
LEGEND	LEO-to-GEO Environment Debris Model
LEO	Low Earth Orbit

LEODEEM	Low Earth Orbital Debris Environmental Evolutionary Model
LUCA	Long-term Utility for Collision Analysis
MASTER	Meteoroid and Space Debris Terrestrial Environment Reference
MC	Monte Carlo
MEO	Medium Earth Orbit
NASA	National Aeronautics and Space Administration
NERF	Normalised Effective Reduction Factor
NFL	No Future Launches
NORAD	North American Aerospace Defence Command
ODPO	Orbital Debris Program Office
ODQN	Orbital Debris Quarterly News
OECD	Organisation for Economic Co-operation and Development
ORDEM	Orbital Debris Environment Model
PIB	Particle-in-a-Box
POST	Parliamentary Office for Science and Technology
SATCAT	Satellite Catalogue
SDA	Space Data Association
SDM	Space Debris Mitigation
SOCRATES	Satellite Orbital Conjunction Reports Assessing Threatening Encounters in Space
SPDA	Space Debris Prediction and Analysis
SRP	Solar Radiation Pressure
SSA	Space Situational Awareness
SSN	Space Surveillance Network
STK/CAT	Satellite Tool Kit's Conjunction Analysis Tools
TLE	Two Line Element
UNCOPUOS	United Nations Committee on the Peaceful Uses of Outer Space
USSPACECOM	United States Space Command

Chapter 1

INTRODUCTION

1.1 Problem Statement

Space debris is a term used to refer to any man-made object in Earth's orbital environment, or re-entering the atmosphere, that no longer serves a useful purpose (IADC, 2002). This debris is found in all orbital regions from Low Earth Orbit (LEO) 200–2,000 km, through Medium Earth Orbit (MEO) 2,000–35,586 km, up to Geostationary Earth Orbit (GEO) 35,786 ± 200 km. LEO is the most densely populated of the three regions (IAA, 2008) and is the focus of this thesis.

Observations of the space debris environment, recent collision events, and modelling studies indicate that we can expect to see continued future growth of the space debris population in LEO that will not be controlled unless debris is actively removed from orbit (Liou and Johnson, 2006). Removing debris via Active Debris Removal (ADR) will require a targeted approach because the costs involved mean that not all debris objects are removable. Therefore, the objective of this thesis is to assess a method of targeting objects that complements methods that have already been proposed in other publications; using network theory to determine target criteria for ADR.

This first chapter provides an overview of space debris, its historical growth, the results of future modelling studies, and methods for tackling the problem and

determining target criteria. This leads into a detailed look at the research aims of this thesis before exploring network theory in Chapter 2.

1.1.1 Classification and sources

Space debris is classified into three categories depending on its size: > 10 cm (large), 1–10 cm (medium), or < 1 cm (small). There are tens of millions of debris < 1 cm in size (NASA, 2009c). These include fragments from historical explosion and collision events, aluminium oxide particles from solid rocket motor firings, and NaK reactor coolant droplets from Radar Ocean Reconnaissance Satellites (Klinkrad, 2006). Debris of this size can erode spacecraft surfaces and cause damage to sensors, electrical cables, and fluid lines (IADC, 1998). To address this problem sensitive parts of spacecraft are designed so that they do not face the highest debris flux. Shielding is also used. For example, Whipple shields are multi-layer screens designed to protect a spacecraft surface from an impact with small or medium-sized debris (UNCOPUOS, 2001; Klinkrad, 2006).

Although debris < 0.5 cm is considered 'sub-measurable' (NASA, 2009a), data is normally acquired in a statistical manner through experimental sensors with high sensitivities (ESA, 2009a). In addition, the retrieval of on-orbit surfaces provides data on debris < 0.1 cm (NASA, 2009a). Surfaces have been retrieved from Space Shuttle missions, such as STS-7, STS-50, and STS-92 (Christiansen et al., 2004), and the Long Duration Exposure Facility (LDEF) (Kinard, 2007).

There are approximately 500,000 debris objects 1–10 cm in size (NASA, 2009c). It is objects in this size range that potentially pose the greatest threat to spacecraft. This is because they are too small for their orbits to be determined adequately, but they are large enough to cause catastrophic damage to operational spacecraft. Whipple shields are only effective against debris up to 1–2 cm, so debris above this size are not shielded against (ESA, 2005).

There are approximately 22,500 debris objects > 10 cm in orbit including non-operational satellites, mission-related objects, and rocket upper stages (Lewis et al., 2011). These objects account for approximately 90% of on-orbit mass in LEO (ODPO, 2011b). The Space Surveillance Network (SSN) of the

United States Department of Defence is the principal source of information on the population of large debris objects. A critical part of the SSN's mission involves detecting, tracking, cataloguing, and identifying man-made objects orbiting Earth, i.e. active/inactive satellites, spent rocket bodies, and fragmentation debris (NASA, 2009c).

When an object has been tracked sufficiently to determine its orbit by the SSN, it is catalogued by the North American Aerospace Defence Command (NORAD). The same object can then be reacquired at a later time by the SSN and identified with confidence. Catalogued objects need to be of sufficient size, above 5 cm for objects in LEO (NASA, 2007), and above approximately 1 m for objects in GEO (Donath et al., 2005; Johnson et al., 2008). Only 6% of the catalogued population are operational satellites (Klinkrad and Johnson, 2009).

Each object in the NORAD catalogue has two unique identifiers: the International Designator and the NORAD catalogue number. The International Designator is assigned at launch by the World Data Center for Satellite Information and consists of three parts: the year of launch, the launch number in that year and a letter designating the separate items associated with the launch (Kelso, 2004). For example, 1998-067A was the primary payload of the 67^{th} launch of 1998 - the Zarya module of the International Space Station. Usually the letter "A" is given to the main payload of the launch, "B" is the associated upper stage, and "C", "D", "E" etc, are assigned to fragments or other items associated with the launch.

The NORAD catalogue number is a unique identifier indicating the sequence in which objects have been added to the NORAD satellite catalogue (SATCAT) (Kelso, 2006). When an object is observed it is given the next ascending number in the SATCAT (Hunt, 2010a). For example, the International Space Station has the NORAD catalogue number 25544.

In addition to the NORAD catalogue, the European Space Agency (ESA) uses the Database and Information System Characterising Objects in Space (DISCOS). DISCOS is a single-source reference for information on all known objects (ESA, 2009b). DISCOS has been built up from data supplied by the

United States Space Command (USSPACECOM) and the SSN (Klinkrad, 1991; Jehn et al., 1993; ESA, 2009b). Although currently relying on non-European sources for its space surveillance, ESA is in the preparatory phase of developing a space situational awareness (SSA) programme that includes tracking debris objects as one of its main goals (ESA, 2010; POST, 2010).

1.1.2 Historical growth

Historical catalogues are used to define the historical growth of the debris population, shown in Figure 1.1. However, the population in Figure 1.1 does not include around 6,500 'analyst satellites' that are not reliably tracked (McKnight, 2010).

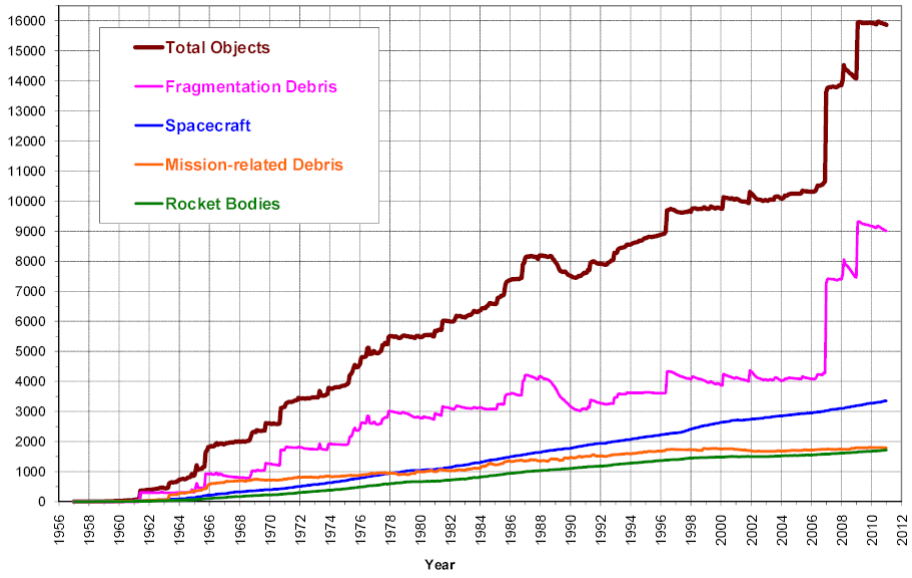

Figure 1.1: Monthly number of catalogued objects in Earth orbit by type as catalogued by the SSN (ODPO, 2011a).

Figure 1.1 shows that until 1996 the growth of the catalogued population was approximately linear at a rate of 260 catalogued objects/year (UCS, 2009; McKnight, 2010). The sharp increase in 1996 was due to the breakup of a Pegasus rocket body which exploded at an altitude of 630 km, generating more than 600 fragments $>$ 10 cm (Matney et al., 1997).

Between 1996 and the end of 2006 the population of fragmentation debris remained approximately constant whilst launches continued to increase the number of spacecraft, rocket bodies, and mission-related debris. However, since the beginning of 2007 there has been a 50% rise in the total number of catalogued objects. In January 2007 the deliberate anti-satellite (ASAT) test that destroyed the Fengyun-1C satellite at 850 km created 3,037 debris objects (ODPO, 2010a). Just after this event was reported, pieces of the debris cloud that was created ranged from below 200 km up to almost 4,000 km in altitude, posing a threat to many operational satellites (Johnson et al., 2008; IAA, 2008; Kelso, 2010). This event increased the debris population > 10 cm by a third, with the majority of the objects residing in long-lived orbits (Johnson et al., 2008). 97% of the fragments were still in orbit in January 2011 (Johnson, 2011).

Between February 2007 and March 2008 three events occurred that had a limited overall impact on the catalogued population of fragmentation debris:

- In February 2007 a Briz-M upper stage exploded in a highly elliptical orbit. Only 85 objects had been observed as of May 2010, although it was estimated that the event generated over 1,000 objects (ODPO, 2007; ODPO, 2010b). These objects have not been observed because of their highly elliptical orbits (Liou, 2010b).
- In February 2008 the deliberate destruction of the satellite USA-193 took place at 250 km (Stansbery et al., 2008). This event had a limited impact on the orbital environment as all of the debris objects it created had decayed by October 2008 (Pardini and Anselmo, 2009).
- Cosmos 2421 fragmented at 410 km in March 2008 creating over 500 debris objects; by May 2010 all but 18 of the objects had decayed (ODPO, 2010b).

However, in February 2009 the population of fragmentation debris grew sharply again due to the first collision involving two intact satellites, Iridium-33 and Cosmos-2251, at 790 km (ODPO, 2009c). This event created 1,875, objects $>$

10 cm of which 93% remained on orbit as of January 2011 (Johnson, 2011). It is likely that the orbital lifetimes of many of the debris will be measured in decades (ODPO, 2009c). The Fengyun-1C ASAT test and the collision between Iridium-33 and Cosmos-2251 increased the population growth rate to approximately 1,250 catalogued objects/year (McKnight, 2010).

Conjunction assessments can also be used to show historical growth in the debris population. Conjunction assessments are made by organisations such as NASA (Newman, 2010), the Space Data Center (SDA., 2010), and the Center for Space Standards and Innovation (CSSI) (CSSI, 2011). These assessments play a critical role in preventing collisions as they aid decisions made by spacecraft operators when collision avoidance manoeuvres are thought to be necessary.

SOCRATES is a source of conjunction assessment data provided by the CSSI that has been issued online for public use since 2004 (Kelso and Alfano, 2005). Figure 1.2 shows the contribution of recent fragmentation events to SOCRATES conjunction events. SOCRATES reports from the last five years show a clear rise in the number of close approaches involving satellite payloads from approximately 7,000 per day in 2005, to nearly 14,000 per day in 2009, and just over 16,000 per day in August 2010. Nearly half of these close approaches involve debris from recent major fragmentation events (Lewis et al., 2009a).

Despite the fact that only 4% of conjunctions involve intact objects, these close approaches should not be ignored. It was the collision between the intact, but non-operational Cosmos-2251 satellite and the operational Iridium-33 satellite that generated the fragmentation debris that now account for 22% of close approaches (Figure 1.2).

Spatial density defines the number of objects per cubic kilometre. A close approach is more likely to occur in a region of high spatial density than a region of low spatial density. Figure 1.3 shows the spatial density distribution of objects $\geq$ 10 cm in LEO.

73% of the total debris population, accounting for 40% of all on-orbit mass, is found around 800–900 km (Klinkrad and Johnson, 2009). The highest spatial densities at some altitudes are due to the popularity of these altitudes for Earth

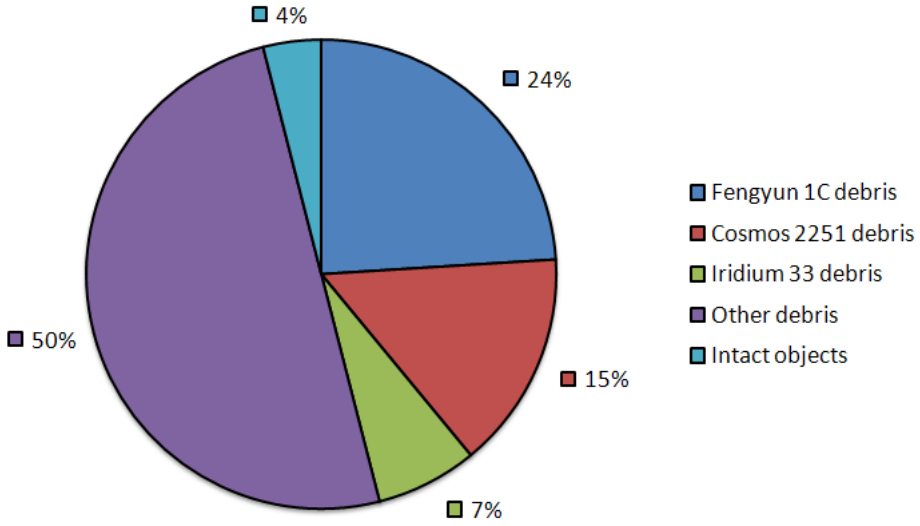

Figure 1.2: Contribution of recent breakup fragments to SOCRATES close approaches (data: CSSI SOCRATES, generated on 9th December 2010). Other debris includes rocket bodies, fuel cores, and fragmentation debris.

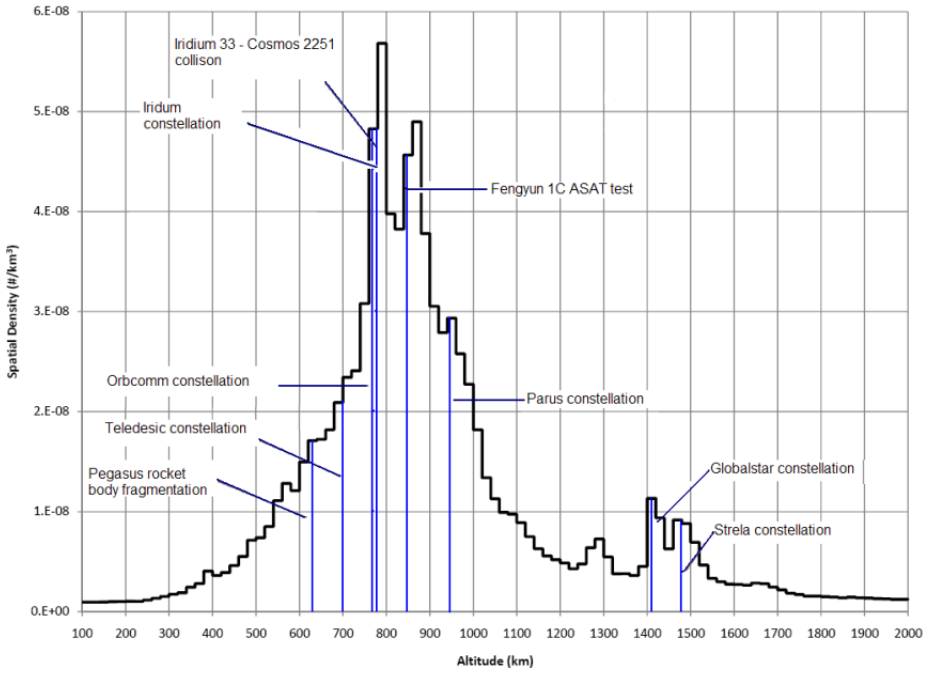

Figure 1.3: Spatial density of objects $\geq$ 10 cm in LEO on 5 June 2009 (grouped in 20 km altitude bins) (ODPO, 2009a).

observation, communication, and surveillance satellites and the rocket bodies associated with their launches. In addition, two major break-up events, the Fengyun-1C ASAT test and the Iridium-33 and Cosmos-2251 collision, have taken place in the region around 800 km.

1.1.3 Instability and future predictions

Stability is defined by determining if the current population of fragmentation debris will increase solely due to collisions (Kessler and Anz-Meador, 2001). Several studies conclude that LEO is unstable (Su, 1993; Kessler, 1991; Rossi et al., 1997; Kessler, 2000; Kessler and Anz-Meador, 2001; Krisko et al., 2001; Liou and Johnson, 2006; Liou and Johnson, 2008; Talent, 2009). However, given the variation of the spatial density across LEO (Figure 1.3), it is more accurate to refer to the stability of altitudes than of LEO as a whole.

Figure 1.4 shows how the on-orbit population $\geq$ 10 cm within some altitudes has moved from stability, through equilibrium, to instability (Klinkrad and Johnson, 2009).

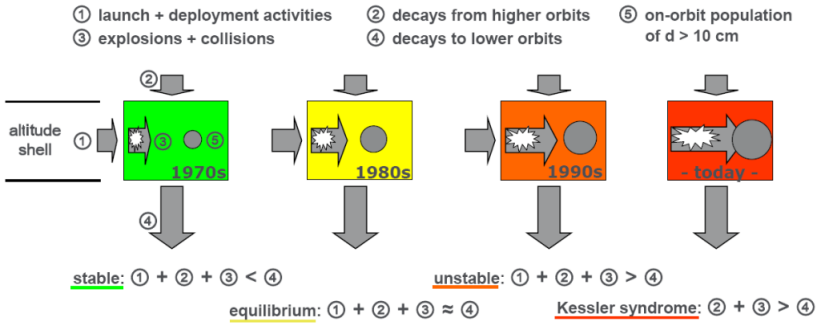

Figure 1.4: From stability to collisional cascading (Klinkrad and Johnson, 2009).

In 1978 it was predicted that collisions between catalogued objects would begin around the year 2000 and, as a result of these collisions, the debris flux would increase exponentially, even if a zero net input rate was maintained (Kessler and Cour-Palais, 1978). If collisions between existing intact objects produce fragments at a faster rate than they are removed by orbital decay, the spatial density of objects will reach a critical density (Kessler, 1991). Two levels of

critical density have been defined: an unstable threshold, where the number of fragments increases with time until equilibrium is reached, and a runaway threshold, where the number of fragments continues to increase for as long as the current population density of intact objects is maintained (Kessler and Anz-Meador, 2001). If launches continue then it is possible to reach a runaway threshold, as new launches add to the population of intact objects.

Collisional cascading (also known as the 'Kessler syndrome') describes the stage of uncontrolled debris growth where collisions between collision fragments (debris resulting from earlier collisions) become important (Kessler, 1991; Walker et al., 2001; Klinkrad, 2006). Altitudes that have a large amount of on-orbit mass and high spatial densities, such as those containing satellite constellations, are at risk from collisional cascading (Walker et al., 2000). McKnight (2010) and Talent (2009) highlight that although the current collision threat in LEO is from small and medium debris, in the future it is the large debris that poses the greatest threat. This is because large debris acts as a reservoir of mass that would become fragments in the event of an explosion or collision.

Space debris models are used to characterise the space debris environment and to predict long-term trends. There are two types of models: environment and evolutionary. Environment models are used to describe the current space debris population. They are used as risk assessment tools by satellite operators to determine properties of the environment, such as impact flux, and as benchmarks for ground-based debris measurements and observations (NASA, 2009d). NASA's Orbital Debris Environment Model (ORDEM) (Xu et al., 2009), Space Debris Prediction and Analysis (SPDA) (Nazarenko and Menshikov, 2001), and ESA's Meteoroid and Space Debris Terrestrial Environment Reference (MASTER) model (Oswald et al., 2005) are environment models.

Evolutionary models are used to simulate historical and future debris populations. Historical simulations model the debris environment from 1957 to the present to validate the methods used for the future simulations (NASA, 2009b). Future projections are used to determine trends and to assess

the effectiveness of mitigation and remediation methods. Examples of evolutionary models are:

- Space Debris Mitigation (SDM) (Rossi et al., 1995),
- Evolve model (EVOLVE) (Reynolds and Eichler, 1995; Krisko et al., 2001),
- Long-term Utility for Collision Analysis (LUCA) (Bendisch et al., 1997),
- Debris Analysis and Modelling Architecture for the Geosynchronous Environment (DAMAGE) (Lewis et al., 2001),
- Debris Environment Long Term Analysis (DELTA) (Walker et al., 2001),
- LEO-to-GEO Environment Debris (LEGEND) model (Liou et al., 2004),
- Low Earth Orbital Debris Environmental Evolutionary Model (LEODEEM) (Narumi et al., 2008), and
- Fast Debris Evolution (FADE) model (Lewis et al., 2009c).

Two forecasting scenarios are: 'business as usual' (BAU) and 'no future launches' (NFL). In a BAU scenario, new launches are included during the simulation period, whereas in an NFL scenario, new launches are excluded. BAU is commonly used as a baseline case, with a historical period of launches used to produce a future launch cycle for the duration of the simulation. NFL is an unrealistic scenario that is often used to model a 'best-case' future. As NFL scenarios exclude future launches they can also provide an assessment of the current LEO debris environment (Liou and Johnson, 2008). Both BAU and NFL modelling studies suggest that the debris population will continue to increase in the future and that collisions between objects will drive the long-term future evolution of the debris environment (Liou and Johnson, 2006; Liou and Johnson, 2008; Lewis et al., 2009b; Liou and Johnson, 2009; Liou, 2010a). The population growth is currently linear, but the Liou and Johnson (2009) BAU modelling study predicts a fast non-linear

growth if no interventions are taken. Furthermore, a 2010 BAU study predicts that the population will increase by 75% by 2210 (Liou et al., 2010).

Figure 1.5 shows the results of two NFL scenarios constructed using data before (2006) and after (2009) the Fengyun-1C ASAT test and the Iridium-33/Cosmos-2251 collision. Even without future launches Figure 1.5 shows that the debris population is going to increase in the future. This predicted increase is due to collisions.

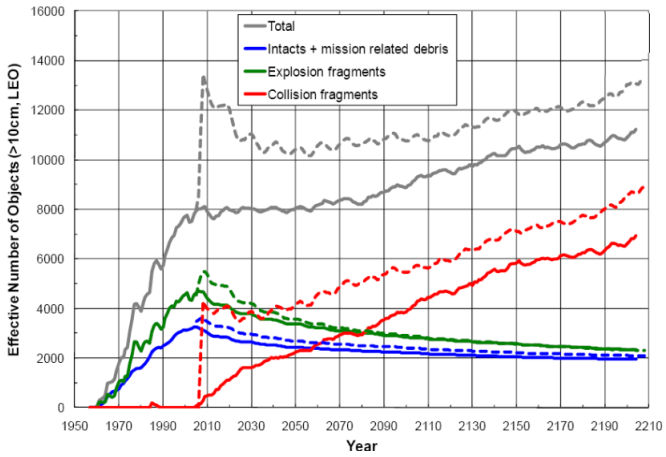

Figure 1.5: Two NFL scenarios: NFL from 2006 (solid line) and NFL from 2009 (dashed line) (Liou, 2010a).

Figure 1.6 shows the variation in the cumulative number of collisions between objects $\geq$ 10 cm for NFL and BAU scenarios. One BAU scenario does not include any post-mission disposal (PMD), the other includes 90% PMD. For both of the BAU scenarios, on average one collision can be expected every five years up to 2050 (Liou, 2010a). For the NFL scenario, on average one collision would be expected every eight years in the same time frame. Similarly, Lewis et al. (2009a) predict that the cumulative number of collisions will be between five and 11 by 2050 resulting in an average expected collision rate of one collision every 3.6 to eight years.

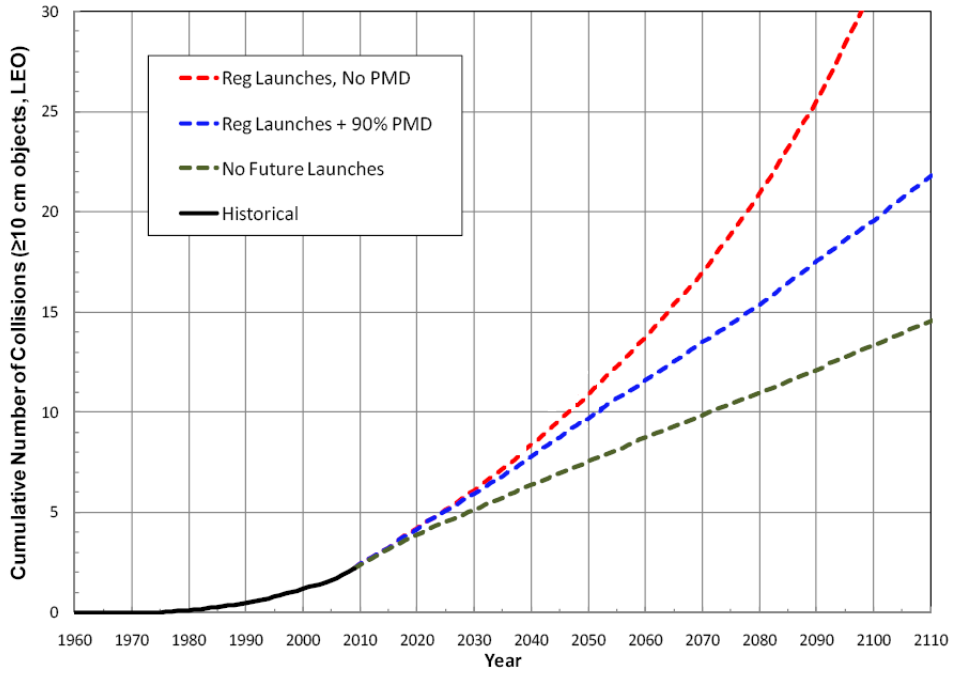

Figure 1.6: Cumulative number of collisions predicted in NFL and BAU scenarios (Liou, 2010a).

1.1.4 Mitigation

Kessler and Cour-Palais (1978) stated the expected problems of future population growth and instability of the orbital environment. In the 1990's, mitigation policies were proposed to manage the creation of debris to stabilise the environment. The Inter-Agency Space Debris Coordination Committee (IADC) was created in 1993 by four space agencies to bypass the legal and diplomatic aspects constraining the development of legally binding agreements at the United Nations (UN) (ODPO, 2011a). The IADC is now a forum of representatives from 12 member organisations.

In 2002 the 'IADC Space Debris Mitigation Guidelines' were issued (IADC, 2002). In 2007 the United Nations Committee on the Peaceful Uses of Outer Space (UNCOPUOS) Scientific and Technical Subcommittee Working Group on Space Debris approved the use of new guidelines (based on the 2002 IADC version) as voluntary mitigation measures (ESA, 2007). These guidelines

bypassed the legal subcommittee and were endorsed by a full UN General Assembly Resolution (Weeden, 2009). The guidelines are designed to minimise the generation of debris (in LEO and GEO) in both the short-term and the long-term:

Short-term (IADC, 2007):

- Limit debris released during normal operations
- Minimise the potential for breakups during operational phases
- Limit the probability of accidental collision in orbit
- Avoid intentional destruction and other harmful activities

Long-term (IADC, 2007):

- Minimise potential for post-mission breakups resulting from stored energy
- Limit the long-term presence of spacecraft and launch vehicle orbital stages in LEO after the end of a mission
- Limit the long-term interference of spacecraft and launch vehicle orbital stages with the GEO region after end-of-life (EOL)

The mitigation guideline that calls for the limitation of the long-term presence of spacecraft and launch vehicle orbital stages is represented by the '25-year rule'. Modelling studies determined that a 25-year post-mission lifetime would be effective at stabilising the population and minimising the generation of new debris even when launch rates are increased (Walker and Martin, 2004; Liou and Johnson, 2005).There are five UN treaties that outline general principles for managing space debris in addition to the IADC and UN guidelines. However, there are no dedicated obligations with which space agencies and satellite operators are required to comply and the 25-year rule has not been universally applied (UNCOPUOS, 2007; NASA, 2008).

The premise of the 25-year rule is to reduce orbital lifetime by manoeuvring satellites at the end of their useful lives into orbits that would be subject to an

atmospheric drag force leading to the object's re-entry within 25 years. Atmospheric drag force is given by,

$$\mathbf{F}_D = \frac{1}{2}\rho S C_D V_r^2 \left(\frac{-\mathbf{V}_r}{|V_r|}\right), \tag{1.1}$$

where ρ is the atmospheric density, S the reference area for the object, C_D is the object's drag coefficient, and V_r is the velocity vector of the orbiting object relative to the atmosphere (Stark et al., 2003). Atmospheric drag is effective up to about 800 km (Sheriff and Hu, 2001). The drag force takes energy out of an orbit causing altitude and eccentricity to decrease. As the object's altitude decreases, the atmospheric density encountered rises exponentially, accelerating its decline in altitude (Knipp, 2005). The process continues until the orbit is no longer sustainable, and the object re-enters the atmosphere.

The mean atmospheric density at 600 km altitude is of the order of 10^{-13} kg/m^3, compared to about 1.3 kg/m^3 at sea level (Benson, 2011). However, atmospheric density varies with solar activity. The 10.7 cm radio flux, 'F10.7 cm', is accepted as an accurate representation of solar activity (Vallado and Finkleman, 2008). A high 10.7 cm flux indicates an active solar period and a low flux indicates a quiet period (Stansbery and Foster Jr., 2004).

Changes in atmospheric density as a result of changing solar flux directly affect the decay rates of objects in LEO (ODPO, 2009b). As a result, the lifetime of debris in orbit (and effectiveness of mitigation) varies with the solar cycle, a period of $\approx$ 11 years in which the Sun's activity varies between a quiet minimum and an active maximum. The effect of the solar cycle on the lifetime of debris is shown in Figure 1.7.

During solar cycle maximum, the temperature of the Earth's upper atmosphere increases from 700 °C to 1500 °C (NASA, 2010). As the Sun's activity increases towards solar maximum, the atmosphere expands and the atmospheric density increases. The increase in atmospheric density makes drag more effective at higher altitudes, thus affecting more orbits and causing debris to re-enter the Earth's atmosphere at a higher rate during solar maximum than at other times (Stansbery and Foster Jr., 2004; Stokely et al., 2009).

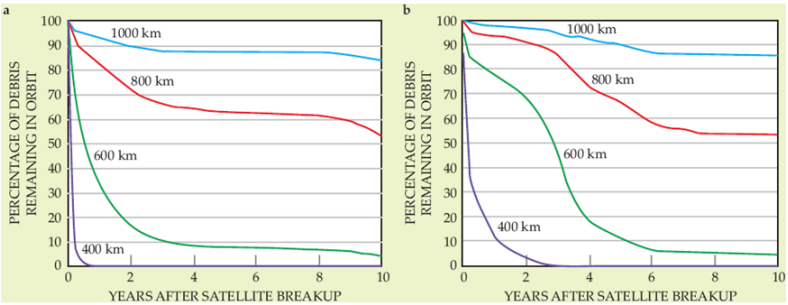

Figure 1.7: The percentage of debris remaining in a circular orbit at different altitudes is shown a) at a time of maximum solar activity (1st January 1980) and b) a time of minimum solar activity (1st January 1986) (Wright, 2007).

However, Emmert et al. (2004) indicate that the thermosphere, an upper layer of the Earth's atmosphere which reaches from $\approx$ 90 km to $\approx$ 600 km, is currently cooling and contracting. Between 1970 and 2010 thermospheric density reduced by a few percent per decade (Saunders et al., 2011) and this decline in thermospheric density is predicted to continue as part of a long-term trend (Keating et al., 2000; Picone et al., 2005; Saunders et al., 2011). Cooling lowers the density of the atmosphere and means that the drag sink is less effective at removing objects.

1.1.5 Remediation

Despite the effectiveness of mitigation (when applied), its continued application will not stop the growth of the debris population entirely due to the existing instability of several densely populated orbital altitudes (Walker et al., 2001; UNCOPUOS, 2007; Liou and Johnson, 2009). Therefore, in addition to current mitigation measures, remediation is needed (Liou and Johnson, 2006).

ADR has been proposed as a means of remediation and is described in several studies as a necessary and effective way to control the growth of the debris population (Bastida-Virgili and Krag, 2009; Lewis et al., 2010; Liou and Johnson, 2009; Nishida et al., 2009). ADR will involve manoeuvring debris into immediate de-orbit or into lower orbits to reduce the overall orbital lifetime of

the objects (IAA, 2010).

The International Academy of Astronautics (IAA) reviewed several ADR techniques in 2008 and 2010 and determined the following four to be feasible for removing large debris objects: drag augmentation, momentum exchange tethers, electrodynamic tethers, and orbital transfer using attached propulsion modules (IAA, 2008; IAA, 2010). These are outlined below:

- Drag augmentation –Drag augmentation involves increasing the area-to-mass ratio (AMR) of an object using an inflatable or deployed structure. By increasing the AMR of an object, the drag force has a greater impact on a satellite thus further reducing its orbital lifetime. Inflatable structures such as the Innovative Deorbiting Aerobrake System (IDEAS) (Santerre et al., 2008), the Inflatable Deorbit Device (iDoD) (Maessen et al., 2007), and the Gossamer Orbit Lowering Device (GOLD) (Nock et al., 2009) have been developed to test these concepts. iDoD uses inflatable tubes with sheets of mylar between them to act as sails to increase the AMR on debris objects up to 1,000 km (Noca et al., 2010). GOLD is designed to be effective up to 1,500 km (Nock et al., 2009).

- Momentum exchange tethers –After rendezvous with a debris object, a 'chaser' spacecraft would be connected to it by a non-conductive tether (Hoyt and Forward, 2000). The tether would be deployed, maintaining tension using a gravity gradient. The new tether system would orbit with the orbital angular velocity of the centre of mass of the system –the debris object would have a speed below that expected for its orbital altitude and the chaser spacecraft would have a speed in excess of that appropriate for its orbital altitude (Izquierdo et al., 2000; IAA, 2010). When the tether is detached, the momentum transfer decreases the debris object's perigee and increases the chaser spacecraft's apogee (IAA, 2010). The debris will enter a lower orbit, reducing its orbital lifetime.

- Electrodynamic tethers –A tether made of conducting material can be deployed from a satellite or debris object to reduce its orbital lifetime via electrodynamic drag (Iess et al., 2002; Hoyt, 2009; Pearson

et al., 2009; Furukawa et al., 2009; Kawamoto et al., 2009; Pardini et al., 2009). An electromotive force is created due to the current flowing through the tether as the debris and attached tether travel through the Earth's geomagnetic field. Once a current flows through the tether, kinetic energy is converted into electrical energy and a Lorentz force acts in a direction opposed to the orbital motion creating electrodynamic drag (Hoyt, 2009). The tether length determines the current and time taken for a reduction in altitude; tethers that are 5–10 km long will reduce debris orbital altitudes by 2–50 km per day (Pardini et al., 2009).

Tethers can be reusable or expendable and do not require propellant to operate. However, if they are to be reused, then a voltage would need to be applied to reverse the current in the tether to re-boost its orbit (Kawamoto et al., 2006). The Electrodynamic Debris Eliminator (EDDE) (Pearson et al., 2009), the Terminator Tape (Hoyt and Forward, 2000; Hoyt, 2009), and the Terminator Tether (Hoyt and Forward, 2000; Hoyt, 2009), are examples of tether technology that are under development. Pearson et al. (2009) propose that EDDE could remove 2,465 objects with mass > 2 kg from LEO within seven years. The risks associated with having multiple tethers in orbit at once are not discussed as part of this proposal.

- Attached Propulsion Modules –Attaching a propulsion source to a debris object would allow for controlled de-orbit or re-entry (IAA, 2010). However, although attached propulsion modules would provide controlled de-orbit they have a significant mass cost for their operational lifetime (Yoshida and Araki, 1994). Despite this cost, the advantage of this approach compared to tethers or drag augmentation devices is that propulsion modules are reliable technologies (Bonnal and Bultel, 2009).

All four of these proposed technologies are yet to be fully demonstrated (Alby and Bonnal, 2010). Whilst each has its advantages, the methods share some common disadvantages. The main disadvantage is that the proposed ADR methods require physical contact with the debris objects. The physical interface

with large, uncooperative objects presents a major technological challenge. Debris objects may have residual angular momentum, no grasping interface, and mostly brittle surfaces (Bischof et al., 2002; Kaplan, 2009; IAA, 2010). The successful rendezvous with these uncooperative objects will likely require the development of optical and range sensors to accurately manage the rendezvous manoeuvre (Kawamoto et al., 2010; Terui, 2010; Noca
et al., 2010; Bellido, 2010).

Residual angular momentum could be dealt with by applying external torques (Kaplan, 2009). Other proposed solutions to this problem would be to deploy a net to grasp and retrieve an object or to use magnetic control to 'de-tumble' the objects to remove their residual spin before capture
(Hoyt, 2009; Carroll, 2009; Ruault et al., 2010; Lappas et al., 2010). A technology named 'Grapple, Retrieve, and Secure Payload' (GRASP) has been designed by Tethers Unlimited, Inc. to chase and rendezvous with a debris object using inflatable booms to deploy a net to capture the debris (Hoyt and Forward, 2000). After capturing a debris object a module containing a de-orbit technology such as an electrodynamic tether, momentum exchange tether, attached propulsion module, or drag augmentation device could be attached to the debris (Hoyt and Forward, 2000; Bonnal and Bultel, 2009).

Another disadvantage of the aforementioned techniques is that the addition of an ADR system into orbit increases the risk of on-orbit collisions, especially for methods that increase the area-to-mass ratio of a debris object, such as drag augmentation devices. However, it is claimed that the drag augmentation device, GOLD "does not generate new debris objects" due to its thin-film envelope design (Nock et al., 2009). The thin-film envelope is a spherical structure made of gossamer that is designed to interact with a debris object by absorbing it, increasing its AMR and reducing its orbital lifetime. However, it is not clear how the structure would remain intact when it came into contact with the debris and this claim is yet to be tested in orbit.

A disadvantage of drag augmentation devices, electrodynamic tethers, and momentum exchange tethers is that they are vulnerable to debris impact. A 100 km long tether of 1 mm thickness has an area of 100 m^2, so a collision that

could cut the tether would be expected every few days (Eichler and Bade, 1993). The main risk to tethers is from small debris or meteoroid impact, although it is believed that the collision risk can be mitigated by increasing the width or using a double strand or braided tether design to increase robustness (Pardini et al., 2009). Kawamoto et al. (2006) examined the survival probability of three types of tether, 10 km in length, orbiting at 800 km (Figure 1.8). A net is expected to have an 80% chance of survival after one year in orbit. A braided tether has a better chance of survival (approximately 25% after one year) than a single tether which would not be expected to survive more than 100 days in orbit. Despite the risk of collision, tethers have shorter de-orbit times compared to drag augmentation methods (Pardini et al., 2009). Therefore, if a tether could be used to de-orbit a debris object within 100 days, it would be considered suitable as a ADR method.

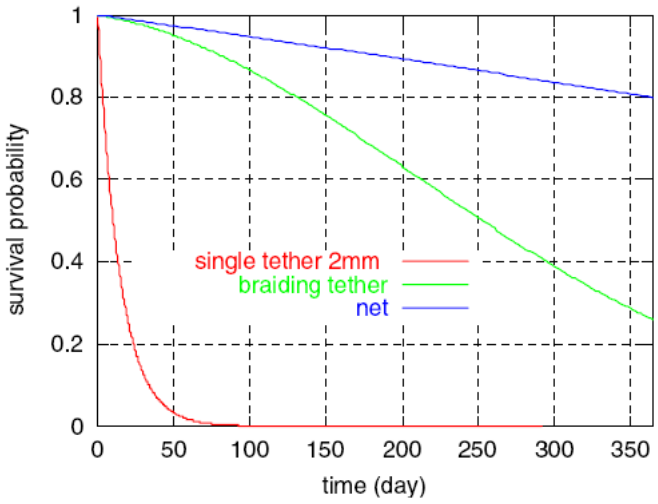

Figure 1.8: The survival probability of a single 2 mm tether, a net, and a braided tether (made of multiple strands of tether material) (Kawamoto et al., 2006).

The de-orbit of large debris objects also presents a challenge in terms of safety on the Earth's surface. An uncontrolled de-orbit manoeuvre would be acceptable for a debris object that was expected to break up in the atmosphere (objects with mass < 20 kg) (IAA, 2005). However, if the object was not expected to break up, contained hazardous materials, or posed a greater than 1 in 10,000 risk of causing casualties, then a controlled re-entry would be required

(NASA, 1995; IAA, 2005). This makes attached propulsion modules a strong candidate for ADR as they can provide a controlled re-entry.

1.2 Measuring effectiveness

Regardless of the technology chosen to implement ADR, the process will be considered successful if it leads to long-term stability of the debris environment (IAA, 2010). Therefore removal criteria are needed to target debris objects that will play a detrimental role in the future debris environment, with the aim of reducing the probability and severity of future collisions (Bastida-Virgili and Krag, 2009; Liou and Johnson, 2009). McKnight (2010) suggests that between ten and 50 objects will need to be removed during a period of 100 years to prevent one collision. The removal criteria need to be cost-effective as cost estimates (in US $ for FY2009) range from $1,000–$20,000 per object for small and medium-sized debris (Phipps and Campbell, 2009; McKnight, 2010) and $500,000–$100 million per object for large, intact debris objects (Wiedemann et al., 2004a; Wiedemann et al., 2004b; Helly, 2009; Nock et al., 2009; Bonnal and Bultel, 2009; Starke et al., 2009; McKnight, 2010). Bonnal and Bultel (2009)'s proposal of an Orbital Transfer Vehicle that delivers deorbiting kits to debris objects in LEO fits into this cost estimate; between $8 million and $27 million per debris object.

A large part of the total cost will come from the fuel required to reach the ΔV needed to access debris objects. For a satellite of dry mass 2,177 kg located at an altitude of 800 km transfer to an orbit with a lifespan of less than 25 years would signify a ΔV of 80 m/s. Assuming a specific impulse of 300 s, this would require 60 kg of fuel, while direct de-orbiting with atmospheric re-entry would mean a cost of 190 m/s (150 kg of fuel) (IAA, 2005). If fuel costs $10,000 per kg (Chapman, 2010), then the cost of fuel required for removal of one object at 800 km will be in the range of $0.6 million–$1.5 million. However, the total ΔV required to remove objects might be reduced if an ADR system was capable of multiple removals and could focus on clearing narrow inclination bands, thus requiring small plane changes (Carroll, 2009).

The measurement of how well a concept has performed and whether it has succeeded requires a clear objective with which to compare the outcome. For remediation of the space debris environment it is not enough to say the aim is to 'reduce the debris population'. Instead a clearer goal is needed, such as, 'to reduce the debris population $\geq$ 10 cm in size at 900 km altitude to 2009 levels by 2045, and then maintain a 0% growth rate'. When a clear goal has been established, there is a point of reference by which to measure the outcome of remediation.

The following measures are used in this thesis to assess the effectiveness of ADR in simulations of the future environment:

Liou and Johnson (2009) introduced an Effective Reduction Factor (ERF) to quantify the effectiveness of ADR scenarios in LEGEND simulations. The ERF is the ratio of the total number of objects reduced during the simulation to the number of objects removed via ADR during that time period (Liou and Johnson, 2009). A 'No ADR' modelling scenario is used a benchmark.

The Effective Reduction Factor is,

$$ERF(t) = \frac{N(t) - N_S(t)}{CN_R(t)}, \tag{1.2}$$

where $N(t)$ is the effective number of objects in a 'No ADR' scenario at time, t, $N_s(t)$ is the effective number of objects in the ADR scenario at time, t, and $CN_R(t)$ is the cumulative number of objects removed at time, t (Liou and Johnson, 2009). For example, if ERF = 15 this means that for every object removed from the simulation using ADR, the total population will be reduced in number by 15 at the end of the simulation period (Liou and Johnson, 2009). The higher the ERF value, the more effective the chosen ADR strategy is at identifying a set of objects that have the greatest potential of contributing to the growth of the future debris environment (Liou and Johnson, 2009).

However, not all objects will contribute equally to the growth of the future environment (Liou and Johnson, 2009; Lewis et al., 2009b). This can be illustrated using the above example of a situation in which the ERF value is 15.

In this case, if three objects were removed via ADR at the end of the simulation there would be 45 fewer objects in the environment. If 20 objects were removed via ADR there would be 300 fewer objects in the environment. As the removals will be based on removal criteria it may appear that removing the first three objects and reducing the population by 45 would be more cost-effective than removing 20 as the subsequent 17 objects would not be ranked as highly by the removal criteria. Lewis et al. (2009b) addressed this issue by introducing the Normalised Effective Reduction Factor (NERF),

$$NERF(t) = \frac{N(t) - N_S(t)}{N(t) - N_T(t)}, \tag{1.3}$$

where $N_T(t)$ is the number of target objects at time, t (Lewis et al., 2009b). As before, $N(t)$ is the effective number of objects in a 'No ADR' scenario at time, t, $N_s(t)$ is the effective number of objects in the ADR scenario at time, t, and $CN_R(t)$ is the cumulative number of objects removed at time, t (Liou and Johnson, 2009).

The NERF is the ratio of ERF for an ADR scenario to ERF calculated in a simulation in which no collisions are permitted, thus assuming that the removals in an ADR scenario result in no further collision activity (Lewis et al., 2009b). This method takes the goal of stabilising the environment into account (Lewis et al., 2009b).

1.3 Literature review

There have been a variety of proposals for determining removal criteria. In the 1980's and 1990's objects at an altitude of 1,000 km were at the greatest risk of collision and rocket bodies between 950–1,050 km made up 75% of on-orbit mass (Ash et al., 1993). Removal criteria were determined based on Kessler's collisional cascade predictions for objects between 700–1,500 km focussing on intact rocket bodies (Corporation, 1988; Ramohalli, 1989; Ash et al., 1993). Since 2009 several more detailed remediation strategies have been suggested:

A study by Alary (2010) suggested removing debris starting with the 'biggest' objects. It is assumed that 'big' objects are likely to be the most massive. Whilst the mass of an object affects the outcome of a collision, (the number of collision fragments that are generated), it does not directly affect the likelihood of a collision occurring. On its own, this is not a robust criterion for selecting ADR targets.

Talent (2009) develops a prioritisation list to remove objects that pose the greatest risk of being involved in future collisions. The removal criteria are based on differential collisional rate equations that are part of a particle-in-a-box (PIB) model (Talent, 2009). The PIB approach involves treating the LEO environment as a box with global average characteristics in which all objects can move about and all objects are described as one equivalent particle with characteristics defined by the total number of objects, total cross-sectional area, and total mass on orbit (Talent, 1990; Talent, 1992).

The Talent (2009) study suggests that removing two large, derelict objects per month would stabilise the environment. 24 rocket bodies with apogee 652–982 km, and perigee 628 –936 km are identified as the targets for the first year of removal (Talent, 2009). The result of removing 24 rocket bodies per year is shown in Figure 1.9.

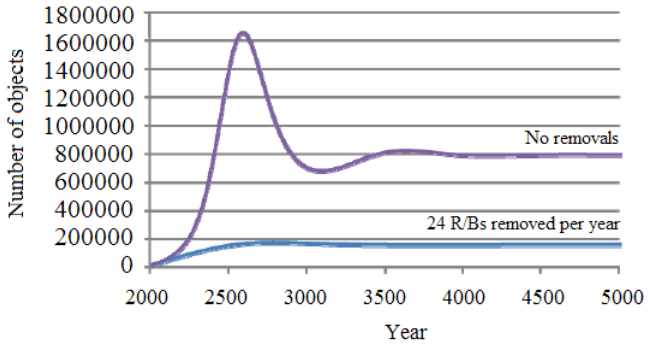

Figure 1.9: Comparing a non-remediation scenario to one in which 24 rocket bodies are removed per year (Talent, 2009).

Whilst the PIB model highlights the problem with not applying any remediation to the environment, rocket bodies are assumed to be the only candidates for removal and this assumption holds for 3,000 years. Although the

study ranks the rocket bodies for removal based on their relative threat to the environment, it assumes that there will be 72,000 rocket bodies to remove in this time period. This does not take into account the threat that other types of objects pose to the environment.

Unlike Talent (2009), Alfano et al. (2009) suggest prioritising objects for removal based on several parameters more closely related to individual objects in the near-term: the density of orbits, close approach statistics for individual objects, cumulative probabilities of collision, and estimated consequences of conjunctions. This approach acknowledges that several features need to be assessed to determine the 'most threatening' debris i.e. those objects most likely to be involved in collisions, creating further debris in the future (Alfano et al., 2009). For example, the study identifies 16 'bad actors' (objects that were involved in more than 2,000 conjunction events under 5 km) in conjunction assessments from August 2009. However, some of the close approach statistics are out of date (Alfano et al., 2009). This is problematic when considering the accuracy of the identification of the 16 'bad actors'. Solving this problem will involve collecting up-to-date information.

McKnight (2010) proposes targeting large, intact objects based on inclination. The study states that although all debris below 700 km is likely to re-enter within 25 years and 50% of debris up to 900 km is likely to re-enter within 25 years, a 'lethal' hazard exists at 850 km and annual collision probability between 600–1000 km is expected to double from 2009 levels by 2035 (McKnight, 2010). It is also noted that 10% of objects in LEO pose 80% of the total collision cross-section (McKnight, 2010). Therefore, removing this small portion of the objects would significantly reduce the overall risk of collision.

The advantage of focussing on narrow inclination bands is that there is the opportunity for multiple removals, reducing the ΔV and cost per object removed (Carroll, 2009). Upon reviewing the debris population in 2010, the 70.89–71.11° and 97.03–99.27° inclination bands were found to have the highest spatial densities in LEO (McKnight, 2010). However, these two narrow regions only contain 179 targets thus ignoring the other 1,171 objects that make up the 10% of objects providing 80% of the collision hazard as previously stated.

Kawamoto et al. (2009) and Kawamoto et al. (2010) propose the removal of 100–150 large, intact objects from regions of high spatial density identified by inclination and altitude. The regions the studies focus on are determined by simulations using the LEODEEM model (Kawamoto et al., 2006):

- 900–1,000 km, 82–83°,
- Sun-synchronous orbit, 98–100°,
- 1,500 km, 64–75°, 83° and 52°.

Figure 1.10 shows the growth suppression of the effective number of objects in LEO if ADR had begun in 2006 and 100 large, intact objects had been removed from 82–83°, 900–1,000 km (Kawamoto et al., 2006; Kawamoto et al., 2009).

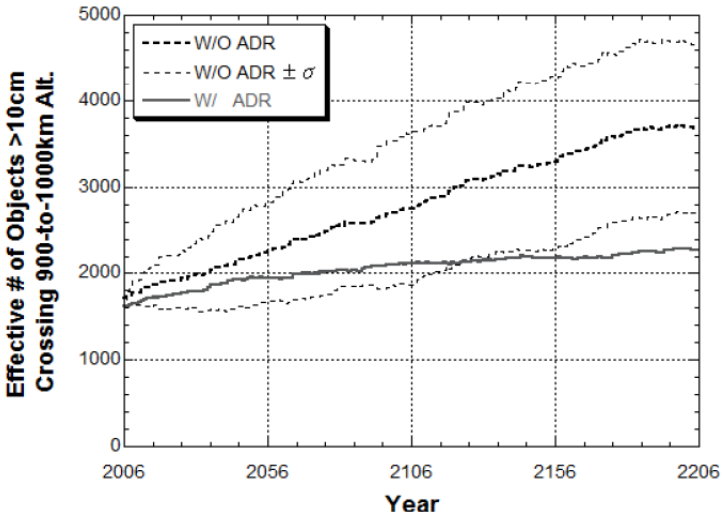

Figure 1.10: Results from ADR and non-ADR scenarios in a LEODEEM study (Kawamoto et al., 2006).

According to Figure 1.10, this method has the potential to significantly reduce the growth of the population at 900–1,000 km. However, the time-scale for the removal of 100 objects is not specified so it is not known how many objects would be targeted per year and if the objects are considered to be immediately removed from orbit or whether they are moved to lower altitudes to reduce their orbital lifetime. If the objects were moved to lower altitudes then, although the

number of objects between 900–1,000 km would be reduced, the numbers below 900 km would increase.

The approach taken by Bastida-Virgili and Krag (2009) involves targeting regions of space based on the spatial density of objects, focussing on specific types of objects found in those regions. The study only considers the removal of payloads and rocket bodies as they have larger cross-sections, known geometry, and higher mass compared to other debris objects (Bastida-Virgili and Krag, 2009). Large cross-sections and high mass indicate that the debris would have a significant impact on the environment in the event of a fragmentation event. Known geometry is important when considering the physical interface with a debris object.

The regions that the study identified for ADR were (Bastida-Virgili and Krag, 2009):

- 290 objects at 1000 km ± 100 km, 82±1°,
- 140 objects at 800 km ± 100 km, 99±1°,
- 40 objects at 850 km ± 100 km, 71±1°.

These regions were identified in a 200-year NFL study using DELTA, from which the number of catastrophic collisions vs. altitude vs. inclination was analysed (Bastida-Virgili and Krag, 2009). The study concluded that ADR of a few objects based on selected regions is more effective than ADR of many objects based on mass or area (Bastida-Virgili and Krag, 2009).

A problem with the Bastida-Virgili and Krag (2009) study is that the initial population that was used did not include the results of the major fragmentation events that have occurred since 2006 (Bastida-Virgili and Krag, 2009). Two other regions were identified as possibly being suitable for ADR (750 km ± 100 km, 86° ± 1° and 1400 km ± 100 km, 82° ± 1°), but they were not considered further. However, as noted in the paper, one of the two rejected regions has seen a catastrophic collision, thus an up-to-date initial population may have changed the conclusions of the study.

The first part of the study assumed that the objects selected for removal would be removed instantaneously at the start of a simulation year (Bastida-Virgili and Krag, 2009). In the second part of the study it was assumed that ADR missions would lower the orbit of the targeted debris so that they would re-enter within 25 years. No consideration was given for mission success rate in either part of the study.

The Liou and Johnson (2009) approach uses a ranking of

$$R_i = \text{collision probability} \times \text{mass of debris object}, \tag{1.4}$$

for each object based on the definition of risk,

$$risk = \text{likelihood of problem occurring} \times \text{outcome of the event}, \tag{1.5}$$

to determine removal criteria.

Liou and Johnson (2009) compared the effectiveness of three ADR strategies to a non-mitigation scenario over a simulation period of 200 years using LEGEND. The R_i values for all objects with a non-zero collision probability were calculated at the start of each simulation year and sorted in descending order (Liou and Johnson, 2009). In the three different ADR scenarios the top five, ten, or 20 highest ranked objects were removed before the simulation continued. Figure 1.11 shows the results of this study.

The effective number of objects is the total number of objects that spend all or part of their orbital period in LEO (Liou, 2006). A non-removal scenario predicts a fast non-linear growth of the future debris population, whereas the three ADR scenarios predict a slower growth of the population (Liou and Johnson, 2009). The study concluded that five objects need to be removed per year starting in 2020 to stabilise the environment (Liou and Johnson, 2009). However, the ranking approach means that objects that have the potential for many collisions may remain in the simulation if they are not ranked highly at the beginning of the simulation year. Consequently these objects may go on to cause a collision.

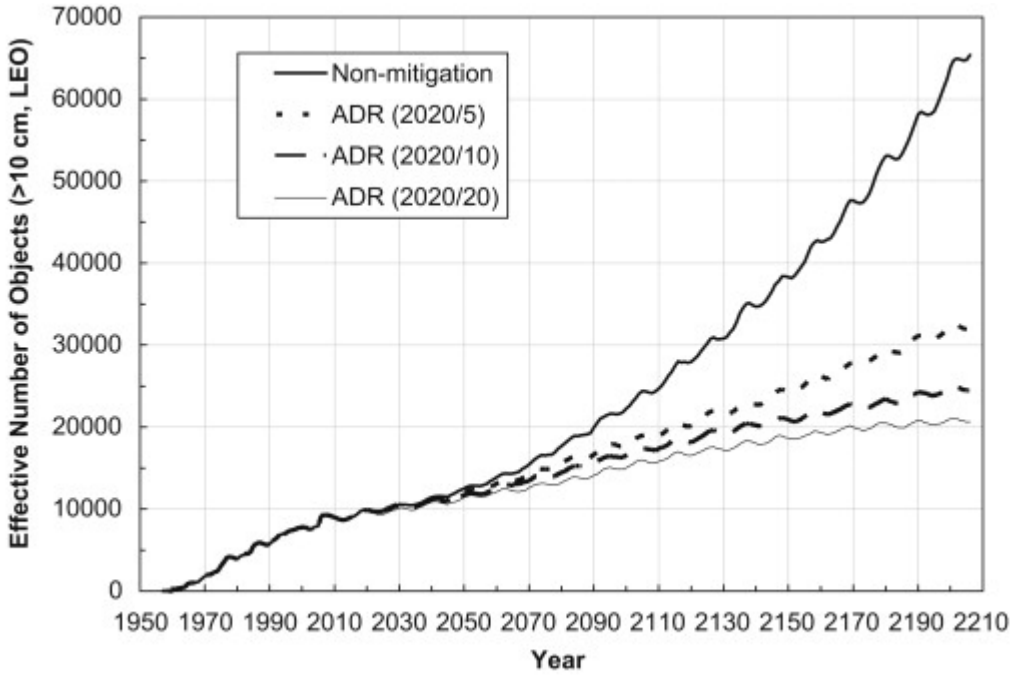

Figure 1.11: LEGEND ADR study in which five, ten and 20 objects are removed and compared to a non-mitigation scenario (Liou and Johnson, 2009).

Unlike the other studies discussed here, this study does not consider the cost of removal, for example, by targeting narrow inclination bands as mentioned in other studies. However, Liou (2009) acknowledges that alternative target selection criteria (size, altitude, inclination etc) may be more practical, although such criteria will need to be evaluated in simulations to investigate their cost-effectiveness. Indeed, in a follow-up study, Liou's results suggest targeting rocket bodies in the regions of 800 km and 1000 km (ODPO, 2011b).

1.4 Contributions and aims

The methods for developing targeted removal criteria in the reviewed literature do not take into account either the consequences of individual events or include enough detail about the debris objects to accurately determine if they should, or can, be removed. Using network theory is designed to address both of these problems; on networks, debris-creating events or conjunctions are not viewed in

isolation and the characteristics of the events and the objects can be built into the network theory measures.

The idea for using of network theory developed out of research into complexity science. Many complexity science publications use network theory to analyse datasets, from airline routes to neurological pathways and social groups (Achacoso and Yawamoto, 1992; Newman and Park, 2003; Bagler, 2009). Data from conjunction assessments and future modelling studies is ideally represented as a network because the space debris environment is a system composed of many objects that can interact with one another. Using this novel approach meant that the first two aims of the research were to use networks to represent various aspects of the space debris environment and to analyse these 'space debris networks' to determine their characteristics. In order to follow on from research in the literature and address the problems posed by ADR, the final aim is to assess the use of network theory for determining ADR target criteria.

Networks are maps of interactions (Rosvall, 2006). Network theory is an area of study developed from systems theory to quantitatively measure the general properties of a network and the individual properties of the components of a network. Chapter 2 introduces network theory and looks at various types of networks and their characteristic features. The concepts of *complexity* and *robustness* are also introduced.

Chapter 3 introduces 'space debris networks' based on DAMAGE modelling studies and SOCRATES conjunction assessments. The processes for obtaining data from DAMAGE and SOCRATES are discussed alongside the reliability of each method. DAMAGE and SOCRATES space debris networks are presented separately to assess their general characteristics in relation to the need for ADR.

The case studies in Chapter 4 apply network theory to DAMAGE and SOCRATES datasets to address the issue of determining ADR criteria. In the first case study the use of *weighted* measures are assessed. In the second case study the use of *centrality* measures are addressed.

Chapter 5 discusses the findings of the thesis in relation to the original aims.

Other issues such as political, financial, and technological difficulties that relate to ADR are also discussed. The conclusions about the success of using networks to represent and analyse the space debris environment, and for determining target criteria for ADR are discussed in Chapter 6. In addition, the potential for future work will be presented.

Chapter 2

NETWORK THEORY

2.1 Network types

The individual elements of a network are called *vertices* and the interactions between them are called *edges*. In space debris networks a vertex represents an orbiting object and an edge represents a conjunction event between the objects (Lewis et al., 2010). Two vertices that are joined by an edge are called *neighbours*.

The most basic measures of a network are the *order* and the *size*. The number of vertices is the *order*, n, of the network, and the number of edges is the *size*, m. A network of order, n cannot have a size, m, greater than $\frac{n(n-1)}{2}$ if the vertices within the network only have one edge connecting to each of their neighbours (Calderelli and Vespignani, 2007). However, if *multi-edges* are permitted, then the size and order of the network are not constrained. A multi-edge is defined as a collection of two or more edges connecting the same two vertices on a network. A network with multi-edges is called a *multigraph* (Figure 2.1).

A network is represented mathematically using an adjacency matrix,

$$A = \begin{pmatrix} a_{ij} & \dots & a_{in} \\ \vdots & \ddots & \vdots \\ a_{nj} & \dots & a_{nn} \end{pmatrix}. \tag{2.1}$$

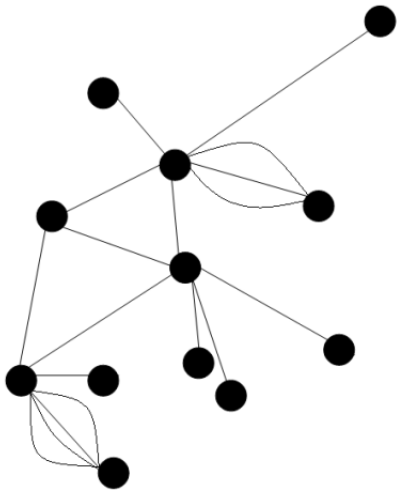

Figure 2.1: A multigraph with multi-edges.

If there is an edge between vertex i and vertex j then $a_{ij} > 0$. If there is no edge between vertex i and j then $a_{ij} = 0$. If the majority of values in an adjacency matrix are 0 then it can be called a *sparse matrix*. For computational purposes, if a network is represented by a sparse matrix, then it is more efficient to store the data in an incidence table which requires $O(|m|)$ space compared to an adjacency matrix which requires $O(|n^2|)$ (Gross and Yellen, 2005). An incidence table is also suitable for storing multigraph data (Weiss, 1997).

Networks and their corresponding adjacency matrices vary according to the type of vertices and edges that are found on the network. In the simplest case A is a $n \times n$, symmetric matrix (Newman, 2008). A symmetric adjacency matrix represents an *undirected network* (Figure 2.2 a, b, d) (Eq.2.2). In a *directed network*, such as one representing email correspondence within a group of people, edges connect vertices according to the direction of flow, as shown in Figure 2.2 c. The adjacency matrix is asymmetric as a result (Eq.2.3).

An *unweighted* network has a binary adjacency matrix, where $a_{ij} = 1$ or 0 (Eq.2.4) (Figure 2.2 a, b, c). However, the edges in *weighted networks* have weights associated with them that describe their value relative to one another (Eq.2.5) (Figure 2.2 d) (Newman, 2004). In a weighted network, vertex measures are calculated using edge weights.

$$A_{\text{undirected}} = \begin{pmatrix} 0 & 0 & 0 & 0 & 1 & 0 & 0 & 0 \\ 0 & 0 & 1 & 0 & 1 & 0 & 0 & 0 \\ 0 & 1 & 0 & 0 & 1 & 0 & 0 & 0 \\ 0 & 0 & 0 & 0 & 1 & 0 & 1 & 0 \\ 1 & 1 & 1 & 1 & 0 & 1 & 1 & 0 \\ 0 & 0 & 0 & 0 & 1 & 0 & 0 & 0 \\ 0 & 0 & 0 & 1 & 1 & 0 & 0 & 1 \\ 0 & 0 & 0 & 0 & 0 & 0 & 1 & 0 \end{pmatrix}. \tag{2.2}$$

$$A_{\text{directed}} = \begin{pmatrix} 0 & 0 & 0 & 0 & 1 & 0 & 0 & 0 \\ 0 & 0 & 1 & 0 & 0 & 0 & 0 & 0 \\ 0 & 0 & 0 & 0 & 1 & 0 & 0 & 0 \\ 0 & 0 & 0 & 0 & 1 & 0 & 1 & 0 \\ 1 & 1 & 1 & 0 & 0 & 0 & 0 & 0 \\ 0 & 0 & 0 & 0 & 1 & 0 & 0 & 0 \\ 0 & 0 & 0 & 1 & 1 & 0 & 0 & 1 \\ 0 & 0 & 0 & 0 & 0 & 0 & 0 & 0 \end{pmatrix}. \tag{2.3}$$

$$A_{\text{unweighted}} = \begin{pmatrix} 0 & 0 & 0 & 0 & 1 & 0 & 0 & 0 \\ 0 & 0 & 1 & 0 & 1 & 0 & 0 & 0 \\ 0 & 1 & 0 & 0 & 1 & 0 & 0 & 0 \\ 0 & 0 & 0 & 0 & 1 & 0 & 1 & 0 \\ 1 & 1 & 1 & 1 & 0 & 1 & 1 & 0 \\ 0 & 0 & 0 & 0 & 1 & 0 & 0 & 0 \\ 0 & 0 & 0 & 1 & 1 & 0 & 0 & 1 \\ 0 & 0 & 0 & 0 & 0 & 0 & 1 & 0 \end{pmatrix}. \tag{2.4}$$

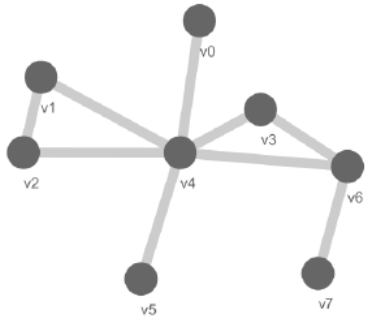

(a) Uni-relational

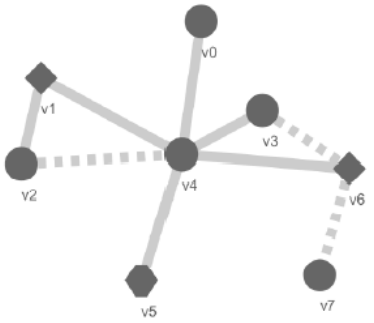

(b) Multi-relational

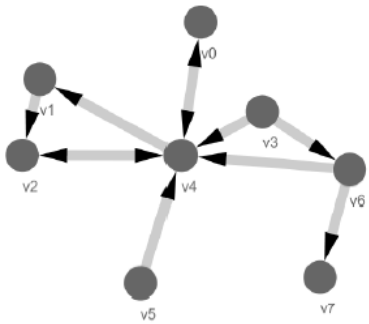

(c) Directed

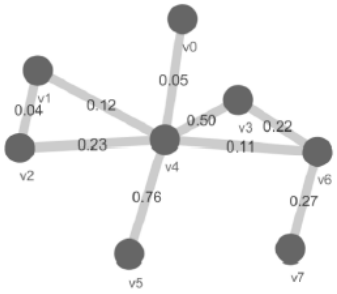

(d) Weighted

Figure 2.2: Network types.

$$A_{\text{weighted}} = \begin{pmatrix} 0 & 0 & 0 & 0 & 0.05 & 0 & 0 & 0 \\ 0 & 0 & 0.04 & 0 & 0.12 & 0 & 0 & 0 \\ 0 & 0.04 & 0 & 0 & 0.23 & 0 & 0 & 0 \\ 0 & 0 & 0 & 0 & 0.50 & 0 & 0.22 & 0 \\ 0.05 & 0.12 & 0.23 & 0.50 & 0 & 0.76 & 0.11 & 0 \\ 0 & 0 & 0 & 0 & 0.76 & 0 & 0 & 0 \\ 0 & 0 & 0 & 0.22 & 0.11 & 0 & 0 & 0.27 \\ 0 & 0 & 0 & 0 & 0 & 0 & 0.27 & 0 \end{pmatrix}. \quad (2.5)$$

A *uni-relational network* has only one type of vertex and one type of edge, which represent all of the vertices and edges homogeneously (Figure 2.2 a,c,d). *Multi-relational networks* contain more than one type of vertex and/or more than one type of edge (Figure 2.2 b). Unless the edges in a uni-relational or multi-relational network are weighted, the adjacency matrices of both types are binary (Eq.2.4).

The mathematical analysis of network and vertex measures provides an insight into how the network and the system it represents is structured. *Vertex measures* are calculated using the elements of the adjacency matrix and they can be used to investigate the roles that individual parts play in a network as a whole. Vertex measures can be averaged over the whole network to give *network measures* that are used to analyse the global topology of the network. Various vertex and network measures for both unweighted and weighted networks are detailed in the following sections.

With the exception of Section 3.1.3 (in which measures were calculated within DAMAGE), in this thesis, network and vertex measures are calculated using stand-alone code written in C++. The original code (written by the author, under guidance) was a basic version written in C (Appendix A). This version was upgraded by Dr F M Bélanger to provide a faster, more efficient data analysis package. For a dataset containing approximately 8,400 vertices and 15,200 edges, it takes $\approx$ 24 hours to calculate all of the network and vertex

measures detailed in Section 2.2.

A freely available software tool, 'Cytoscape' is used to display the networks in this thesis. Cytoscape is open-source software designed to represent and analyse molecular interaction networks (Shannon et al., 2003; Cline et al., 2007). This software is used because it is easy to import data, it has a clear user interface in which to manipulate the networks, and it is easy to export data for network analysis. There are various options available for the layout of the network; these are based on algorithms that optimise the visualisation. It is difficult to understand the topology of large networks based solely on these visualisations, but Cytoscape provides the option of manipulating the view so that specific vertices and edges can be isolated. Figure 2.3 shows a close-up view of vertices and edges on a weighted space debris network drawn in Cytoscape.

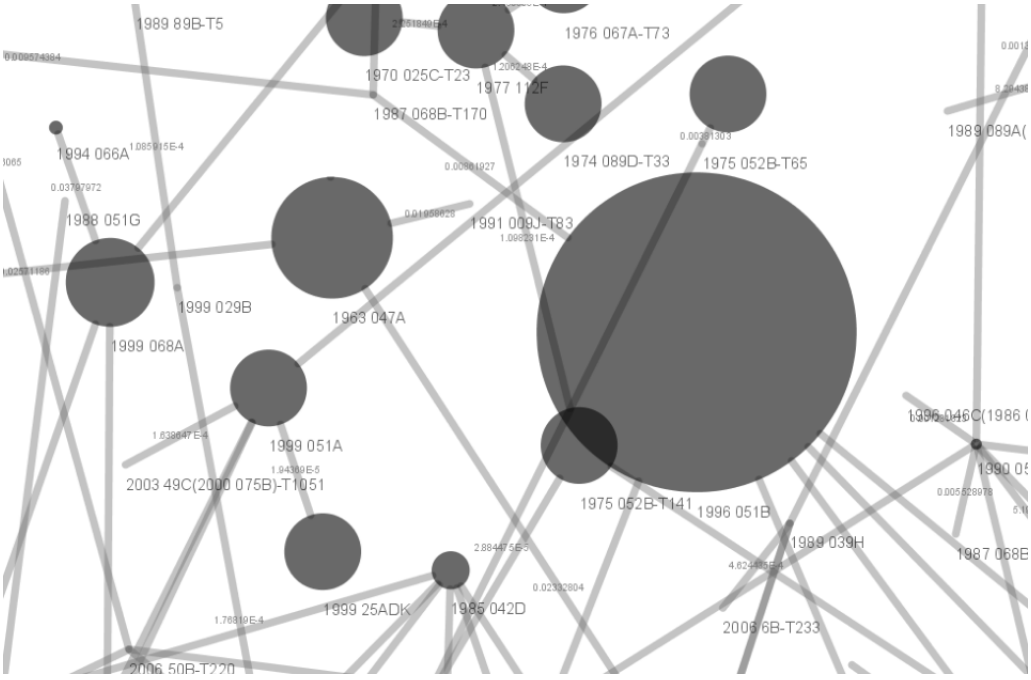

Figure 2.3: Vertices and edges on a weighted space debris network. The vertices represent debris objects that are identified by their International Designator.

2.2 Network and vertex measures

2.2.1 Degree centrality

Centrality measures are used to identify vertices that are 'important' to the structure of a network (Barthelémy, 2004; Borgatti, 2005; Hwang et al., 2006). The degree centrality (referred to as *degree*), k_i describes the connectivity of a vertex. The degree is calculated using adjacency matrix elements,

$$k_i = \sum_{j}^{n} a_{ij}. \tag{2.6}$$

The network degree, $\bar{K}$, is the average value of k_i,

$$\bar{K} = \langle k_i \rangle = \frac{1}{n} \sum_{i}^{n} k_i. \tag{2.7}$$

For a weighted network, the equivalent measure of degree is strength,s_i,

$$s_i = \sum_{j}^{n} a_{ij} w_{ij}, \tag{2.8}$$

where w_{ij} is the weight on the edge between vertices i and j.

The degree of a vertex on a space debris network represents the number of conjunctions involving an orbiting object (Lewis et al., 2010). In space debris networks edges are weighted in terms of the probability of a conjunction occurring (Lewis et al., 2010). Therefore, strength signifies the importance of a vertex on the network in terms of the number of conjunctions, weighted by the probability of those conjunctions occurring. An object represented by a vertex with many edges representing conjunctions that all have a low probability will be less 'important' than a vertex representing an object involved in a few high probability conjunctions.

A topological characterisation of a network can be obtained in terms of the degree distribution, $P(k)$, defined as the probability that a vertex has degree, k

(Boccaletti et al., 2006). *Random networks* have a binomial degree distribution; in these networks the average vertex represents the most probable degree value on the network (Calderelli and Vespignani, 2007) (Figure 2.4 a) . Figure 2.4 b shows a random network, a simplified version of the US road network, in which most vertices share a similar degree and there are no vertices with a degree significantly higher than any other (Barabàsi, 2007).

Networks with a power-law distribution (Figure 2.4 c) have many vertices with low degree, and a few vertices with high degree. This means that the average degree does not represent a 'typical' vertex (Calderelli and Vespignani, 2007). The vertices with a high degree compared to other vertices in the network act as *hubs* (Albert and Barabàsi, 2002; Barabàsi and Bonabeau, 2003).

Figure 2.4 d shows a simplified version of a network of airline routes between US cities which has a power-law distribution. There are a few major airports (the hubs) that are served by a large number of airlines flying to many smaller airports that are served by fewer individual flights (Figure 2.4 d).

The degree distribution, $P(k)$, in Figure 2.4 b follows a power law such that,

$$P(k) \sim k^{-\gamma}, \tag{2.9}$$

where γ is a constant exponent i.e. the probability that a vertex has degree, k decays as a power law (Barabàsi et al., 2001). If the degree exponent lies between 2 and 3 then the networks are called 'scale-free' (Faloutsos et al., 1999; Barabàsi et al., 2001; Albert and Barabàsi, 2002; Dorogovtsev and Mendes, 2002). Some authors argue that because many networks appear to be 'scale-free' then there is a 'universal architecture' that can be found in all networks with a power-law degree distribution (Barabàsi and Albert, 1999; Goh et al., 2001). However, this is disputed by other authors (Comellas and Miralles, 2009). Fox-Keller (2005) argues that degree distribution is dependent on a network's specific constraints, such as its size and order. Furthermore, Li et al. (2005) believe that the literature on scale-free networks is sensationalised and does not present rigorous proof of the properties of scale-free networks. Determining whether or not all networks with a power-law degree distribution

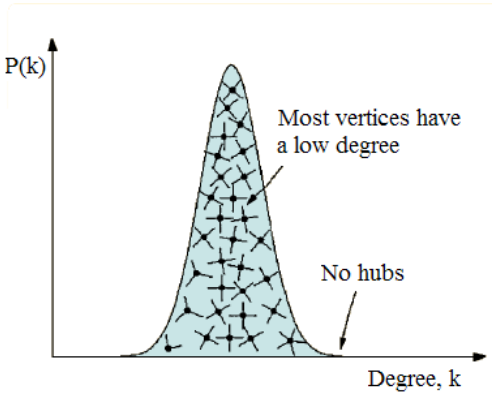

(a) Binomial degree distribution.

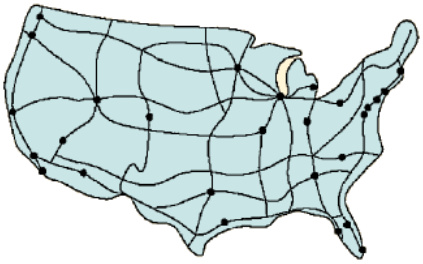

(b) US road network

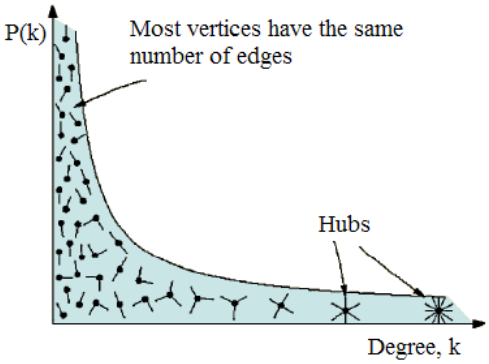

(c) Power law degree distribution.

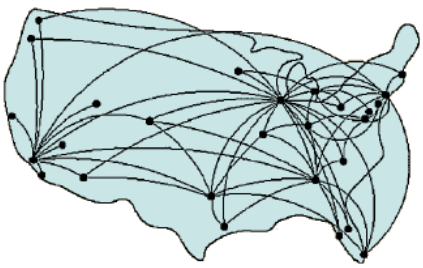

(d) US airline network

Figure 2.4: Network types.

are 'scale-free' is outside the scope of this thesis. However, the degree distribution can still be used to characterise space debris networks. In addition, another network measure can be used to determine whether or not a network contains hubs: assortativity.

2.2.2 Assortativity

Network *assortativity*, R, measures the correlation between the degrees of vertices,

$$R = \sum_{e=1}^{m} \frac{\left(\left(\frac{j_e k_e}{m}\right) - \left(\frac{j_e + k_e}{m}\right)^2\right)}{\left(\left(\frac{j_e^2 k_e^2}{m}\right) - \left(\frac{j_e + k_e}{m}\right)^2\right)}, \tag{2.10}$$

where j_e and k_e are the degrees of two vertices at the end of edge e (Newman, 2002a). Assortativity values can be positive or negative, corresponding to *assortative* or *disassortative* networks respectively. Networks with a binomial degree distribution are assortative and networks with a power-law degree distribution are disassortative. The vertices in an assortative network are likely to be connected to vertices with a similar degree, whereas the vertices in a disassortative network are likely to connect with vertices that have different degrees, thus forming hubs.

Many real-world networks suffer the loss of vertices, either through accidental failure or in deliberate attacks. Deliberate attacks can remove vertices randomly or in a targeted manner. Networks can be managed via the protection of hubs or to enhance the deliberate destruction of the network (Albert et al., 2000; Holme et al., 2002; Motter and Lai, 2002; Shargel et al., 2003; Dybiec et al., 2004; Chassin and Posse, 2005; Gallos et al., 2005; Mitra et al., 2007; Moreira et al., 2009; Carvahlo et al., 2009). Vertices chosen at random in a disassortative network are likely to have a low degree and not be central to the network topology. Whilst these networks are resilient to random removal, they are extremely vulnerable to targeted attacks, i.e. to the selection and removal of the hubs (Albert et al., 2000; Barabàsi and

Bonabeau, 2003; Jing et al., 2007).

Real-world networks fit into one of two categories: those that need protecting from loss in order to maintain connectivity, for example;

- power supply (Carreras et al., 2001; Crucitti et al., 2004; Albert et al., 2004; Chassin and Posse, 2005; Carvahlo et al., 2009; Wang and Rong, 2009),
- communication (Cohen et al., 2000; Latora and Marchiori, 2005; Mitra et al., 2007; Rosato et al., 2007; Hidalgo and Rodriguez-Sickert, 2008a; Hidalgo and Rodriguez-Sickert, 2008b; Schneider et al., 2009), and
- air transportation (Scott et al., 2005; Latora and Marchiori, 2005; Bagler, 2009),

and those that are seen as undesirable and that need attacking to reduce connectivity, for example;

- disease epidemics (Pastor-Satorras et al., 2001; Liljeros et al., 2001; Dybiec et al., 2004; Christley et al., 2005; Reis et al., 2007; Hidalgo, 2008), or
- terrorist associations (Carpenter and Stajkovic, 2006; Carley, 2009).

In the first category, hubs need to be protected in order to minimise loss of connectivity to a whole network. This can be clearly illustrated by imagining the disruption caused to global travel if a major hub airport such as London Heathrow or Chicago O'Hare were closed due to increment weather or a terror threat directed specifically at one of the airports. Space debris is problematic and therefore fits into the second category. On a space debris network assortativity measures the correlation between the number of conjunctions involving debris objects and those with which they interact (Lewis et al., 2010). If it is found that space debris networks are disassortative and hubs are present, it would indicate that there is at least one way of determining removal criteria with network theory.

Figure 2.5 highlights the differences between accidental failures and attacks on assortative and disassortative networks. Accidental, random failure on an assortative network can break down the network (Figure 2.5a). In contrast, disassortative networks are more robust when faced with accidental, random failure as the overall connectivity is higher in the resulting network than in the assortative network when the same vertices are removed (Barabàsi and Bonabeau, 2003) (Figure 2.5b). However, Figure 2.5c illustrates the vulnerability of disassortative networks to targeted attacks. When the hubs of the network are removed, the connectivity is severely reduced. In this example, removing a smaller number of vertices in a targeted attack was more effective at reducing the connectivity of the network than losing a larger number of vertices due to random removal.

2.2.3 Closeness centrality

Another measure of centrality is the *closeness* of a vertex in a network. Closeness is calculated as the mean shortest-path distance from i to all other vertices in the network,

$$D_i = \frac{1}{n-1} \sum_{j}^{n} d_{ij}, \tag{2.11}$$

where d_{ij} is the shortest-path distance between vertices i and j.

The closeness statistic for the network is,

$$\bar{D} = \langle D_i \rangle = \frac{1}{n} \sum_{i}^{n} D_i. \tag{2.12}$$

The smaller the closeness centrality of a vertex is, the shorter the average distance from one vertex to any other (Borgatti, 2005). Low values of closeness for objects on a space debris network would indicate an unstable environment in which a conjunction could affect many other objects (Lewis et al., 2010).

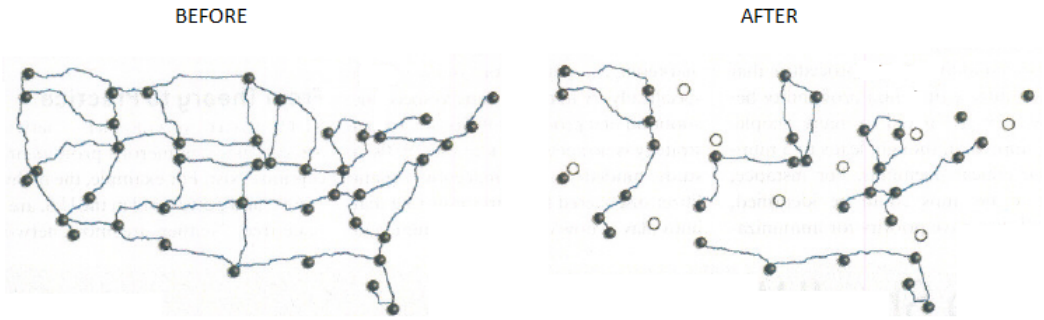

(a) Assortative network, accidental failure.

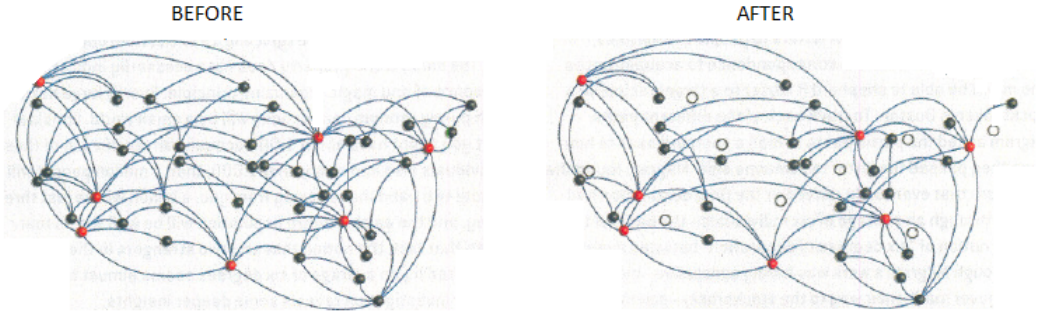

(b) Disassortative network, accidental failure

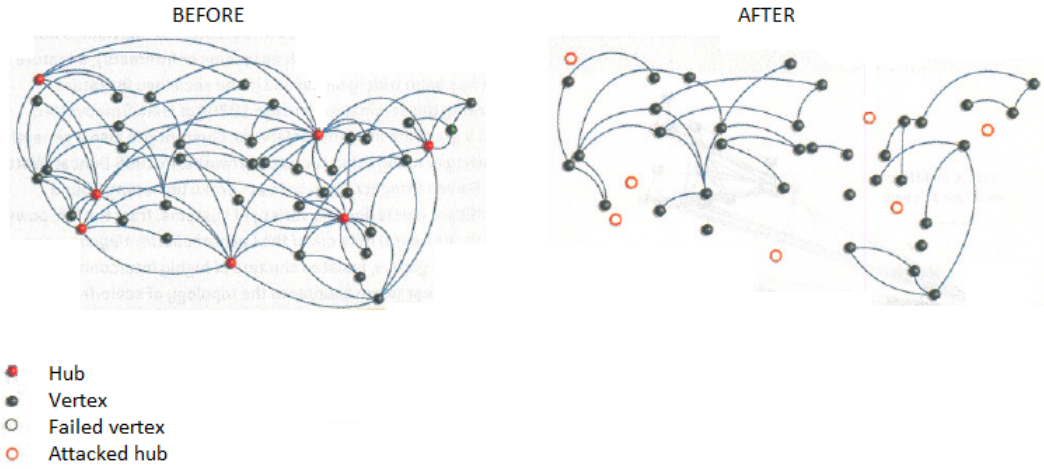

(c) Disassortative network, deliberate attack.

Figure 2.5: Comparing accidental failure and deliberate attack on assortative and disassortative networks (Barabàsi and Bonabeau, 2003).

2.2.4 Betweenness centrality

Measuring the importance of vertices to the structure of a network using degree centrallity overlooks vertices with low degree that may be crucial for connecting different regions of a network (Barthelémy, 2004). On a space debris network, *betweenness centrality* measures the role played by a debris object in a series of conjunction events (Lewis et al., 2010). A series of conjunction events would be represented by chains of vertices in the networks.

Betweenness centrality assumes that the flow between vertices is indivisible and a vertex is central to the extent that it falls on the shortest path between pairs of other vertices (Freeman, 1977). This centrality measure systematically takes into account flow moving from each vertex to every other vertex on the network (Borgatti, 2005).

Betweenness centrality is calculated in two phases and will be demonstrated here using an example network (Figure 2.6). The first phase computes distances and shortest path counts using a breadth-first search; the second phase visits all vertices to accumulate values for individual vertex betweenness (Freeman, 1977; Lewis et al., 2010).

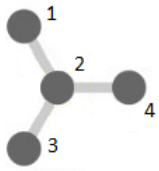

Figure 2.6: An example network of four vertices and three edges.

First phase

A breadth-first search algorithm is used to navigate a network from one vertex to another. The process involves calculating distances between all possible pairs of vertices on a network . This is accomplished one pair at a time, where one vertex acts as the starting point for the search, the *parent* vertex and, another vertex is the end point, the *source* vertex (Figure 2.7). The network *geodesic* is the average of the shortest-path distance between each pair of vertices. When visiting a new vertex, a breadth-first search stores adjacent vertices not yet visited in a queue, thus exploring the neighbours before the search for the source vertex continues (Donato et al., 2007).

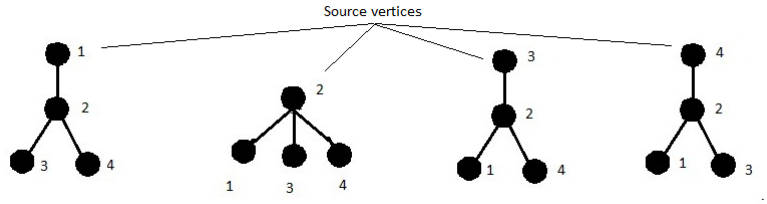

Figure 2.7: The example network has four vertices so there are four possible combinations for the breadth first search; in each variation there is a different source vertex.

The shortest-path distances between each pair of vertices are as follows:

$v_1 \rightarrow v_2$ shortest-path distance = 1
$v_1 \rightarrow v_3$ shortest-path distance = 2
$v_1 \rightarrow v_4$ shortest-path distance = 2
$v_2 \rightarrow v_3$ shortest-path distance = 1
$v_2 \rightarrow v_4$ shortest-path distance = 1
$v_3 \rightarrow v_4$ shortest-path distance = 2

Second phase

The accumulation process is completed using the following steps (Newman, 2001; Zhou et al., 2005; Lewis et al., 2010):

1. A variable b_i^s, taking the initial value 1, is assigned to each vertex, i.

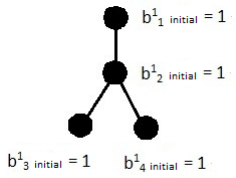

Figure 2.8: Using vertex, v_1 as the source, assign the initial value of 1 to each vertex.

2. Go through the vertices, i in order of their distance from the source vertex, s, starting from the furthest. The value of b_i^s is added to the corresponding variable on the parent vertex of i, i.e. the vertex connected to i and closer to vertex s. If i has more than one parent, b_i^s is divided equally between them.

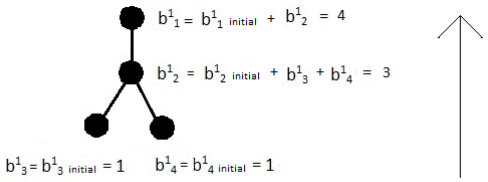

Figure 2.9: Start from vertices v_3 and v_4 and add the initial values of b_i^s towards v_1.

3. Go through all vertices in this fashion and record the value b_i^s for each vertex i. Repeat the entire calculation for every source vertex s.

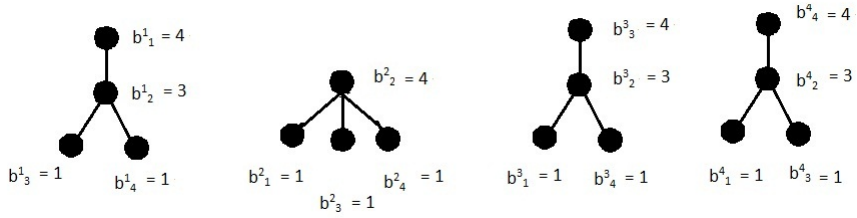

Figure 2.10: Stages 1 and 2 are repeated using each of the four vertices as the source vertex.

The betweenness for each vertex i is then obtained as,

$$B_i = \sum_{s}^{n} b_i^s. \tag{2.13}$$

Network betweenness is then calculated as,

$$\bar{B} = \langle B_i \rangle = \frac{1}{n} \sum_{i}^{n} B_i. \tag{2.14}$$

For the example network this is:

$B_1 = b_1^1 + b_2^1 + b_3^1 + b_4^1 = 4 + 1 + 1 + 1 = 7$
$B_2 = b_1^2 + b_2^2 + b_3^2 + b_4^2 = 3 + 4 + 3 + 3 = 13$
$B_3 = b_1^3 + b_2^3 + b_3^3 + b_4^3 = 1 + 1 + 4 + 1 = 7$
$B_4 = b_1^4 + b_2^4 + b_3^4 + b_4^4 = 1 + 1 + 1 + 4 = 7$

$\bar{B} = B_1 + B_2 + B_3 + B_4 = 34$

2.2.5 Clustering

Clustering measures the tendency for cliques (clusters of vertices) to form in the neighbourhood of a given vertex such that if vertex i is connected to vertex j, and vertex j is connected to vertex k, it is likely that i is also connected to k (Calderelli and Vespignani, 2007). The clustering coefficient, c_i, is

$$c_i = \frac{2}{k_i(k_i - 1)} \sum_{j \neq k}^{n} \sum_{k}^{n} a_{ij} a_{ik} a_{jk}. \tag{2.15}$$

The clustering coefficient of the network is the average of c_i over all vertices,

$$\bar{C} = \langle c_i \rangle = \frac{1}{n} \sum_{i}^{n} c_i. \tag{2.16}$$

On a space debris network clustering measures the likelihood that an orbiting

object is part of a triangular cluster (Lewis et al., 2010). If the clustering coefficient of space debris networks is high, this would suggest that most objects would not be involved in a series of conjunction events as the vertices would not form chains.

2.2.6 Complexity

Complexity science is the study of systems made of a large number of parts that interact in such a way that the system's overall behaviour cannot be simply described by the behaviour of the individual parts. Complex systems lend themselves to being represented as networks because the parts and interactions between the parts can be modelled as vertices and edges. Network theory can be used to define statistical properties that characterise the structure and behaviour of complex systems, illustrate how the parts of complex systems interact with one another using network models, and to predict the behaviour of complex networks based on network and vertex measures (Newman, 2002b).

Identifying whether or not a system is complex is subject to much debate in the literature and even specialist texts do not attempt to define "complex" (Bar-Yam, 1997). However, Calderelli and Vespignani (2007) argue that a system may be considered complex if it:

1. displays variety that is only limited by the size of the system i.e. the network degree exponent $2 < \gamma < 3$,

   It was stated in Section 2.2.1 that if a network's degree distribution has a degree exponent $2 < \gamma < 3$ then it is called a scale-free network. This is a quantifiable measure that can be used to assess the system in question. However, in practice only an estimate of γ can be calculated (Clauset et al., 2009).

2. exhibits *emergence*.

   Emergence is defined as the unpredictable appearance of novel properties during interactions between parts of a system (Goldstein, 1999).

> Emergence is often linked to the action of *self-organisation* by which a system evolves from a disorganised, unstable state to one with a structure and stability (Prigogine and Stengers, 1984; Collier and Burch, 1998).

Two systems that exhibit scale-free power law size distributions and self-organising properties are the asteroid belt and particles in Saturn's rings. The asteroid belt is found between the orbits of Mars and Jupiter (Gradie and Tedesco, 1982). Formation of the asteroid belt is part of the self-organisation process that formed the solar system (Collier, 2004). The asteroids in the belt are a variety of sizes. The size distribution of the small asteroids (0.4–5.0 km diameter) is scale-free with a power law exponent, $\gamma = 2.3$ (Ivezic et al., 2001; Gladman et al., 2009). The particles of size 1–10 cm that form Saturn's rings also have a scale-free size distribution with a power law exponent, $\gamma \approx 3$ (Zebker et al., 1985; Brilliantov et al., 2009). This system also exhibits evidence of self-organisation (Shepelyansky et al., 2009; Brilliantov et al., 2009).

The space debris environment will be examined to determine if it has a scale-free degree distribution and is self-organised. If it is found to have these properties they will indicate that the environment is complex. Scale-free properties link back to the concept of hubs that could be targeted for ADR. ADR would also interrupt the process of self-organisation, but would not stop it if collisional cascading was not prevented.

2.2.7 Network robustness

Vertex and network measures can be used to understand how a network behaves in response to the addition or removal of vertices or edges. As assortativity and centrality measures are a useful way of identifying vertices that are important to a network's structure they can be used to identify susceptible vertices that could be targeted for removal (Bonacich, 1987). Weighted networks are especially vulnerable to centrality driven attacks (DallAsta et al., 2006).

Robustness defines the ability of a network to remain complete when vertices are removed (Schneider et al., 2009). Three measures of robustness are: *breakdown*

of the giant component, *connectivity*, and *change in network diameter*.

A *component* of a network contains vertices that are connected to each other. The component of a network containing more than half of all of the connected vertices is called the *giant component* (Janson et al., 1993; Molloy and Reed, 1998). Removing a portion, p of vertices can act to reduce the robustness of the giant component. A critical portion, pc exists and when $p > pc$ the network disintegrates into smaller components that no longer connect with other parts of the network, thus reducing its robustness (Newman, 2002b; Wang and Chen, 2003). When this happens the network is described as 'failed' (Cohen et al., 2000). The value of pc provides a measure of the network's robustness. Cohen et al. (2000) found that the Internet, a disassortative network, is extremely robust to random removals as $pc > 0.99$. This indicates that the Internet is resilient to random failure of its vertices, and it would remain essentially connected even if 99% of its vertices were removed in a targeted attack (Cohen et al., 2000).

Connectivity is measured using the beta index,

$$\beta = \frac{m}{n}, \tag{2.17}$$

the ratio of the size of the network to the order of the network (Dekker and Colbert, 2004). A network with a high number of edges compared to the number of vertices is highly connected, and therefore robust. Removing vertices from a network also removes edges and so, to most effectively reduce the connectivity and robustness of a network, the vertices with high degree should be removed. However, as noted in the network measures section above, the degree centrality is not the only measure of 'importance' of a vertex. Removing other central vertices will also impact on the overall connectivity of the network.

A network is described as robust if its *diameter* is small and simple measure of a network's response to failure or attack is a change in its diameter (Shargel et al., 2003). The diameter is the maximum shortest-path length, $d_{ij(max)}$ between pairs of vertices; when the diameter is small, the removal of a few vertices will not affect the connectivity of the network because the remaining

vertices will stay connected along other chains. A small diameter is undesirable for the space debris environment, as it would indicate that there were many chains along which series of conjunction events could occur. Effective ADR would act to increase the diameter, making the network less robust.

The nature of the instability of the space debris environment means that the debris population will increase due to collisions. An increase in the number of predicted collisions or reported conjunctions would result in an increase of network connectivity; this would mean a decrease in the diameter and an increase in the size of the critical portion. All of these indicate that the instability of the space debris environment will result in robust space debris networks. In addition, the process of collisional cascading may be represented by chains within the network indicating the potential for a series of conjunction events to occur.

Chapter 3

SPACE DEBRIS NETWORKS

3.1 DAMAGE networks

3.1.1 Modelling process

DAMAGE is capable of modelling historical and future populations from LEO to GEO. The model was designed using an object-oriented framework and consists of a computational model of the environment ('Environment') and several support models to evolve the environment (Lewis et al., 2001). The support models are: 'Atmosphere', 'Break-up', 'Collision', 'Launch', 'Propagator', 'Event Manager', and 'Mitigation' (including ADR).

Environment: The computational model of the environment contains information on the initial reference population of orbiting objects ≥ 10 cm (Lewis et al., 2001). This information includes: the launch date of the object, its International Designator, orbital elements, mass, and diameter. Within this model the user can set the length of the simulation and the simulation time-step.

The user can also define the number of Monte Carlo (MC) runs determined necessary to provide reliable statistics for the simulation. The Monte Carlo method is used because random variables are utilised as part of the future projection. As the results from a future projection provide an estimate of an unknown value, repeating forecasts allows for the variability in the model

output to be measured. For example, a study by Liou (2008) showed that future simulations in LEGEND required 10–40 MC runs for accuracy within 5 -10% of the 'true' outcome.

Propagator: All orbiting objects in DAMAGE simulations are propagated forwards using a semi-analytical orbital propagator (Lewis et al., 2004). The propagator accounts for the main forces that perturb the orbit of an object:

- Gravitational harmonics –The oblateness of the Earth and its irregular mass distribution create gravitational anomalies that are represented by spherical harmonics (Brookes, 1994). These harmonics cause effects such as perigee precession.
- Luni-solar gravitational perturbations –These are the additional gravitational forces that are exerted on Earth-orbiting objects by the Sun and the Moon (Stark et al., 2003). In LEO the Earth's gravitational force is dominant, but in MEO, highly elliptical orbits, or GEO, luni-solar gravitational perturbations act to alter the inclination of orbiting objects (Lewis et al., 2001).
- Solar radiation pressure (SRP) –Electromagnetic radiation from the Sun exerts a small pressure on objects causing orbit oscillations, most notably for objects with high area-to-mass ratios (Lewis et al., 2001; Stark et al., 2003). The effects of SRP are variable due to changes in solar flux and also depend on the orbiting object's mass and condition of its surfaces (Bar-Sever and Kuang, 2004).
- Atmospheric drag –This force acts to reduce the semi-major axis, and eccentricity of an orbiting object, eventually leading to re-entry (Stark et al., 2003). The effects of atmospheric drag on objects in DAMAGE simulations is determined within the 'Propagator' support model and it is calculated by the 'Atmosphere' support model.

Atmosphere: The solar flux, atmospheric density, and atmospheric scale height are set within the atmosphere model. Models of historical populations in

DAMAGE use historical monthly averaged solar flux F10.7 cm values whereas future projections use a long-term F10.7 cm projection based on a repeating sine function (Lewis et al., 2009c; Lewis et al., 2010). The atmosphere support model uses the third generation Committee on Space Research (COSPAR) International Reference Atmosphere (CIRA-72) atmospheric model to provide atmospheric density and atmospheric scale height data (Jacchia, 1971; Lewis et al., 2009a).

Collision: Collision probabilities between objects $\geq$ 10 cm in DAMAGE are estimated using an algorithm based on 'Cube' used in the LEGEND evolutionary model (Liou et al., 2004; Lewis et al., 2005). The Cube approach was designed to estimate long-term collision probabilities between orbiting objects by uniform sampling at each time step in the simulation (Liou et al., 2003).

The Cube approach involves dividing the volume of Earth orbit into small volume elements called 'cubes'. Objects are propagated in time steps along their orbits through the cubes. If more than one object occupies a cube during one time step, its collision probability with other objects in the cube is calculated. Each time step is assumed to be small enough so that the collision characteristics between two objects, i and j, do not vary and thus the collision probability, $P_{i,j}$ between the two objects can be considered constant (Liou et al., 2003). Thus, for any object, i, that has a finite collision probability with a second object, j, within the same cube at time, t, the collision probability is,

$$dP_{i,j}(t) = s_i s_j V_{imp} \sigma dU dt, \tag{3.1}$$

where s_i and s_j are the spatial densities of i and j in the cube, V_{imp} is the relative velocity between the two objects, σ is the combined cross-sectional area of the two objects, dU is the volume of the cube, and dt is the time interval (Liou and Johnson, 2009). The total residential probability in one cube divided by the volume of the cube gives the spatial density of objects within that volume (Walker et al., 1997). When the collision probability is calculated, a random number generator is used to draw a number to compare to $P_{i,j}$, to

determine whether the collision occurs (Liou, 2006).

The main advantage of the Cube approach is that it is fast and efficient because collision probabilities are only calculated when the cubes are occupied by more than one object (Liou, 2006). However, a drawback is that even if two objects are spatially close to one another, but have a cube boundary separating them, then their collision probability is not considered. To accurately model the collision nature of the environment it is necessary to set the cube volume to be small; but due to the short-term perturbations suffered by the orbiting objects, the cubes are usually set to 10 km^3 (Liou et al., 2003; Liou, 2006). The collision support model in DAMAGE allows the user to determine the volume of the cubes.

Break-up: The break-up model determines how many fragments are created in a collision or explosion. Since the Martin et al. (2004) study, the NASA break-up model has been employed as standard within many evolutionary models, including DAMAGE (NASA, 2008; Lewis et al., 2010). The NASA break-up model generates fragments down to 1 mm for collision and explosion events (Krisko, 2004). It includes the size distribution of collision or explosion fragments, the area-to-mass ratio of the fragments and the ΔV distribution with respect to the parent object (Liou et al., 2004). The distribution of the number of fragments in relation to the mass of the object involved in a catastrophic collision is shown in Figure 3.1.

The breakup model requires a definition of the characteristic length, l_c to define the size of an object,

$$l_c = \frac{(l_x + l_y + l_z)}{3} \tag{3.2}$$

where l_x is the largest shadow dimension of the object, l_y is the second largest shadow dimension that is perpendicular to l_x, and l_z is the third largest shadow dimension which is perpendicular to l_x and l_y (Klinkrad, 2006). Shadow dimensions are used because the characteristic length defines the object's size as it would be portrayed in space (Hill and Stevens, 2008).

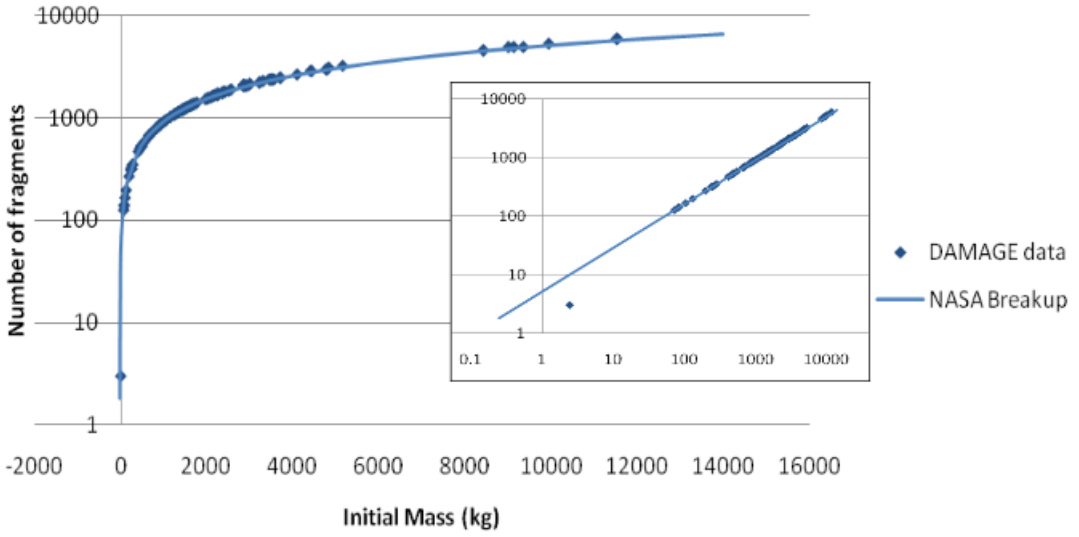

Figure 3.1: The distribution of number of fragments of different masses generated by the NASA break-up model in DAMAGE.

In space debris models, collisions between objects in space are defined as *catastrophic*, *damaging*, or *low-velocity*. If the ratio of kinetic energy to target mass is > 40 J/g, then a collision is catastrophic (Johnson et al., 2001). The outcome of a catastrophic collision is the total fragmentation of the target object, whereas a non-catastrophic collision (damaging or low-velocity) only results in minor physical damage to the target (Hanada and Liou, 2008).

The number of debris created in a catastrophic collision is dependent on the mass of the two objects that collide and the angle and orientation at which they strike each other (ODPO, 2009c). The breakup model calculates the number of fragments, N_f with a diameter, d larger than l_c as,

$$N_f(d \geq l_c) = 0.1 \times \hat{m}^{0.75} \hat{l_c}^{-1.71}, \tag{3.3}$$

where $\hat{m}$ and $\hat{l_c}$ are normalised. The parameters are normalised to make the quantities dimensionless; they are expressed as 'per unit'. $\hat{l_c}$ is,

$$\hat{l_c} = \frac{l_c}{metres}, \tag{3.4}$$

and $\hat{m}$ is,

$$\hat{m} = \frac{m_p v_i}{1000}, \tag{3.5}$$

where m_p is the mass of the impact projectile and v_i is the impact velocity (Klinkrad, 2006).

Event Manager: The event manager allows the user to choose if the 'mitigation' and 'launch' support models are used. Collision detection, close approach detection, and fragmentation can also be activated or deactivated using this support module.

The launch support model is used to model historical and future launch traffic that adds to the population of orbiting objects. In DAMAGE the future launch traffic is generated by using statistics from ESA's DISCOS covering a historical period of launches, for the duration of a simulation (Lewis et al., 2010).

The mitigation support model allows the user to include mitigation and/or remediation strategies in a future simulation. The mitigation options include passivation, operational debris suppression, and post-mission disposal. The success rate of post-mission disposal can also be varied.

The options for remediation within the support model include:

- variable removal criteria,
- concept of operations including: a choice of the number of objects to be removed by one removal system and the number of removal systems on one launch vehicle, and
- removal parameters such as the total number of objects to be removed and when remediation should start and end.

3.1.2 Reliability of DAMAGE

The reliability of DAMAGE and its usefulness as a source of data for this thesis are examined here. A 'hindcast' can be used to determine how accurate the

output is. In a hindcast, a model is run, providing data for a period of time in the past for which there is already real-time data. The model output can then be compared to the known historical data. Figure 3.2 shows the comparison between a historical evolution of the satellite and debris population using DAMAGE with historical catalogue data.

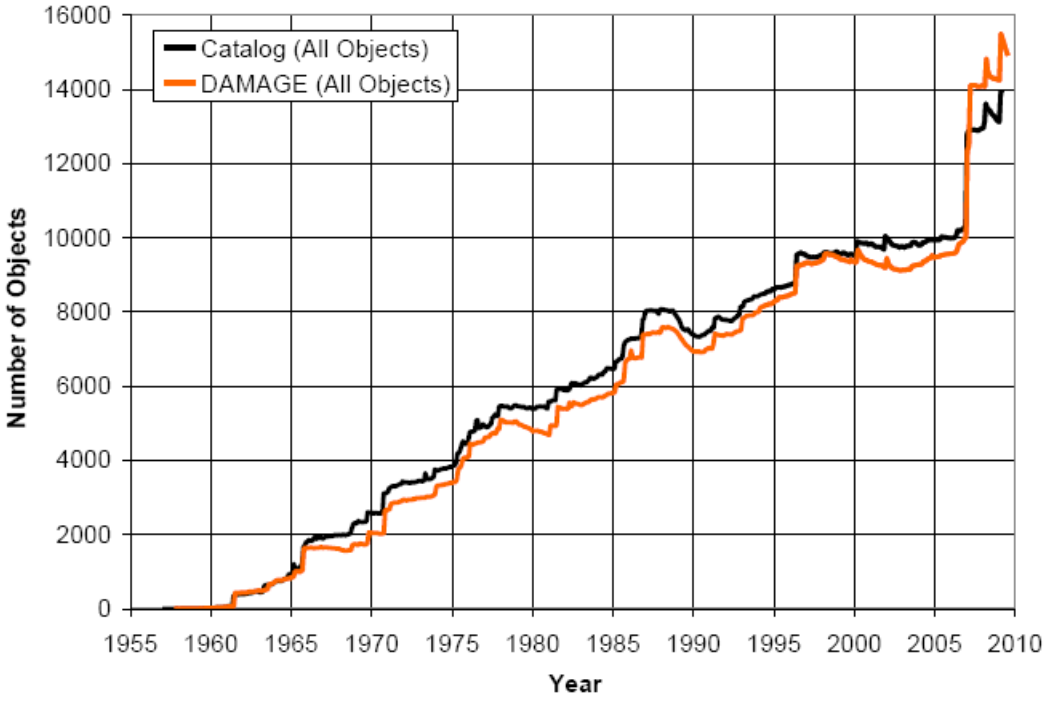

Figure 3.2: Comparison of DAMAGE historical evolution with historical catalogue data (data: NASA) (Lewis et al., 2009a).

DAMAGE performs well confirming that it is a reliable model. However, a hindcast cannot determine how well any debris model will forecast a future population and no forecast model can predict the future with 100% accuracy. The debris environment is a multi-body system with many unknown variables that cannot be predicted in advance. This is overcome by estimating the variables, such as the solar flux data using long term F10.7 projections as described earlier.

Another problem concerns the use of the Monte Carlo method. Reliable statistics are established in DAMAGE by using several MC runs. These MC

runs are used to determine the variability in the modelling output. However, in most publications only the mean and standard deviation are presented so the variability in the results is lost. Reducing the results to the mean average does provide a clear way of presenting the results of several MC runs as Figure 3.5 shows. However, the drawback of only presenting the mean average is that it does not represent any of the modelled outcomes. For example, the final predicted population in 2210 in Figure 3.3 is between ∼11,000 and ∼20,500, but the mean is plotted as ∼15,500.

Figure 3.5 shows the mean average results from a LEGEND modelling study based on 150 MC runs (the first 50 of which are shown in Figure 3.4). This figure clearly shows the trend predicted by the modelling study, but it does not show the variation in the predicted outcomes. Decisions about important issues like ADR removal criteria are based on modelling studies such as these; therefore, if only the mean average is used to determine a result, it is important to take the variability into account and to undertake further modelling studies to confirm the accuracy of the average results.

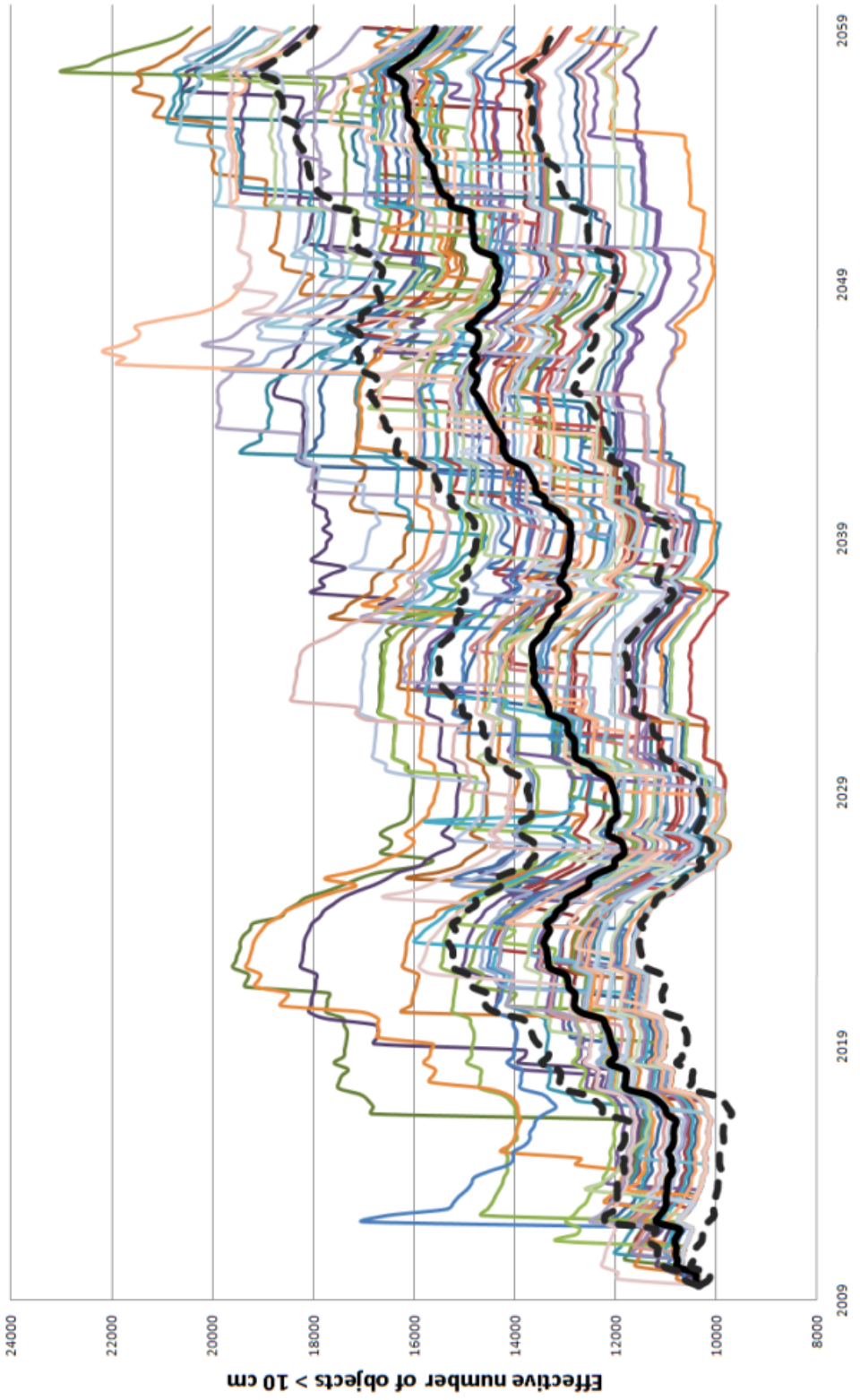

Figure 3.3: 50 MC runs in DAMAGE no ADR study results showing mean and +/- 1 standard deviation results.

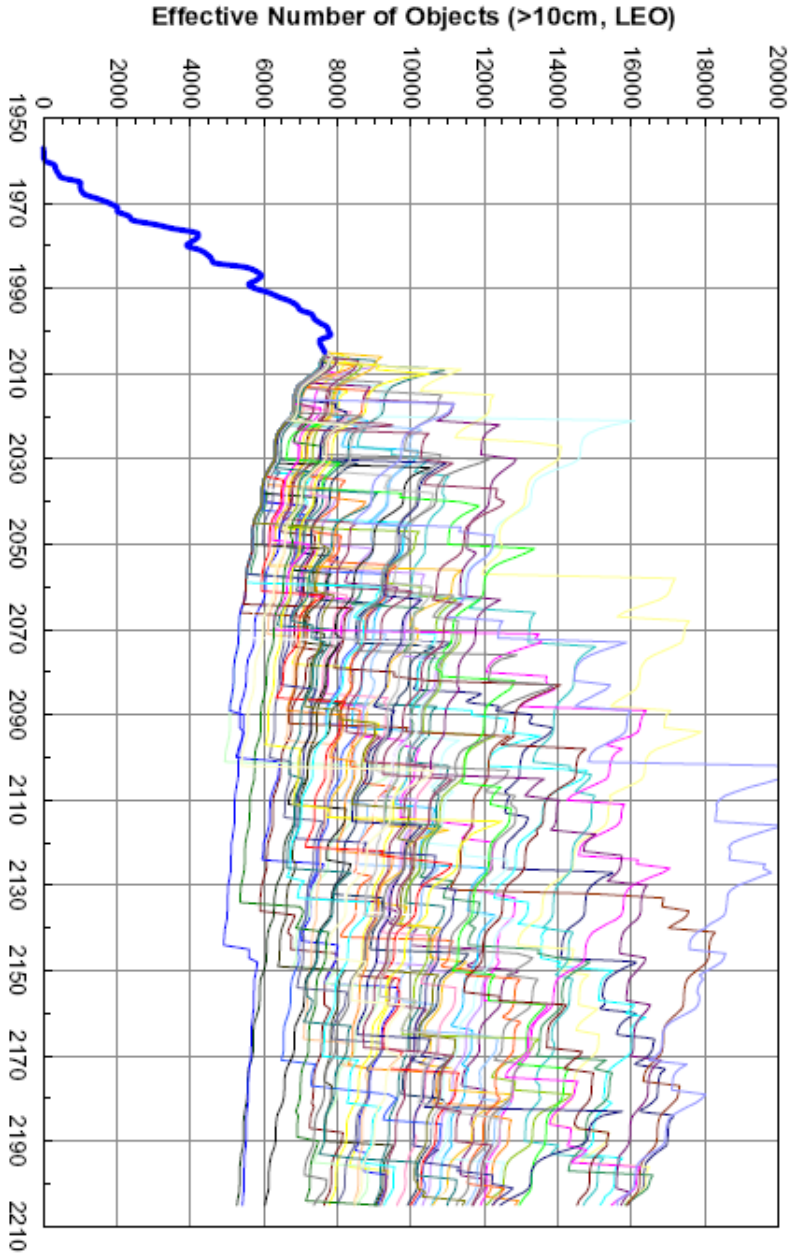

Figure 3.4: First 50 MC runs (Liou and Johnson, 2008).

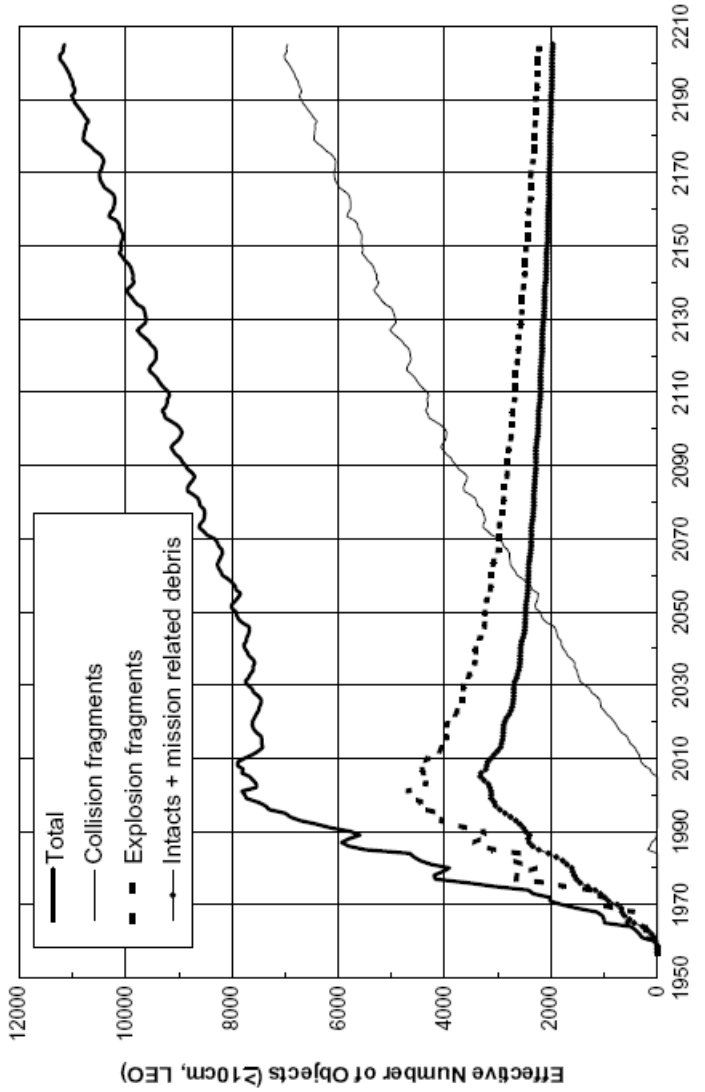

Figure 3.5: Average of all 150 MC runs (Liou and Johnson, 2008).

3.1.3 DAMAGE networks

The objective of this section is to investigate the features of the space debris environment, as modelled in DAMAGE simulations, using network and vertex measures. The space debris networks presented here are used to represent conjunctions (uni-relational) and the heritage of objects (multi-relational) in the space debris environment.

Uni-relational networks

The network in Figure 3.6 was generated using a combination of two MC runs from a 40-year (2000–2040) BAU simulation of LEO. If two orbiting objects occupy the same cube during any time-step in the simulation their corresponding vertices are joined by an edge representing the conjunction (Lewis et al., 2010). This is a uni-relational network; there is only one type of vertex, therefore the vertices represent a mix of payloads, rocket bodies, mission-related debris, explosion fragments, and collision fragments. For example,"AM" is a rocket body, 1978 34B, whereas "X" and "Y" are fragments from historical break-ups of a rocket body and satellite (1978 100D and 1981 31A, respectively)(Lewis et al., 2010).

Vertex	**A**	**I**	**X**	**Z**	**AM**
Degree	1	7	2	4	5
Clustering coefficient	0.0	0.0	0.0	0.0	0.0
Closeness	9.5	4.4	4.2	4.1	4.6
Betweenness	51	1689	1339	1741	1133

Table 3.1: Centrality and clustering statistics on the five vertices selected from the 52 vertices in the network in Figure 3.6 (Lewis et al., 2010).

The vertex measures for the five vertices, "A", "I", "X", "Z", and "AM" in Figure 3.6 are shown in Table 3.1. "I", "Z", and "AM" are important to the structure of the network because of their high degree and betweenness centrality. For example, object "I" has a betweenness value 33 times higher than object "A" (Lewis et al., 2010).

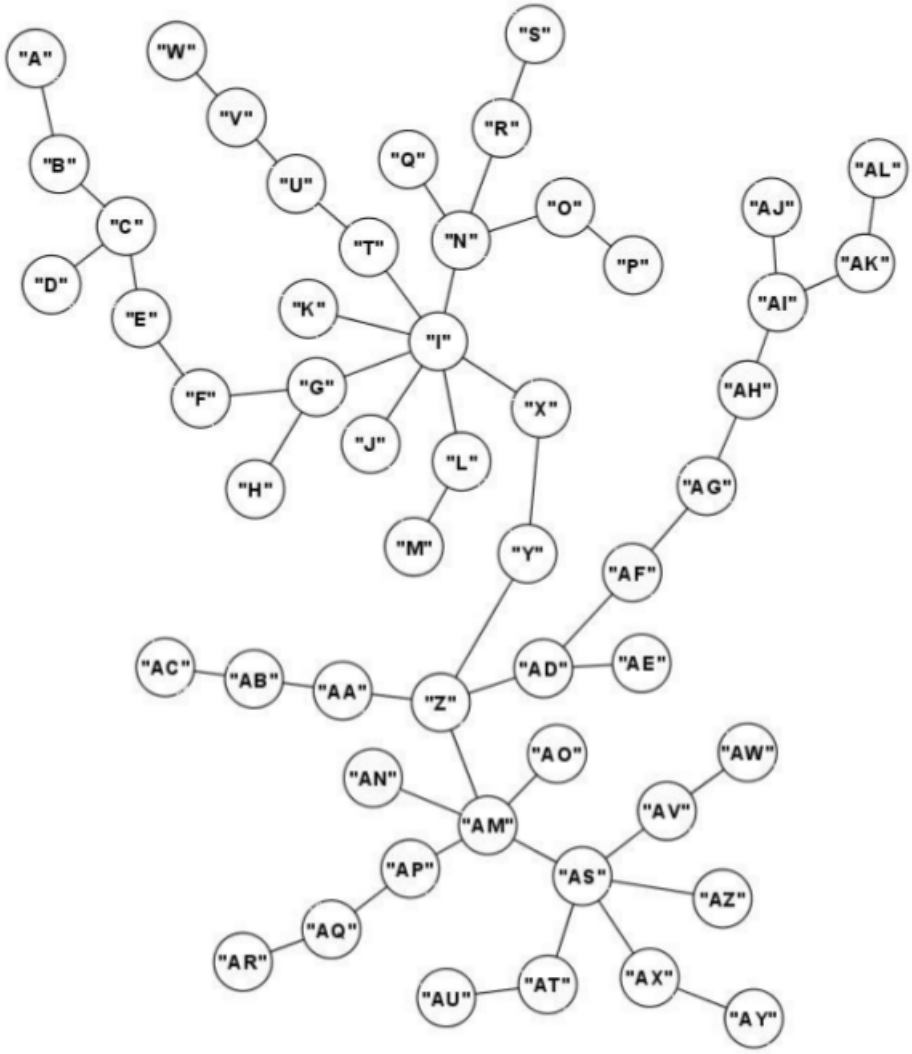

Figure 3.6: Uni-relational network formed from two MC runs (Lewis et al., 2010).

Removing "I" and "AM" reduces the maximum number of connected vertices from 52 to 15 and the network betweenness centrality decreases from $\bar{B} = 324.54$ to $\bar{B} = 27.3$ (Lewis et al., 2010). Reducing the network betweenness will reduce the connectivity of the network which will reduce its robustness. This reduces the likelihood of a collisional cascade and indicates that the environment as a whole could be made more stable.

Vertex "A" has a higher closeness centrality compared to the other vertices in Table 3.1. This is because, like other vertices such as "AL", "AC", and "W", "A" is a vertex with degree, $k = 1$ that lies on the periphery of the network. Here, high values of closeness indicate that the vertices are not important to the structure of the network. Therefore "I", "X", "Y". and "AM", are all more important than "A".

The vertices "X" and "Y" have important roles in the network because although they have a low degree, and are only connected to two other objects, they are part of chains (Lewis et al., 2010). Chains provide collision feedback routes and their presence is indicated by the lack of clustering. Therefore, removing "X" or "Y" would split the network into two parts preventing collision feedback routes.

Multi-relational networks

A multi-relational network was generated from one MC run of a 25-year (2001–2026) BAU simulation study. The network features three types of vertex and three corresponding types of edge (Figure 3.7). This network is partly directed (the edges connecting vertices representing fragments to vertices representing intact objects are labelled "is a fragment of"), but is treated as undirected for this study.

The multi-relational network edges represent the relationships: "conjunction","is a fragment of", or "is a member of" corresponding to interactions between the following types of vertices (Lewis et al., 2010):

- intact objects, such as payloads and rocket bodies,
- fragments generated by the break-up model in DAMAGE, and

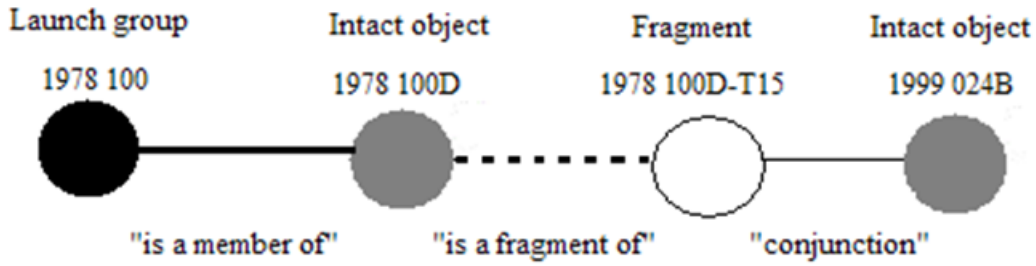

Figure 3.7: Multi-relational network vertices and edges. The 'launch group' and 'intact object' labels are the International Designator of the objects, and the 'fragment' labels are derived from the parent object's International Designator (Lewis et al., 2010).

- launch groups added by DAMAGE for every object involved in a conjunction event.

The multi-relational network generated from the 25-year DAMAGE simulation is shown in Figure 3.8. Unlike the uni-relational network in Figure 3.6 different types of objects are represented by different types of vertices. The types of vertices show the heritage of the objects that were involved in conjunctions during the simulation. Every fragment came from an intact object, and every intact object came from a launch. The launch groups are not physical objects, but are illustrated because one launch may be responsible for several conjunctions, e.g. vertex "D". Similarly fragments are connected to their parent objects to show their heritage.

This network shows how fragmentation events and launches affect the growth of the space debris population (Lewis et al., 2010). For example, "D" was a rocket body involved in an explosive break-up and became the parent object to fragment objects. Despite not being involved in a conjunction "D" is a hub and plays a central role in the multi-relational network (Lewis et al., 2010). If "D" is removed it will change the network structure. Vertices can be removed in fictitious "what if? " scenarios to show the consequences of a launch or conjunction to the structure of the network, for example how would the network look if the explosion of "D" hadnt taken place?

The individual vertex measures for vertices "A", "B", "C", "D", and "E" are

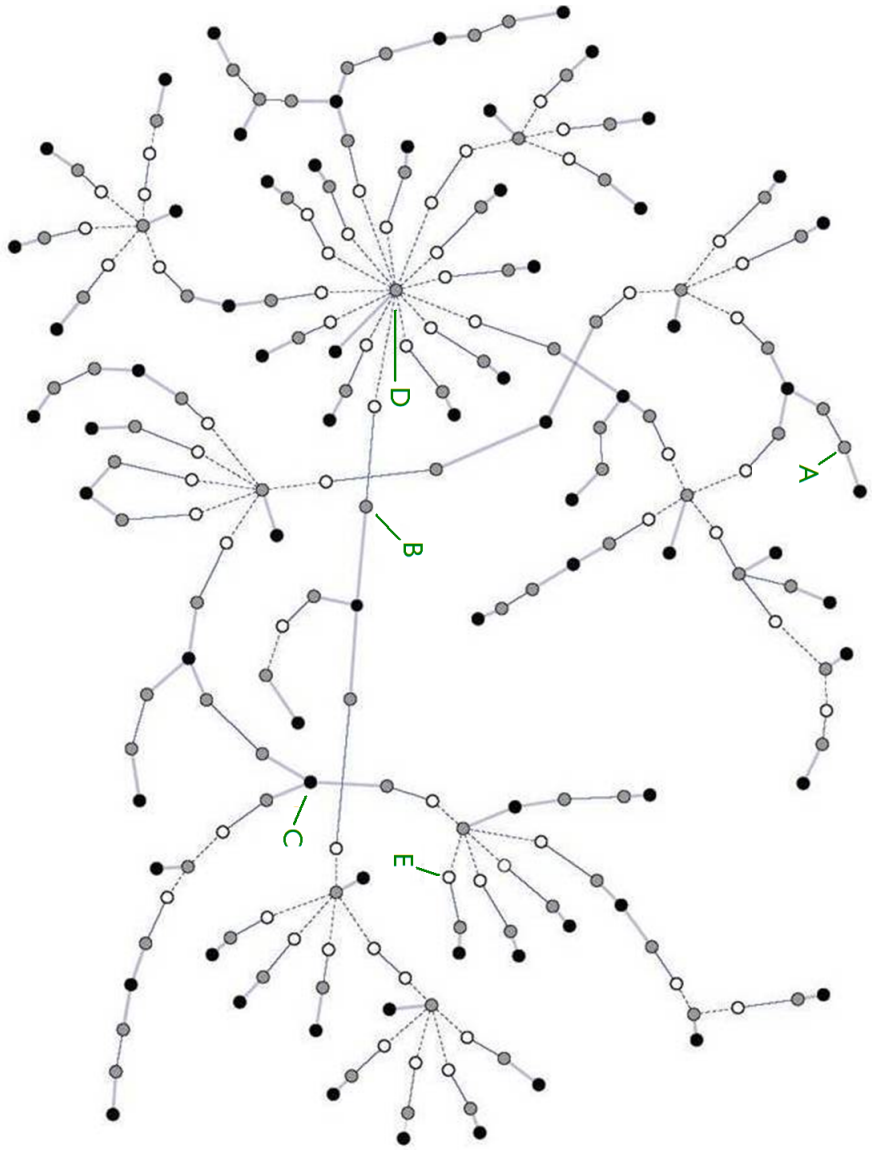

Figure 3.8: Multi-relational network formed from one MC run (Lewis et al., 2010).

Table 3.2: Statistics for the selected vertices in Figure 3.8 (Lewis et al., 2010).

Vertex	**A**	**B**	**C**	**D**	**E**
Object	1988 002G	1988 102J	1993 030	1987 068B	1992 093B-F135
Degree	2	2	3	15	2
Clustering	0.0	0.0	0.0	0.0	0.0
Closeness	15.19	13.50	20.53	12.13	23.85
Betweenness	660	12912	14034	34947	1096

shown in Table 3.2. Figures 3.9 and 3.10 show the effectiveness of removing objects based on their betweenness centrality. Vertices "B", "C", and "D" have betweenness centralities higher than vertices "A" and "E"; the betweenness centrality of vertex "D" is almost 32 times greater than that of vertex "E" (Lewis et al., 2010). When vertices "A" and "E" are removed from the original network in Figure 3.8 the network in Figure 3.9 remains. Removing only "A" and "E" has little effect on the structure of the network; no chains are broken, and the beta index only falls by 0.0001.

When vertices "B", "C", and "D" are removed from the network in Figure 3.8 the network in Figure 3.10 remains. In this case, the giant component is destroyed, reducing the connectivity of the original network to leave seven smaller networks. Removing "B", "C", and "D" results in the total removal of 51 edges and 46 vertices. This process breaks chains and completely removes the effects of the explosion of "D". This is because removing vertices may also involve removing the neighbours of the chosen vertex, because unless its neighbour is involved in a conjunction, it will be completely unconnected to the rest of the network. For example, in this multi-relational network, removing an intact object would automatically result in the removal of its parent object.

Complexity and robustness

Individual and re-combined MC runs are used here to illustrate the robustness and potential complex nature of space debris networks. In order to model the space debris environment as a network based on DAMAGE simulations it is unavoidable that they will be constructed as a series of Monte Carlo runs (Lewis et al., 2010). Therefore, it is possible to examine the networks that represent individual Monte Carlo runs and then join them together. The likelihood of interactions is calculated based on the likelihood of interactions in each Monte Carlo run; in a weighted network this could be represented, by weighted edges. However, the networks here are unweighted. As such the network measures used are also unweighted and do not include the conjunction probability.

The following networks were generated using a combination of one, two, three,

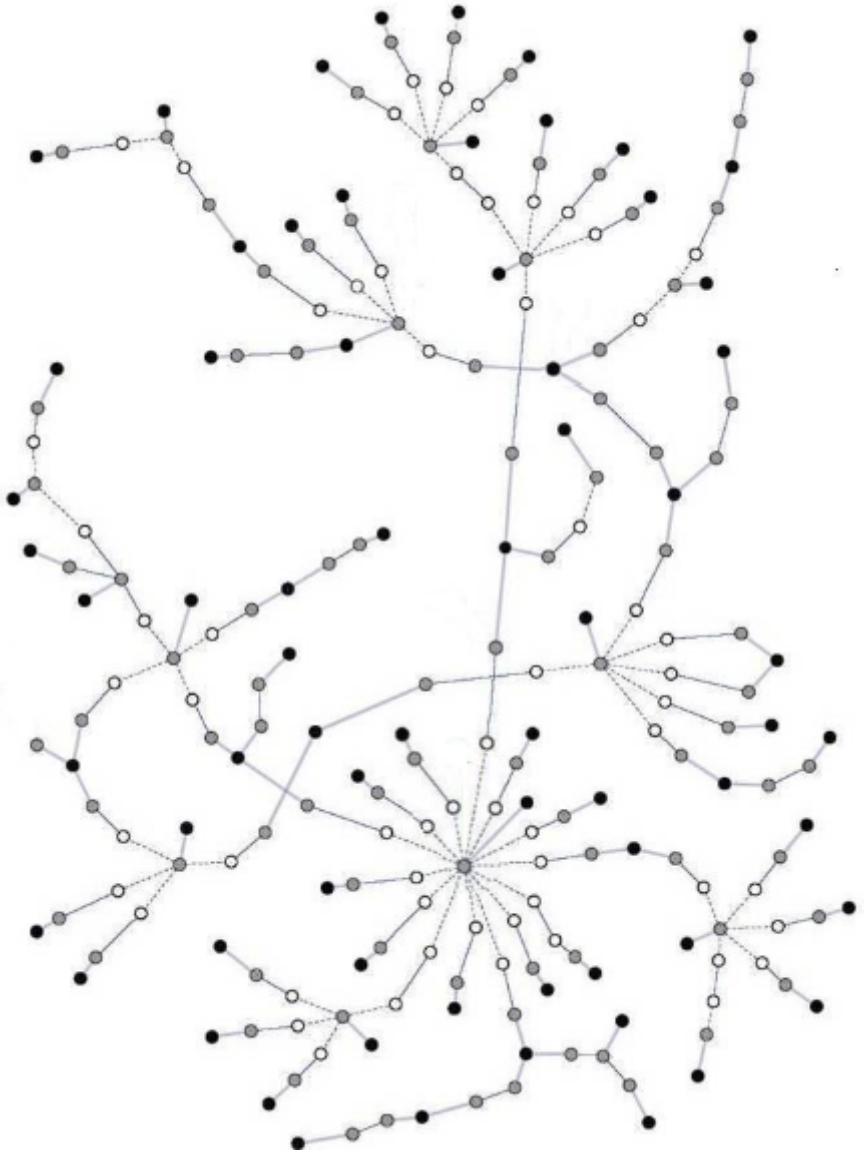

Figure 3.9: Vertices "A" and "E" are removed from the network in Figure 3.8.

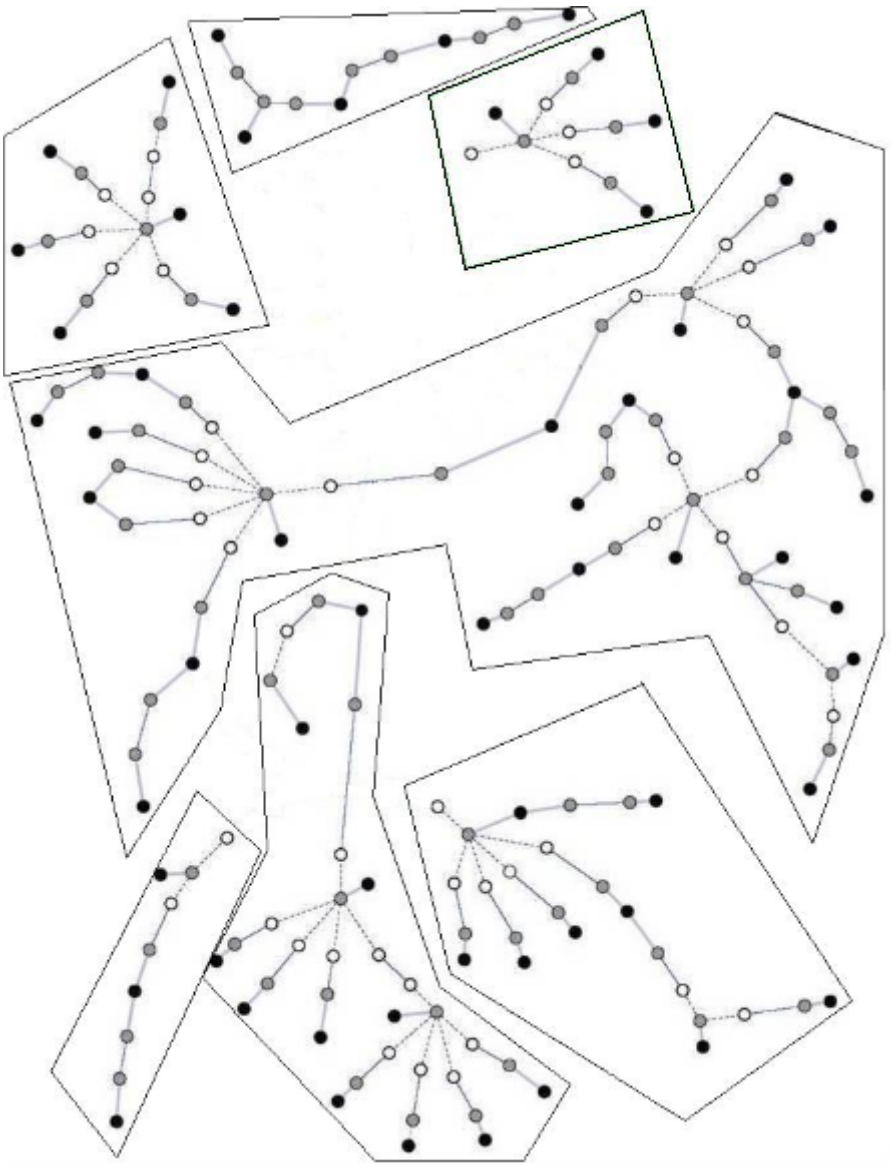

Figure 3.10: Seven smaller networks remain when vertices "B", "C", and "D" are removed from the network in Figure 3.8.

and four MC runs from a 40-year (2000–2040) BAU simulation (Lewis et al., 2010). Figure 3.11 shows the network built from one MC run. Each of the individual MC runs in the simulation produced similarly disconnected networks, in which most objects were only connected to one other object, forming pairs or short chains of up to 12 vertices in length (Lewis et al., 2010).

Figure 3.11: The network formed from one MC run (Lewis et al., 2010).

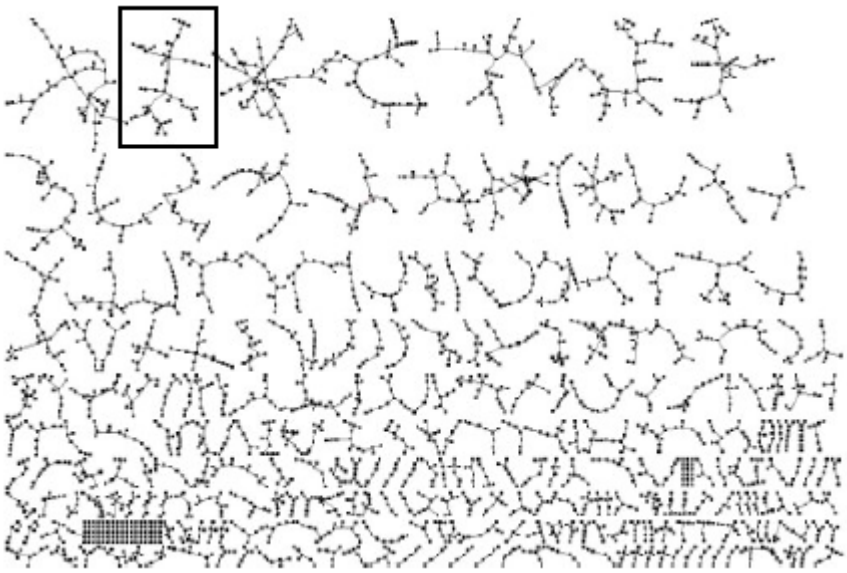

Figure 3.12: The network formed from two combined MC runs (Lewis et al., 2010).

When two individual MC runs are added together (Figure 3.12) the vertices form small networks (up to order 52) that are disconnected from each other (Lewis et al., 2010). This indicates that the addition of further MC runs will increase the order of the networks; when data are added from the third and

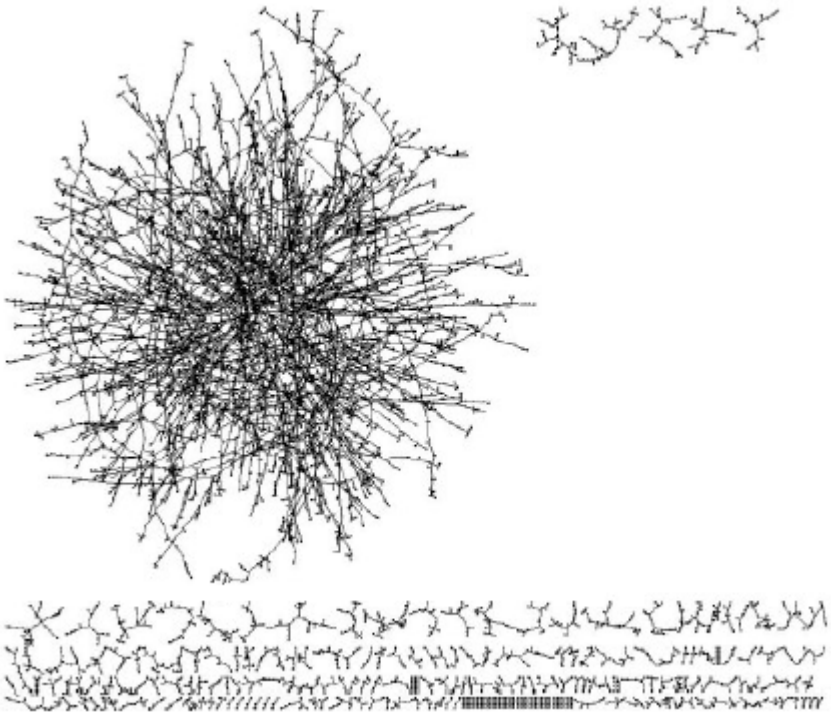

Figure 3.13: The network formed from three combined MC runs (Lewis et al., 2010).

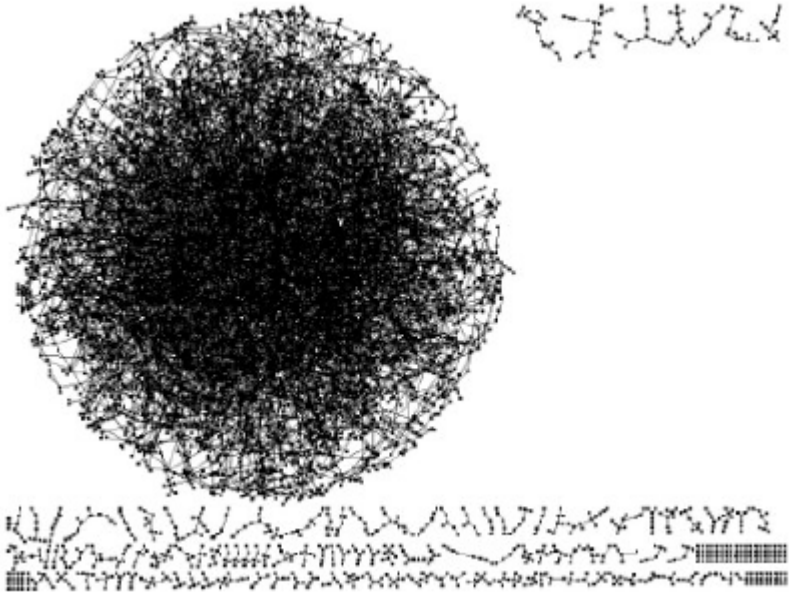

Figure 3.14: The network formed from four combined MC runs (Lewis et al., 2010).

fourth MC runs (Figures 3.13 and 3.14) the order increases to a maximum of 5,537 (Lewis et al., 2010) in Figure 3.13. Although some of the vertices are still connected in pairs and chains, it is estimated that more than 80% of the vertices in Figure 3.13 and 3.14 are part of the interconnected giant component making the networks robust.

All of the networks in Figures 3.11 to 3.14 are disassortative and their structures indicate that there is a move towards complexity as more vertices are added (Lewis et al., 2010). However, although the order increases as the number of MC runs increases, the space debris population is not getting bigger. Instead, as MC runs are added, more of the individual objects in the total simulation population are likely to be represented in the networks.

3.2 SOCRATES networks

3.2.1 Conjunction assessment process

Conjunction assessments are made by SOCRATES as follows: twice a day SOCRATES obtains an updated database of the orbital elements of unclassified orbiting objects from the NORAD Space Track website (Spacetrack, 2009; Kelso and Alfano, 2005). These orbital elements are in the form of Two Line Element (TLE) sets, one of several standardised formats for describing orbital elements (Hunt, 2010b). This database is split into 'payloads only' and 'all objects' (Kelso and Alfano, 2005; Kelso, 2009b). SOCRATES uses Analytical Graphics Inc.'s Satellite Tool Kit's Conjunction Analysis Tools (STK/CAT) that incorporates the simplified general perturbations theory (SGP-4) orbital propagator (AGI, 2011). The TLEs are propagated in time and converted into osculating elements (Klinkrad, 2009). STK/CAT calculates the collision risk between the objects in the 'payloads only' list and the objects in the 'all objects' list and reports on the minimum distance, maximum probability, and the time of close approach for each conjunction (Kelso, 2009b).

Maximum probability is calculated to give consistent results for all

conjunctions, despite varying uncertainties in positional covariance data. A large positional uncertainty results in a small collision risk. However, it is only when the positional uncertainties are small that the 'true' probability of collision can be calculated. To calculate the maximum probability a footprint that defines the whole region of potential interaction is projected onto a two-dimensional probability density space (Alfano, 2006). This footprint is rotated to determine the orientation that produces the maximum probability for the conjunction (Alfano, 2006).

Up-to-date conjunction assessments are provided online every day on the SOCRATES website. These have provided a source of data for the networks in this thesis. The author had access to historical SOCRATES data from January 2006 to August 2009 kindly provided by T S Kelso at the CSSI.

3.2.2 Reliability of SOCRATES

TLE age

SOCRATES has successfully demonstrated the use of standard orbital data and basic computer hardware for screening large numbers of satellites for conjunctions assessments (Kelso, 2009a). However, the TLE data used by SOCRATES has uncertainties, mostly caused by atmospheric drag (Knowles et al., 2001). Kelso (2007) states that although the TLE data does not come with covariance estimates, which would provide a measure of the uncertainty, TLE consistency analysis does reasonably approximate the true error of a TLE prediction. However, this analysis is not provided by SOCRATES and lies outside the scope of this thesis.

In addition to the uncertainties in the TLEs, a study of the top five predicted conjunctions in one SOCRATES report in 2008 concluded that conjunction assessments must be interpreted in the context of the age of the TLEs (Finkleman et al., 2008). To illustrate the problem Alfano et al. (2009) studied SOCRATES reports from August 2009. Figure 3.15 shows the variation in the age of TLE data used to provide conjunction assessments in August 2009.

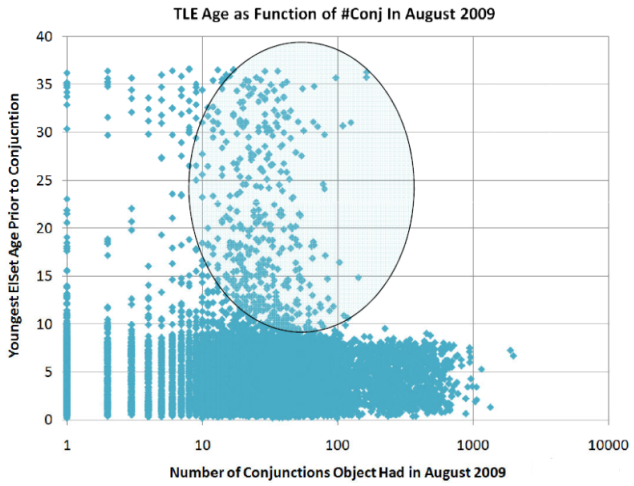

Figure 3.15: The age of TLE data as a function of number of conjunctions in SOCRATES August 2009 (Alfano et al., 2009).

The problem with Alfano et al. (2009)'s analysis is that only the objects involved in a high number of total conjunctions are highlighted as being 'expired'. This ignores the objects involved in a low number of total conjunctions calculated using TLEs of comparable age. It would be better to argue that there could be confidence values associated with TLEs of different ages with the confidence decreasing as TLE age increases, regardless of the number of conjunctions in which an object was involved.

Iridium-33 - Cosmos-2251 collision

Conjunction assessment data from the week leading up to the collision between Iridium-33 and Cosmos-2251 on the 10th February 2009 is studied here to provide an assessment of the reliability of SOCRATES. Whilst a conjunction was predicted between Iridium-33 and Cosmos-2251 during the week leading up to the collision, it was not ranked highly enough, by predicted close approach distance or maximum probability, to be considered a true threat. Figure 3.16 shows the variation over time in the predicted maximum collision probability and the predicted close approach distance between Iridium-33 and Cosmos-2251.

In total, 136,569 conjunctions assessments were made by SOCRATES in the week leading up to the collision. These assessments can be ranked by their

maximum probability. Figure 3.17 shows the ranking of Iridium-33 and Cosmos-2251, the ranking of Iridium-33 and Cosmos-2251 compared to all conjunctions involving Iridium-33, and the rank of Iridium-33 and Cosmos-2251 compared to all conjunctions in the Iridium constellation. The conjunction between Iridium-33 and Cosmos-2251 compared to all conjunctions is ranked between 1,611 and 11 over the course of the week; at the time of the final report it was ranked at 152 (Kelso, 2009a). Of all of the conjunctions in the Iridium constellation, the rank of the Iridium-33 and Cosmos-2251 conjunctions is always less than 200, and the rank of the Iridium-33 and Cosmos-2251 conjunctions compared to all of the conjunctions involving Iridium-33 varies between two and four. Therefore, the TLEs indicate that the conjunction between Iridium-33 and Cosmos 2251 was less likely than other predicted conjunctions involving Iridium-33, or other Iridium satellites.

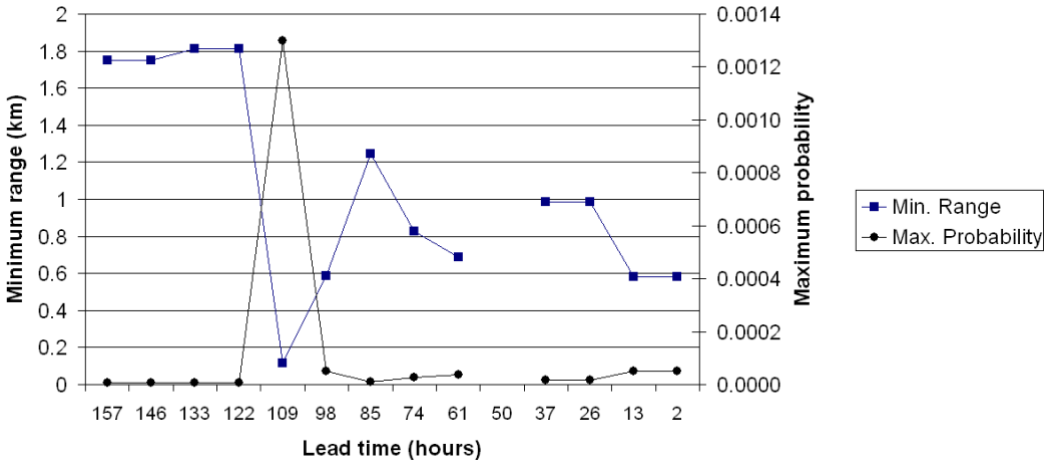

Figure 3.16: SOCRATES maximum probability and minimum distance predictions prior to the collision between Iridium-33 and Cosmos-2251.

The fluctuations in the minimum distance and maximum probability predictions during the week and the errors in the final prediction are most likely due to the inherent uncertainty in the TLE data. However, Figure 3.18 shows that the TLEs used to predict the conjunction were not 'expired'.

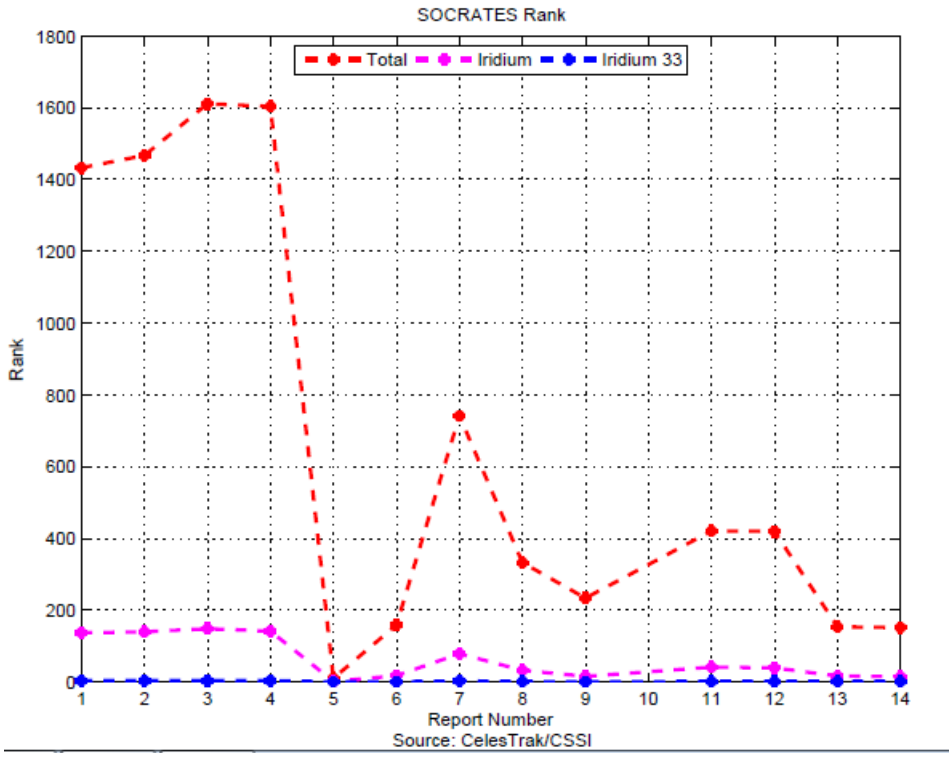

Figure 3.17: Comparison of the Iridium-33/Cosmos-2251 conjunction to all other conjunctions (Kelso, 2009b).

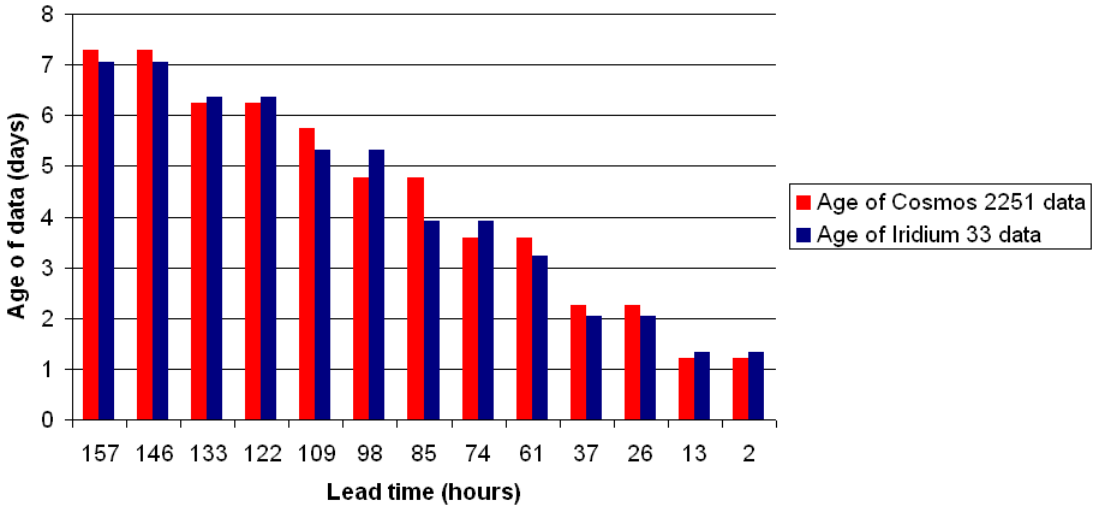

Figure 3.18: Age of the TLE data used in the Iridium-33/Cosmos-2251 conjunction assessments.

Figures 3.16, 3.17, and 3.18 highlight three problems with the SOCRATES data:

- There are errors involved in the prediction. The error in the final predicted minimum distance was 0.584 km.
- The conjunctions with the highest probability are not always the greatest threats (Finkleman et al., 2008). There were 1,095 conjunctions involving Iridium satellites in the week leading up to the collision and the Iridium-33/Cosmos-2251 conjunction was not the most likely to result as a collision.
- Even data considered to be "up-to-date" is not accurate enough to conclusively predict a collision. None of the TLE data used in the Iridium-33 and Cosmos-2251 conjunction assessments could be considered 'expired' because it was all less than eight days old.

Despite these problems, SOCRATES is used here because the conjunction assessments are based on the most comprehensive set of TLE data that is available to the public (Vallado et al., 2006). Although there was no clear indication that the conjunction would result in a collision, SOCRATES did successfully predict the conjunction.

3.2.3 SOCRATES networks

The objective of this section is to investigate the features of the space debris environment when it is represented as a network of SOCRATES conjunction assessments. On a network built from SOCRATES data, edges represent a conjunction and vertices represent the objects in the conjunction. The space debris networks presented here have edges weighted by maximum probability of conjunction.

Conjunction networks

Figure 3.19 shows the network generated from the first of two SOCRATES reports on 12th July 2010. The network is made of four distinct regions:

Order	8421
Size	15251
Diameter	20
Network maximum degree	59
Network degree	3.622
Network strength	6.64×10^{-5}
Assortativity coefficient	-0.354
Clustering	0.005

Table 3.3: Network statistics for SOCRATES data on 12th July 2010.

outliers, the primary part of the giant component, the secondary part of the giant component, and a 'bridge' region. The outliers are objects that were involved in conjunctions that were isolated from other conjunctions and do not connect to the giant component. The primary part of the giant component contains the most vertices and is the large section at the top half of Figure 3.19; the vertices in this region are objects with apogee $<$ 4,500 km and perigee $<$ 1,300 km. The secondary region contains objects with apogee $<$ 4,000 km and perigee $<$ 1,600 km.

The 'bridge' region links the primary and secondary regions together; it contains far fewer objects than either of the main regions, objects with apogee $<$ 2,000 km and perigee $<$ 1,500 km. It is expected that vertices in this region will have low degree and high betweenness centrality, however there is no distinguishing orbital altitudes that suggest that the objects in the 'bridge' region are anything more than artefacts of the network drawing algorithm as they are indistinct from the objects in the primary region. Four sections with example vertices are highlighted in Figure 3.19 and are shown in more detail in Figure 3.20 a-d.

Table 3.3 shows the network measures for the network in Figure 3.19. The size and order of the network show that over 15,000 conjunctions were predicted between 8,421 unique objects on the 12th July 2010. The maximum degree indicates that the most number of conjunctions that a single object was involved in was 59. On average the objects were involved in $\bar{K} = 3.622$ conjunctions although the degree distribution (Figure 3.21) indicates that there

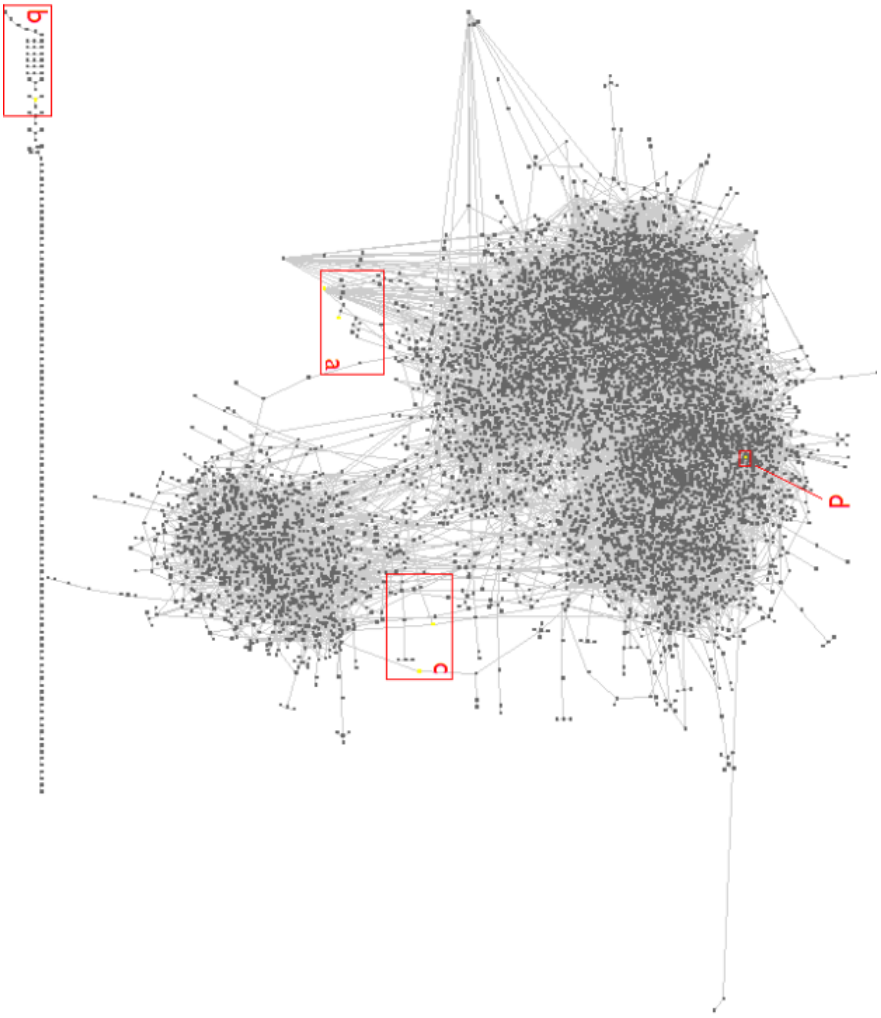

Figure 3.19: 120710 SOCRATES network.

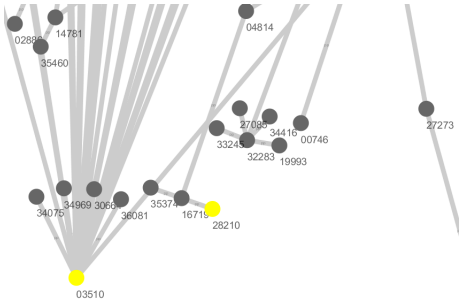

(a) Close-up “28210” and “03510”

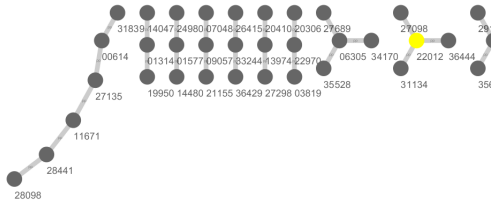

(b) Close-up “22012”

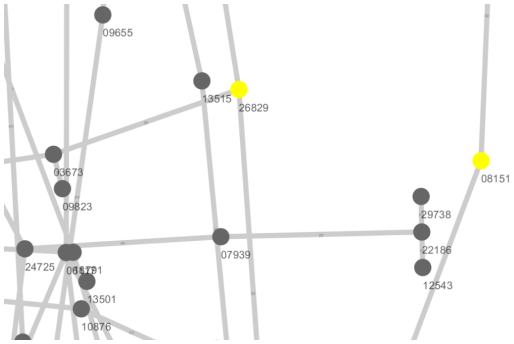

(c) Close-up “26829” and “08151”

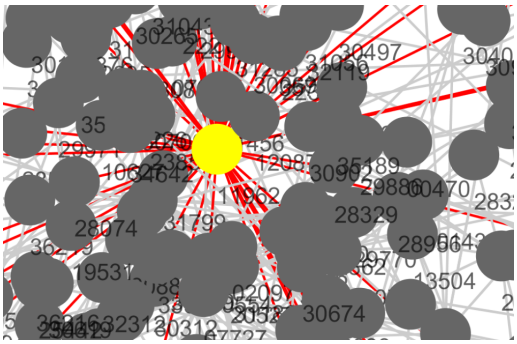

(d) Close-up “11962”

Figure 3.20: 120710 SOCRATES network close-ups.

is a wide spread of objects involved in a higher number of conjunctions.

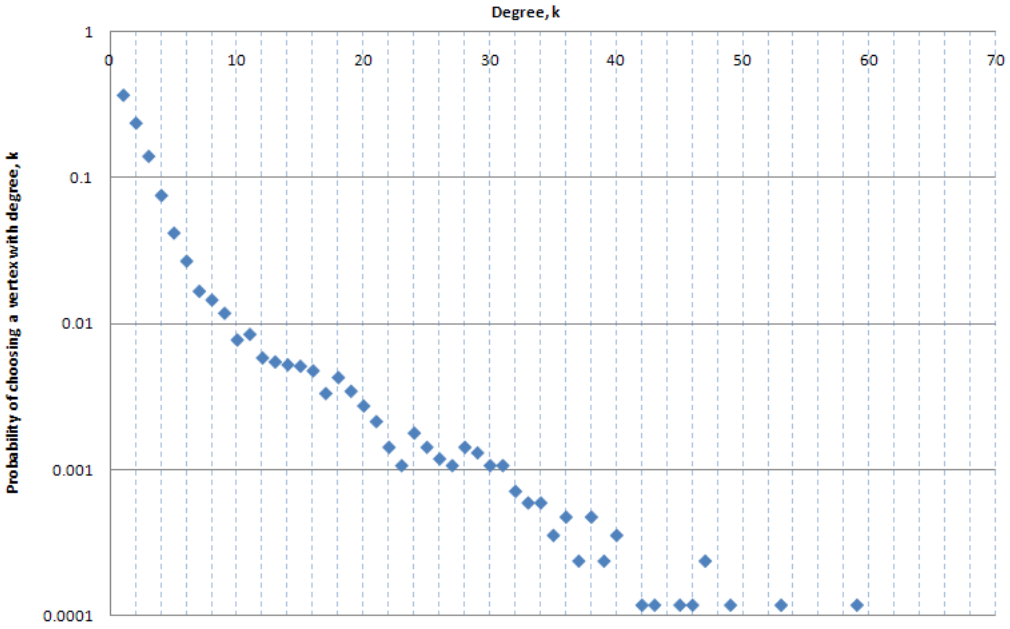

Figure 3.21: Degree distribution of SOCRATES data on 12th July 2010.

The low strength value indicates that the probability of collision on the whole, even for objects involved in a large number of conjunctions, was small. This is reflected in the strength values for the selected objects in Table 3.4. Although "11962" (Figure 3.20d) has the highest degree,"03510" has a degree less than half of the value of "11962", but it has a greater strength, indicating a higher overall probability of collision.

The negative assortativity coefficient value indicates that the SOCRATES network is disassortative and contains hubs. It would be expected that the hubs have high centrality values and some of these can be seen in Table 3.4. Vertices "03510", "26829", "08151", and "11962" have betweenness values several orders of magnitude greater than object "28210" for example. The low betweenness and closeness centrality of "22012" indicate the true nature of the vertex: it lies outside of the giant component.

Although clustering is present in the network ($C = 0.005$) it is not significant enough to indicate that chains would not be able to form. Table 3.4 shows that "03510" (Figure 3.20a) is one of the minority of vertices that is in a cluster.

Table 3.4: Vertex measures for the selected vertices in Figure 3.20.

Vertex	**28210**	**03510**	**22012**	**26829**	**08151**	**11962**
Object	1966 041G	1968 092A	1992 038A	1975 052KH	1975 073F	1980 073A
Degree	1	28	3	3	2	59
Strength	1.78×10^{-7}	0.001739	7.00×10^{-7}	4.70×10^{-6}	4.37×10^{-6}	0.001176
Clustering	0	0.002646	0	0	0	0
Closeness	0.0012	0.0006	0.0001	0.0008	0.0010	0.0006
Betweenness	16559	434692	13	178577	44298.9	1.11×10^{6}

However, “03510”, “22012”, and “11962” are important for another reason: they contribute significantly to the mass reservoir in LEO as they are intact, derelict objects with masses of 150 kg, 158 kg, and 3,300 kg, respectively. This means that they are a potentially large source of collision fragments.

Figure 3.20c shows “26829” and “08151” which have low degree, but high betweenness centrality (Table 3.4). This is because they connect two regions of the giant component. Figure 3.19 shows that there are two distinct, densely connected regions with a few vertices between them which act as bridges.

Complexity and robustness

The network generated from the SOCRATES report on 1st January 2006 (Figure 3.22) is now compared to the network generated from the SOCRATES report on 12th July 2010 (Figure 3.19) to determine how the age of a SOCRATES report affects network structure. It is important to note that conclusions drawn from the analysis are only based on these two datasets.

Table 3.5 shows that in the 4.5 years between the report epochs, the number of objects in the SOCRATES reports has doubled and the number of conjunctions has increased by a factor of 2.4. These increases reflect a substantial change in the environment because of the growth of the space debris population between 2006 and 2010 which includes the Fengyun-1C ASAT test and the collision between Iridium-33 and Cosmos-2251.

The beta index, network degree, and betweenness centrality have all increased, and the closeness centrality has decreased suggesting that the space debris environment in 2010 is now more highly connected than it was in 2006. The 2010 network is twice as disassortative as it was in 2006. Furthermore, the diameter of the network has fallen from $d_{ij(max)2006}= 22$ to $d_{ij(max)2010}= 20$. All of these measures indicate that the 2010 network is more robust than the 2006 network. If this trend continues into the future, it further compounds the need for robust ADR criteria.

Figure 3.23 shows the difference in the degree distributions between the networks. The range of the gamma exponents for both the degree distributions

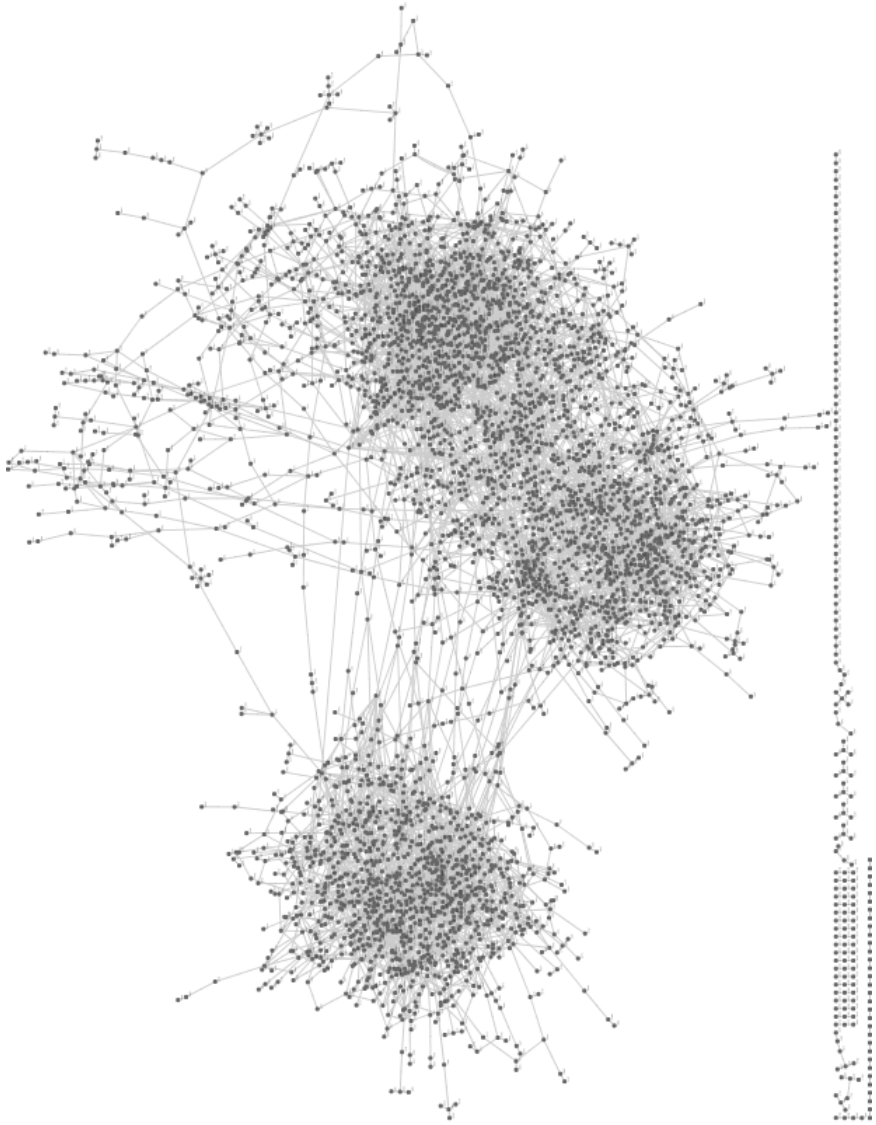

Figure 3.22: Network of the conjunctions reported by SOCRATES on 1st January 2006.

Table 3.5: Network statistics for SOCRATES data on 1st January 2006 and 12th July 2010.

	SOCRATES 010106(0530)	**SOCRATES 120710(0100)**
Order	4242	8421
Size	6322	15251
Beta index	1.490	1.811
Diameter	22	20
Geodesic	8.430	6.610
Network maximum degree	20	59
Network degree	2.981	3.622
Assortativity coefficient	-0.185	-0.354
Clustering	0.007	0.005
Closeness	0.0015	0.0007
Betweenness	36204.3	61950.1

indicate that the networks ate not scale free; the exponent of the degree distribution in 2006 is between $1.745 < \gamma < 2.948$ and the degree exponent of the 2010 network is between $1.797 < \gamma < 2.420$. However, the 2010 network includes a 'fat tail', not seen in the 2006 distribution. This indicates that there are a few vertices acting as hubs with a very high degree compared to other vertices in the network. The fat tail of the 2010 degree distribution is due to the appearance of a few objects in orbit being involved in many conjunctions as a result of the growth of the debris population. The maximum network degree has almost tripled in the 4.5 years since 2006: in the 2006 dataset, the highest degree, k_{max}= 20, in 2010 the highest degree, k_{max}=59. The appearance of hubs is supported by the increase in disassortative mixing seen in the 2010 network.

Representation of objects

In addition to representing objects in the SOCRATES database by their NORAD catalogue numbers, the objects can also be represented by their names e.g."FENGYUN 1C DEB". There are fewer unique names than numbers as, for example,"FENGYUN 1C DEB" can refer to any of the pieces of debris that resulted from the ASAT test on the Fengyun-1C spacecraft. On the other hand, when a new piece of debris from the ASAT test is tracked it is added to the satellite catalogue with a new, unique number. Figure 3.24 shows the network generated from the SOCRATES report on 29th October 2009 with the vertices representing satellite names. Figure 3.25 shows the network generated from the SOCRATES report on 29th October 2009 with the vertices representing satellite numbers. The two networks are compared in Table 3.6.

The network in Figure 3.24 is 75% smaller than the Figure 3.25 network and has 60% fewer conjunctions. In addition, the 'names' network appears to be more robust than the 'numbers' network: the 'names' network has $d_{ij(max)}$=8 whereas the 'numbers' network has $d_{ij(max)}$=18, the geodesic of the 'names' network is 2.2 times smaller then in the 'numbers' network, and the 'numbers' network is less connected than the 'names' network, with β=1.783 and β=4.243 respectively. However, the differences in these measures are artefacts of using

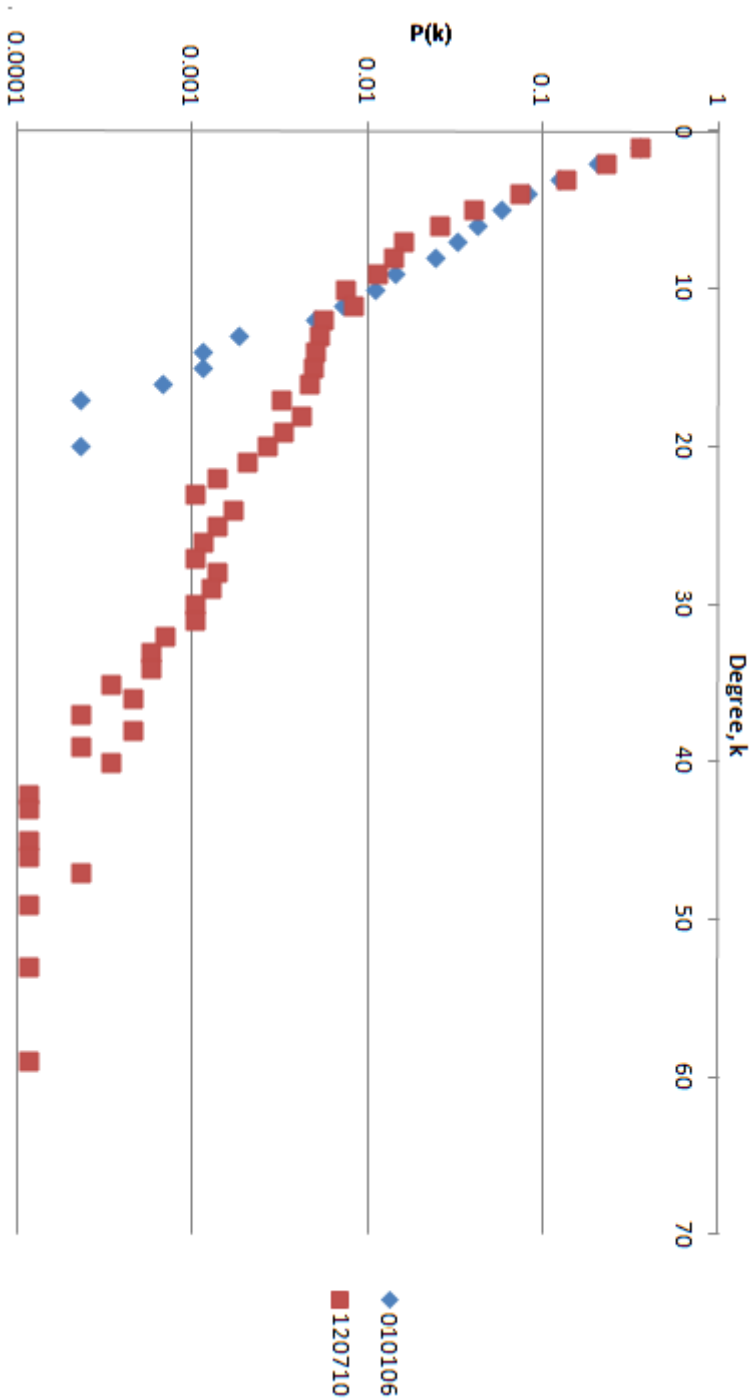

Figure 3.23: Comparison of degree distributions between SOCRATES reports on 1st January 2006 and 12th July 2010.

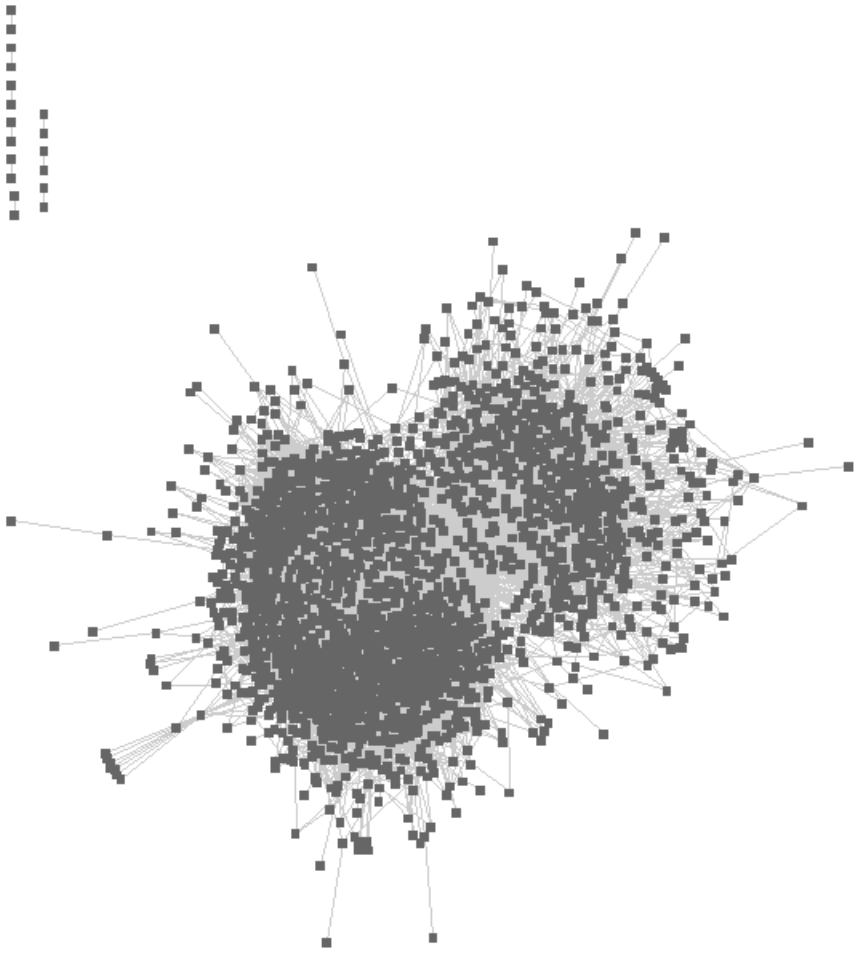

Figure 3.24: Network of generated from SOCRATES report 291009(1244) based on satellite names.

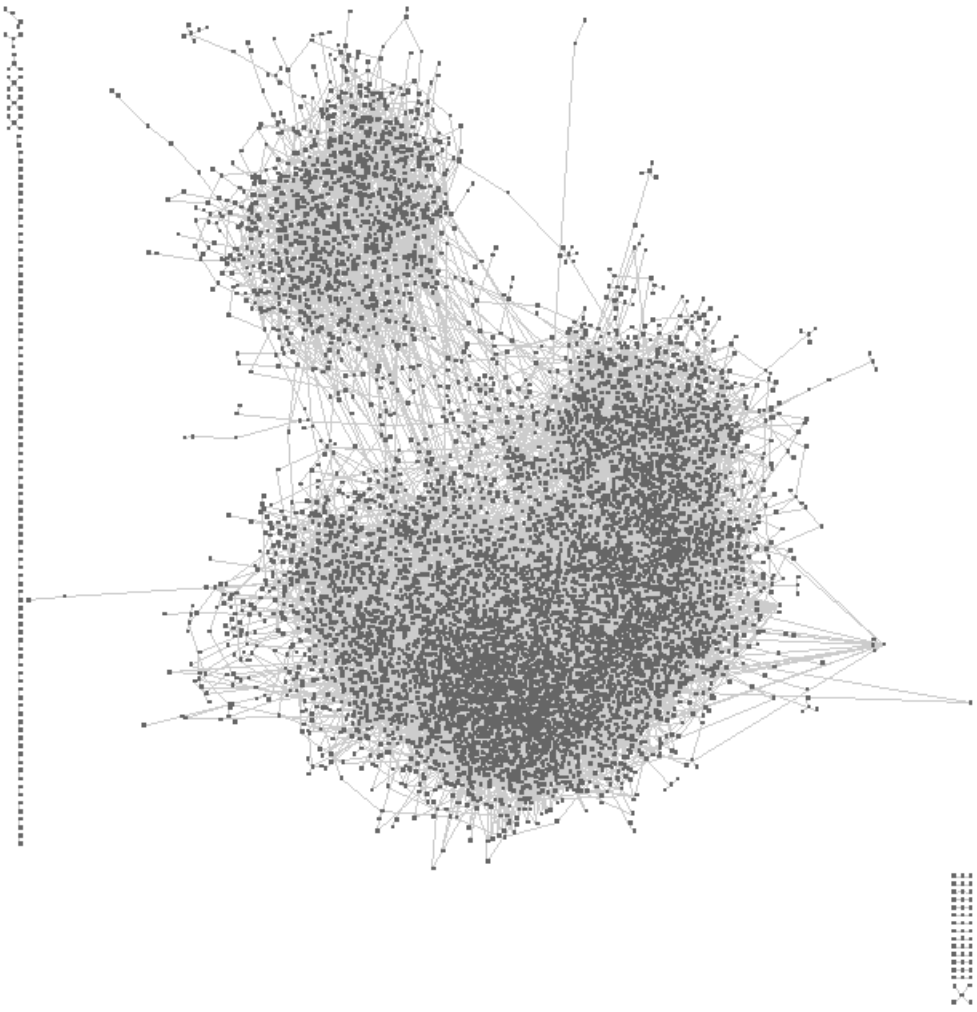

Figure 3.25: Network generated from SOCRATES report 291009(1244) based on satellite catalogue numbers.

Table 3.6: Network measures for networks built using satellite catalogue numbers and satellite names.

	SOCRATES 291009(1244) (names)	**SOCRATES 291009(1244) (numbers)**
Order	2050	8151
Size	8699	14536
Beta Index	4.243	1.783
Diameter	8	18
Geodesic	2.954	6.605
Network maximum degree	980	73
Network Degree	8.487	3.567
Assortativity coefficient	-0.28	-0.31
Clustering	0.104	0.004
Closeness	0.0014	0.0007
Betweenness	7961.58	59546.9

non-unique names to represent the data.

This problem is most clearly seen when comparing the vertices with the maximum degree in the networks. In the 'names' network (Figure 3.24) the vertex with the maximum degree is "Fengyun-1C debris" with 980 neighbours. In reality, there are 1,883 unique pieces of Fengyun-1C debris in the dataset that are represented as individual objects in Figure 3.25. This difference highlights the importance of using unique numerical identifiers when referring to a satellite or debris object to ensure that there is no ambiguity in identification (Kelso, 2004). Therefore, all subsequent SOCRATES networks are generated using the unique satellite numbers.

Chapter 4

CASE STUDIES

The case studies presented in this chapter are used to investigate complimentary approaches to those ADR strategies reviewed in Section 1.3. The case studies also provide a follow-up to the analysis of the DAMAGE and SOCRATES networks in Sections 3.1.3 and 3.2.3, respectively. In Section 3.1.3 it was shown that networks built using data from DAMAGE simulations are disassortative with hubs. The presence of hubs indicated that by targeting vertices of high degree or betweenness centrality, the networks can be broken down. This breakdown would reduce the number of collision feedback routes, but will not necessarily prevent collisions or conjunctions. In Section 3.2.3 it was shown that networks built using SOCRATES conjunction assessments were also disassortative with hubs up to degree $k = 73$ with diameter, $d_{ij(max)}$ up to 20 which indicates that the networks are robust.

Case Study 1 will investigate the effectiveness of targeting objects based on their weighted properties to investigate the hypothesis that weighted networks are vulnerable to centrality driven attacks (DallAsta et al., 2006). In addition, this case study addresses a deficiency in network theory, namely that; the characteristics of an object, such as mass, are labelled as vertex attributes, and no method yet exists to analyse networks that are initially weighted according to their vertices (Bullock, 2009). However, in the space debris environment, the outcome of a conjunction depends upon the mass of the objects involved (Eq.

1.3). Therefore, weighting a network according to the mass of the objects is not an unreasonable approach (Newland et al., 2009).

Case Study 2 will investigate the effectiveness of targeting objects based on their centrality to test the findings of Albert et al. (2000) and Holme et al. (2002). Albert et al. (2000) found that targeting objects on a disassortative network reduces the connectivity of the network more effectively than random removals. Holme et al. (2002) found that the removal of vertices from a network based on the degree and betweenness centralities of the vertices are more harmful than attack strategies based on the initial network, which suggests that the network structure changes as important vertices or edges are removed. If removals based on centrality measures are found to be the most effective, then the values can be recalculated within a DAMAGE simulation each year that objects are removed.

It is expected that using weighted target criteria and criteria based on centrality measures will both be more effective at reducing the connectivity of the network than random removals. Furthermore, it is expected in all cases (targeted and random) that the greatest overall reduction of the debris population will be seen the more objects that are removed.

4.1 CASE STUDY 1: Removals based on weighted measures

4.1.1 Method

This study involved testing the hypothesis that the discriminating power of a network weighted by its edges, combined with statistics that incorporate the weights of the vertices is necessary to achieve the goal of formalising criteria for debris mitigation and removal (Lewis et al., 2010). A 21-year (2009–2030) NFL scenario with 20 MC runs was used by DAMAGE to provide data for this case study. In each of the 20 MC runs, information was recorded about the collision events between intact vs. intact and intact vs. fragment objects $\geq$ 10 cm. The recorded information included the identification, mass, size and orbit of each

object, as well as the collision probability and energy. ADR begins in 2009 and five objects are removed per year until 2030. Five is proposed as the recommended minimum number of objects that need to be removed per year to stabilise the environment based on the findings of Liou and Johnson (2009).

The following six scenarios were compared:

1. No collisions
2. No ADR
3. Removals based on mass $\times$ probability
4. Random removals
5. Removal based on strength
6. Removals based on mass $\times$ strength

4.1.2 Results

The effective number of objects in LEO over the projection period for the benchmark 'Collisions' scenario is shown in Figure 4.1. After an initial decrease, the lack of remediation results in a rise in the population because of collision activity occurring during the projection period. The population falls after 2025, but increases again due to collisions at the end of the simulation. In contrast, the 'No collisions' scenario demonstrates an ideal outcome; collision activity is stopped in 2009 and the population at the end of the simulation is reduced by 30% compared to the start of the simulation. This reflects the results from Liou (2006) and Liou and Johnson (2006) which suggest that without ADR the debris population in LEO is likely to increase due to random collisions between existing on-orbit debris, even if there were no further launches.

Figure 4.2 shows the effect that the four different ADR scenarios have on the debris population. There is an immediate reduction in the population when the ADR strategies are implemented, but this is a random advantage that the ADR

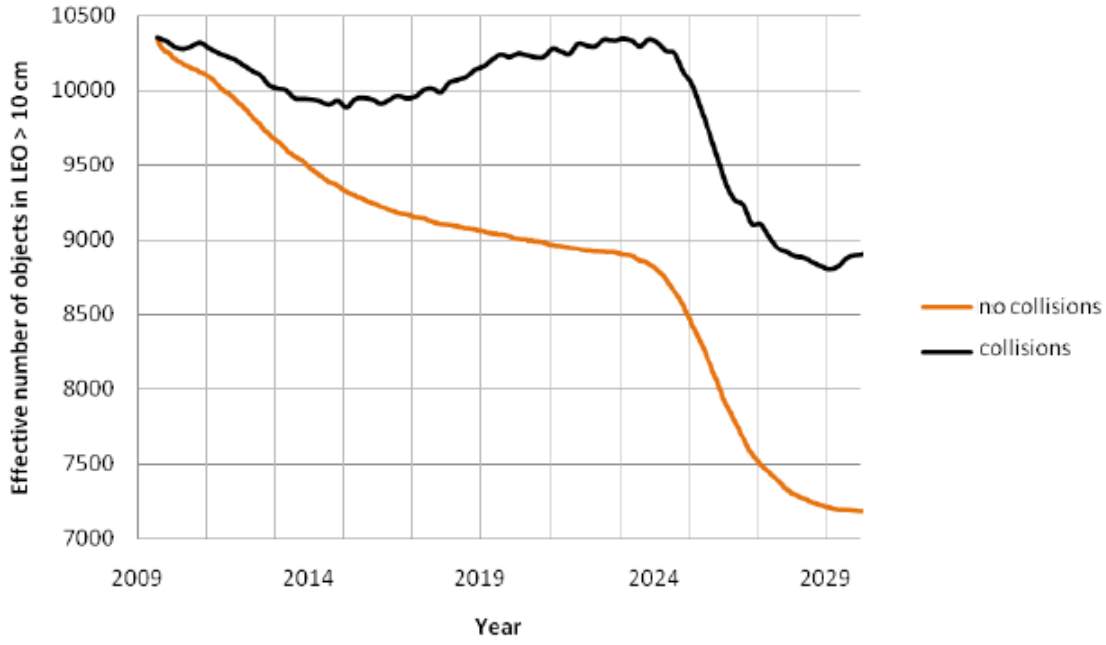

Figure 4.1: DAMAGE-simulated LEO debris populations between 2009 and 2030 for the 'No collisions' and 'Collisions' benchmark scenarios. There is no ADR in either scenario.

Scenario	**Average ERF**	**Average NERF**
Strength	4.54	0.30
Random	-0.21	-0.04
Mass × collision probability	3.98	0.25
Mass × strength	5.05	0.31

Table 4.1: Effectiveness measures for the four ADR scenarios.

scenarios have gained at the beginning of the simulation which is continued through to the end of the projection period.

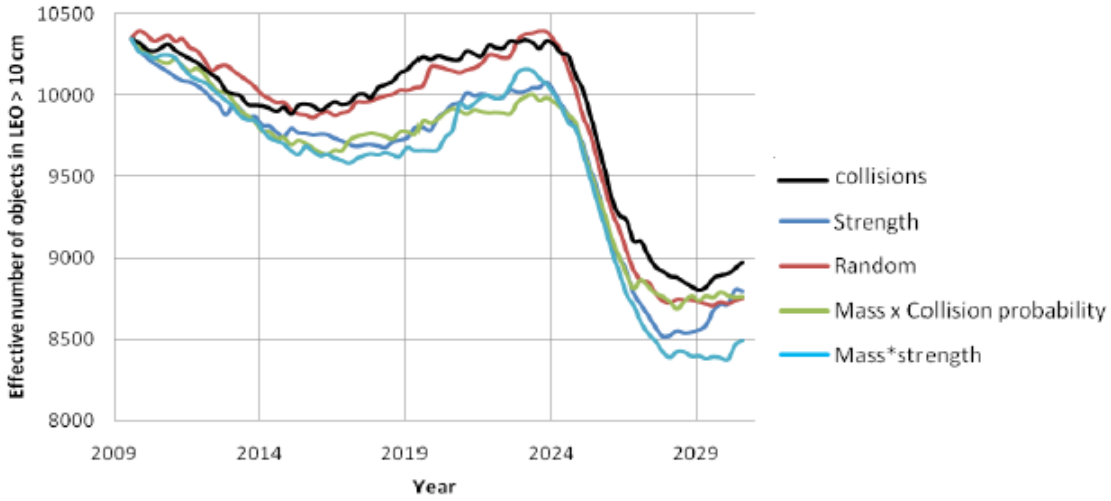

Figure 4.2: Effective number of objects in the 'Collisions' and the ADR scenario simulations in which removals were made randomly or based on strength, mass × collision probability, or mass × strength.

Figure 4.3 shows that the 'strength' and 'mass × collision probability' ADR strategies appear most effective for the first four years of the simulation due to the removal of objects that make a substantial contribution to future collision activity. After this, removals are not as effective but are still necessary for maintaining the impact of ADR on the LEO population, as shown by the NERF (Figure 4.4). For 70% of the projection period, the 'mass × strength' strategy is the most effective.

Table 4.1 shows the average ERF and NERF values for each ADR scenario. The ERF and NERF values for the random removal scenario are both negative

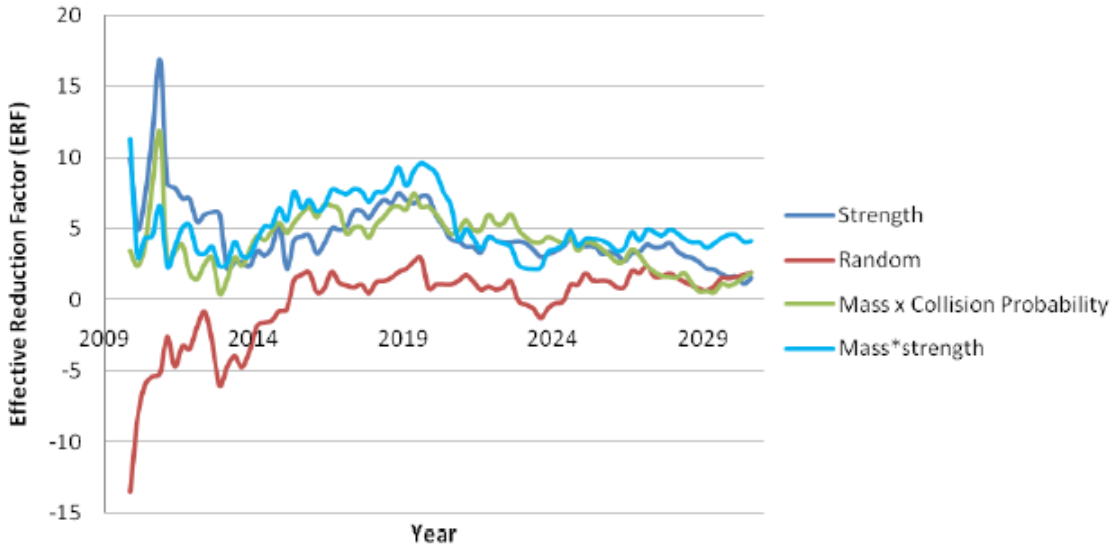

Figure 4.3: Effective Reduction Factor (ERF) between 2009 and 2030 for the four ADR scenarios.

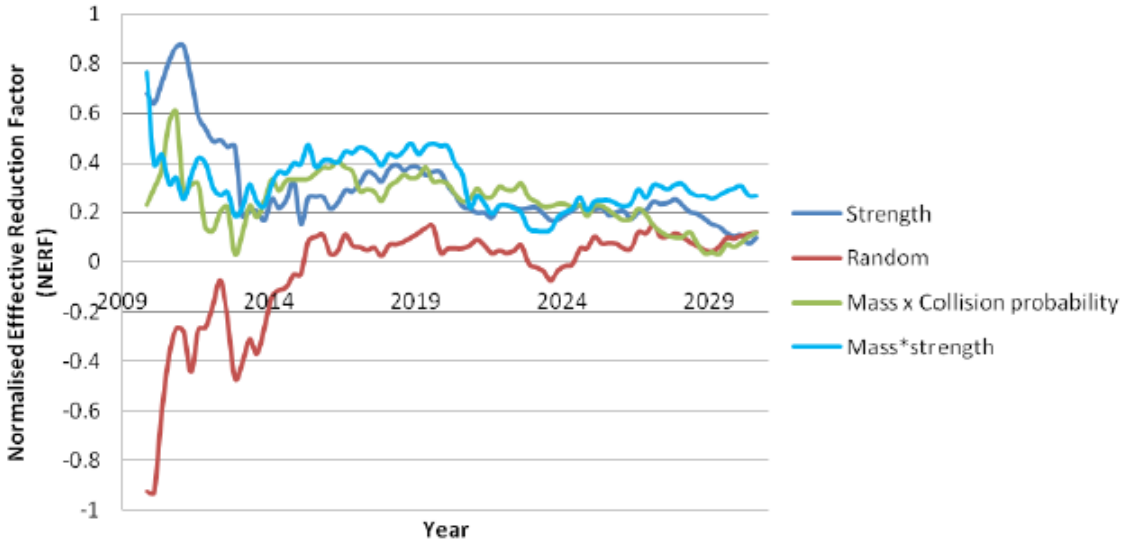

Figure 4.4: Normalised Effective Reduction Factor (NERF) between 2009 and 2030 for the four ADR scenarios.

suggesting that removing objects randomly is worse than the 'Collisions' scenario. However, this finding is counterintuitive because removing any number of objects should result in a reduction of the overall population. This problem may be an artefact of the small number of MC runs that were used. It indicates that the results are not reliable enough to draw meaningful conclusions.

In addition, the apparent effectiveness of each scenario will have been influenced by the short time period that the simulation spanned and the effects of the solar cycle. The simulated solar cycle accounts for the fall in the effective number of objects in Figures 4.1 and 4.2. This is seen by the fall in the effective number of objects, without ADR, due to the move towards solar cycle maximum. The simulation was not run for long enough to determine if it was only the effects of the solar cycle that made the ADR scenarios appear more effective than the 'Collisions' scenario in Figure 4.2. A repeat of this study would require more MC runs to provide reliable results and a longer simulation time so that the effects of ADR could be clearly distinguished from the influence of the solar cycle.

4.2 CASE STUDY 2: Removals based on centrality measures

4.2.1 Method

This two-part study used network centrality measures to identify target objects for removal in an ADR simulation. In the first part, a SOCRATES dataset from the 10th February 2009 is represented as a network. It is the final conjunction assessment before the collision between Iridium-33 and Cosmos-2251. This dataset was chosen to determine if the centrality measures identify either Iridium-33 or Cosmos-2251 as targets. It is expected that neither object will be identified because the network is built using SOCRATES data; data that did not indicate that the two objects would collide.

Five different removal scenarios are used to identify targets in the SOCRATES

network. The different strategies are:

1. Remove no objects (no-ADR, baseline scenario)
2. Random removal
3. Remove objects that have high degree only
4. Remove objects that have low closeness only
5. Remove objects that have high betweenness only

For each scenario the following network measures were recorded: order, size, beta index, diameter, geodesic, maximum degree, average degree, strength, assortativity, clustering, closeness, and betweenness centrality. This information indicated how the network changed when vertices were removed based on their centrality measures and random removal. The success of each of these strategies at reducing the number of objects on the network was measured using the Effective Reduction Factor (Eq. 1.2).

In the second part, after the most successful ADR strategy for short-term network breakdown was identified it was applied to DAMAGE simulations from 2009–2039. A BAU scenario with mitigation measures was used, in which future launches continued to occur to reflect as realistic a scenario as possible. In each of the 50 MC runs, DAMAGE recorded information about all of the conjunction events occurring between objects having a diameter $\geq$ 10cm. Five, ten, and 20 objects were removed each year based on the chosen ADR strategy. These removal strategies were compared to the baseline 'Collisions' and 'No collisions' scenarios. The effectiveness of each scenario was measured using the ERF and NERF.

4.2.2 Results

Network measures

The non-mitigation baseline scenario represents the initial network formed from the SOCRATES dataset (10th February 2009) before any vertices were

removed. Table 4.2 describes the baseline scenario network (1) and the networks representing various removal scenarios in which ten vertices were removed from the network (2-5).

The small change in the beta index ($0.607 < \beta < 0.621$) and the constant diameter ($d_{ij(max)}$=21) in all scenarios indicate that removing ten vertices from this network does not have a great impact on the network structure overall. This is also evidenced by the minor changes in the following measures: geodesic, average degree, strength, and clustering. Nevertheless, the aforementioned measures change the most for the scenarios based on centrality measures.

The change in maximum degree shows that in Scenario 2 only one hub has been removed ($k_{max(2)}$=81). However, all of the centrality measures are effective at targeting high degree objects, reducing the maximum degree of the network by half compared to the baseline scenario. Targeting objects based on their degree centrality (3) is the most effective ($ERF_3 = 13.5$). In this scenario the maximum degree is reduced by 63% meaning that there are less hubs in the network (compared to the baseline) and that the hubs that do remain are considerably smaller.

The assortativity coefficient of the baseline scenario (R_1=-0.233) indicates that the network is disassortative and contains hubs. The random removal scenario is the least effective ($ERF_2 = 1.7$) and the degree-based removal scenario is the most effective (ERF_3=13.5). However, the disassortativity values appear to disagree with the ERF results as the networks in Scenarios 3-5 are more disassortative than the baseline scenario (1). This is because only ten of the most central vertices were removed from each scenario, so hubs, even though slightly smaller, still remain and act to influence the assortativity of the network.

The assortativity, closeness centrality, and betweenness centralities on their own do not indicate whether or not the removals have been effective at altering the structure of the network. Furthermore, the betweenness centrality results highlight a problem with using only 50 Monte Carlo runs; the changes in the results are smaller than the errors. Thus, whilst the betweenness centrality

Table 4.2: Network measures for scenarios 1–5.

Scenario number	**1**	**2**	**3**	**4**	**5**
Scenario	**No ADR**	**Random removals**	**Degree-based**	**Closeness-based**	**Betweenness-based**
Vertices	6406	6389	6271	6324	6323
Edges	10557	10511	10133	10190	10250
Beta index	0.607	0.608	0.619	0.621	0.617
Diameter	21	21	21	21	21
Geodesic	7.14	7.15	7.29	7.29	7.32
Maximum degree	82	81	30	40	40
Network degree	3.30	3.29	3.23	3.22	3.24
Strength	8.76×10-6	8.75×10-6	8.51×10-6	8.33 ×10-6	8.48×10-6
Assortativity	-0.233	-0.234	-0.356	-0.359	-0.339
Clustering	0.005	0.005	0.004	0.004	0.004
Closeness	0.0010	0.0010	0.0010	0.0010	0.0010
Betweenness	49294	49159.8	49110	49510.1	49725.3
ERF	0	1.7	13.5	8.2	8.3

Vertex measure	Satellite	Ranking
Degree	Iridium-33	1730^{th}
	Cosmos-2251	373^{rd}
Betweenness	Iridium-33	1545^{th}
	Cosmos-2251	2472^{nd}
Closeness	Iridium-33	152^{nd}
	Cosmos-2251	203^{rd}

Table 4.3: Network measure rankings of Iridium-33 and Cosmos-2251.

increases for Scenarios 4 and 5, but decreases for Scenarios 2 and 3, the only meaningful observation is that the betweenness centrality remains high in all of the networks. This indicates that removing ten objects from a network of order, $n = 6406$ is not enough to significantly alter its structure even when vertices are targeted.

Finally, Table 4.3 shows how highly the vertices representing Iridium-33 and Cosmos-2251 were ranked compared to all of the vertices according to their degree, closeness, and betweenness centralities. The values show that neither vertex was ranked in the top ten for any of the three centrality measures and therefore, neither was removed from any of the scenarios.

4.2.3 Applying ADR to a DAMAGE simulation

The ERF values in Table 4.2 show that per vertex removed, the degree centrality is most effective strategy. A DAMAGE study was used to investigate how effective the removal based on degree strategy was when removing five, ten, or 20 objects per year as part of a 50 year simulation.

The effective number of objects in LEO over the projection period for the benchmark scenarios is shown in Figure 4.5. Overall, in a 'No collisions' scenario, the population decreases by ≈ 300 objects compared to the 2009 population. However, in the 'Collisions' scenario there is a population rise of ≈ 5000 objects.

Figure 4.6 shows the effect that the three different ADR scenarios have on the

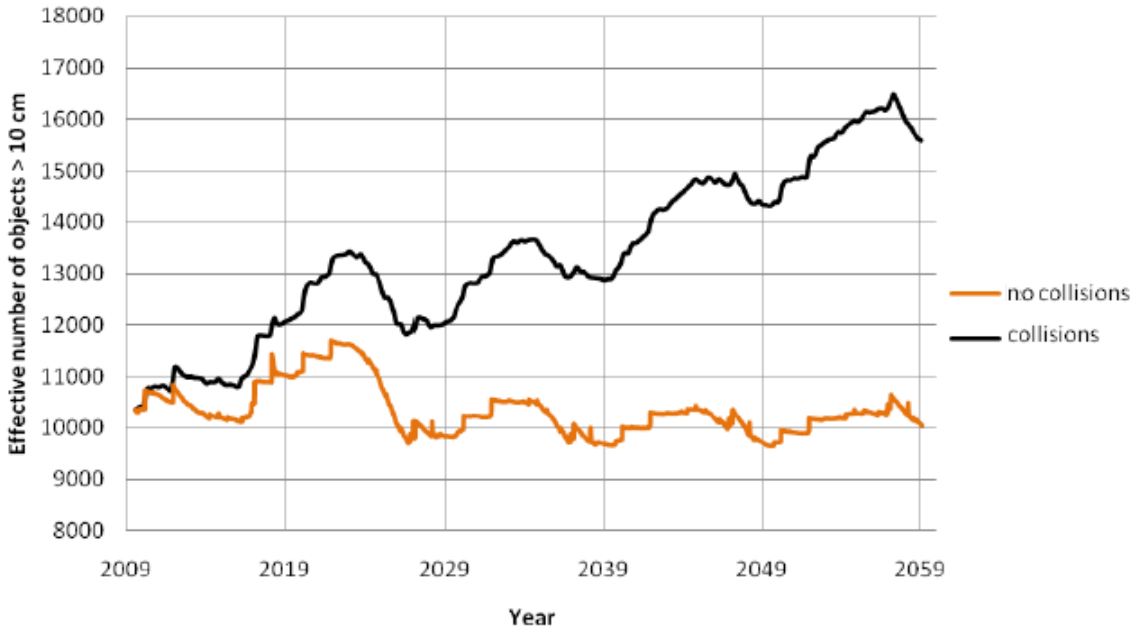

Figure 4.5: DAMAGE-simulated LEO debris populations between 2009 and 2059 for the 'No collisions' and 'Collisions' benchmark scenarios.There is no ADR in either scenario.

debris population during the course of the simulation. All of the ADR scenarios result in a smaller final population than a scenario without remediation. However, in all cases the population rises overall which suggests that ADR strategies based on degree centrality removing five, ten, or 20 objects are not effective enough to stabilise the environment.

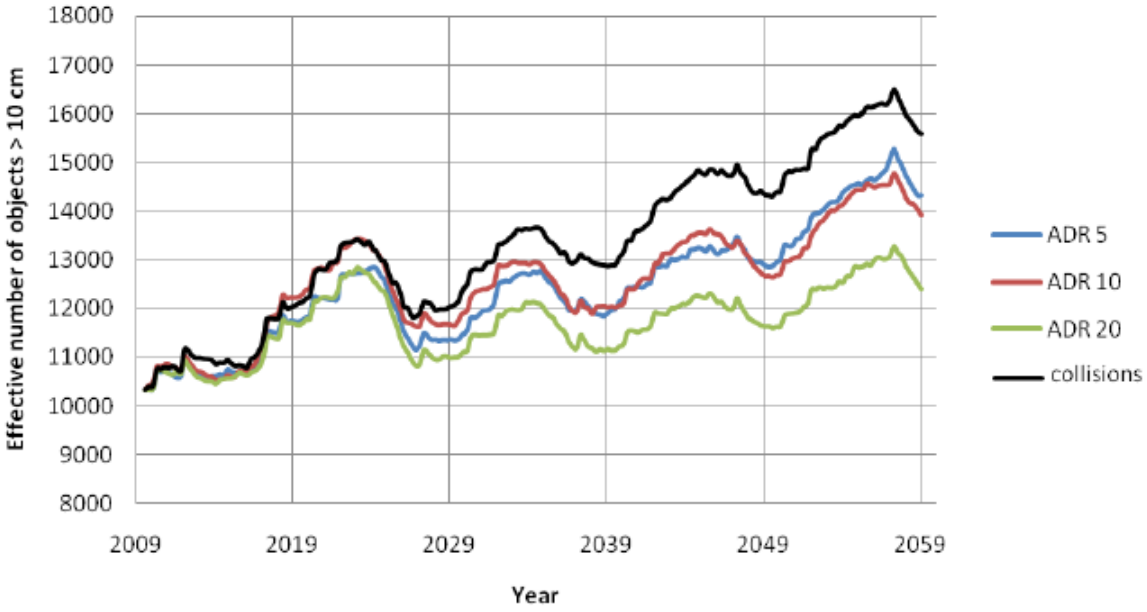

Figure 4.6: Effective number of objects in the 'Collisions' and three ADR scenario simulations in which five, ten, or 20 objects are removed per year.

Figures 4.7 and 4.8 show the variation in ERF and NERF values throughout the duration of the simulations. Table 4.4 shows the average ERF and NERF values for each ADR scenario.

Scenario	Average ERF	Average NERF
ADR 5	7.24	0.33
ADR 10	2.35	0.19
ADR 20	2.83	0.51

Table 4.4: Effectiveness measures three ADR scenarios removing five, ten, or 20 objects per year.

The ERF values in Figure 4.7 and Table 4.4 suggests that removing five objects each year is more effective than removing ten or 20 objects. This does not

correspond to the average effective number of objects in Figure 4.6 which shows that the ADR 5 scenario is the least effective of the scenarios compared to a 'Collisions' situation. This may be due to the use of ERF not NERF, thus the five removals appear more effective than they are. Figure 4.8 shows this is corrected when the target number of objects is taken into account; in fact, in the first year of the simulation, there is an increase in the effective number of objects in orbit despite the five removals in the ADR scenario.

The NERF values in Table 4.4 and Figure 4.8 show that removing the most objects each year (20) is the most effective strategy. The average NERF for ADR 20 is approximately double that of ADR 10; however, it is not four times larger than the ADR 5 scenario. This suggests the possibility that the ADR 10 scenario under-performed due to the occurrence of debris-generating events that increased the population more than the ADR could compensate for. However, it is more likely that the additional five objects in the ADR 10 scenario randomly have a smaller effect on the future enviroment than the five objects in the ADR 5 scenario. This is an artifact of only using 50 Monte Carlo runs.

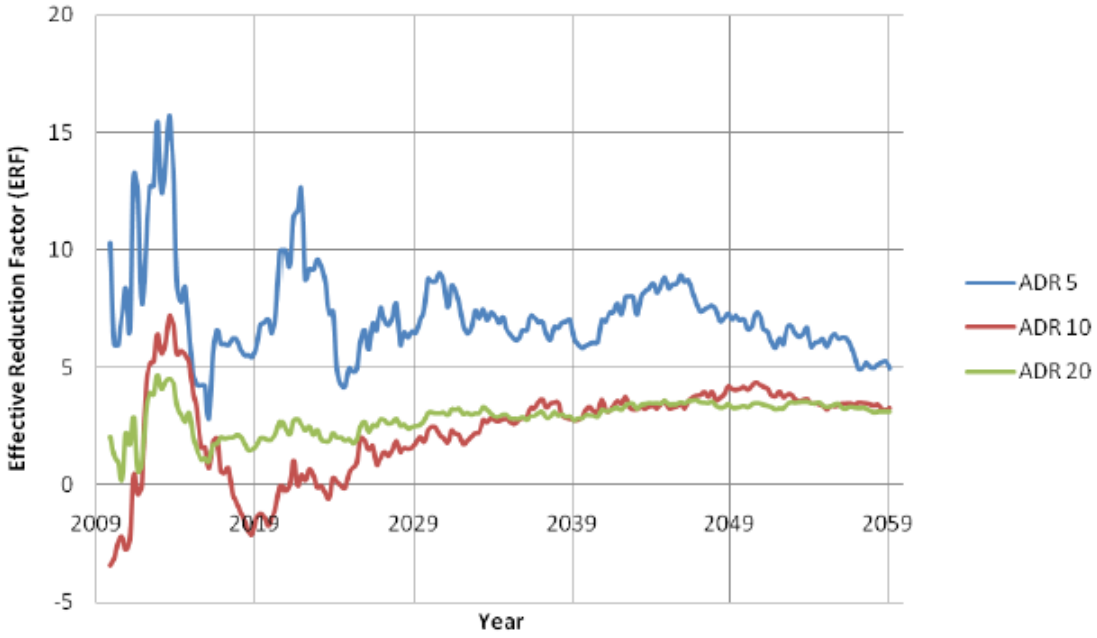

Figure 4.7: Effective Reduction Factor (ERF) between 2009 and 2059 for the three ADR scenarios.

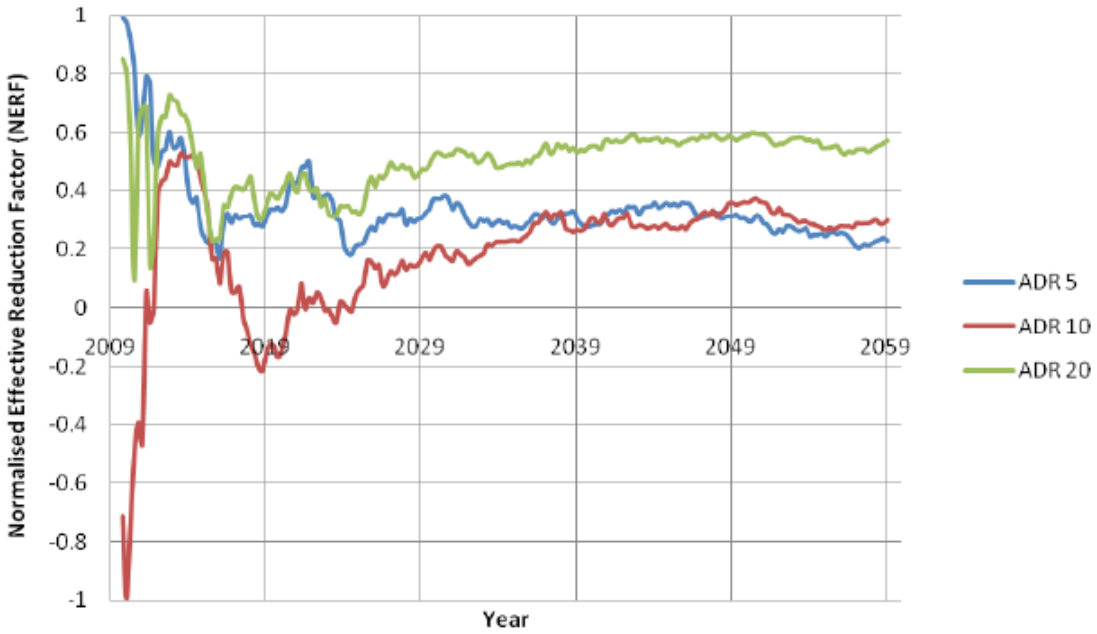

Figure 4.8: Normalised Effective Reduction Factor (NERF) between 2009 and 2059 for the three ADR scenarios.

Chapter 5

DISCUSSION

5.1 Using networks to represent various aspects of the SDE

The first aim of this thesis was to determine if networks could be created from the DAMAGE and SOCRATES datasets to provide a meaningful representation of the space debris environment. The finding is that it is possible to represent two specific aspects of the space debris environment on networks: conjunctions and the heritage of objects. Networks of conjunctions highlight the interactive, dependent nature of the space debris environment. Traditionally, other forms of modelling view individual conjunctions in isolation as single events. However, seen as part of a network, the conjunctions can be understood in terms of chains of events that lead to the overall instability of altitudes in LEO. Preventing these conjunctions, thus increasing the stability of the environment by the removal of objects, is the reasoning behind ADR.

As with conjunctions, individual objects in orbit are often treated in isolation. However, multi-relational networks representing the heritage of objects show that the source of individual objects can be traced back to a single launch vehicle or an explosion. The consequence of an explosion can be seen, not just by the production of debris, but as an additional number of conjunctions that

occur. This provides an indication of the risk that an exploding object poses to the instability of the environment in terms of the conjunctions that the resulting fragmentation debris may have with other objects in the future. Similarly, it further shows the risk that two colliding objects pose to the instability of the environment.This underscores the need for the continued application of mitigation measures and targeted ADR.

5.2 Analysing space debris networks to determine their characteristics

The second aim of this thesis was to analyse space debris networks to determine their characteristics. The networks analysed in Chapters 3 and 4 have provided an insight into the characteristics of space debris networks based on SOCRATES and DAMAGE datasets. It should be noted that, whilst the networks represent the datasets, the findings are based on small studies using data with inherent uncertainties (discussed in more detail in Section 5.3.2).

Disassortativity: The networks presented in this thesis are disassortative with values between $-0.359 < R < -0.185$. This disassortativity indicates that the space debris environment is similar to other 'real world' systems such as airline networks. Like airline networks, space debris networks contain hubs. Disassortative networks are robust to random removals, but vulnerable to targeted attacks on their hubs which indicates that targeted ADR will be an effective method of controlling the growth of the future debris population. However, there need to be enough removals to impact on the topology of the network. Case Study 1 and Case Study 2 showed that only removing between five and 20 objects, does not have much impact on the networks in terms of the changes to measures of robustness. Furthermore, it is not enough to just have target criteria, the criteria need to be effective.

Robustness: The evidence for describing space debris networks as robust is seen in the examples of DAMAGE and SOCRATES networks in Chapter 3 and in the case studies in Chapter 4. The DAMAGE networks built from an increasing

number of Monte Carlo runs (Figures 3.11 to 3.14) show the formation of a giant component after the addition of only 4 MC runs. Analysis of SOCRATES networks shows an increase in the robustness of the networks from β=1.490 to β=1.811 during the growth of the space debris environment between 2006 and 2010. This is reflected in the increased number of objects and greater number of conjunctions. Similarly, the diameter falls from 22 to 20 in the same time period indicating that more chains of conjunctions have formed. The robustness of both DAMAGE and SOCRATES space debris networks reflect the need for remediation of the environment.

Clustering: The lack of clustering on both DAMAGE and SOCRATES networks ($C \approx 0$) also indicates the presence of chains representing series of conjunction events. This means that there are not clusters of objects that could be targeted for removal in order to prevent conjunctions. Instead, the target criteria need to focus on objects with high centrality: either those that connect network components, or those that interact with many other objects. The near-zero value of clustering is unsurprising because high values of clustering are often associated with social networks instead of technological networks; social network literature uses it to describe network density because of the high occurrence of 'cliques' (clusters) of people (Newman, 2003). However, it is common to find 'substantial' values of clustering in a scale-free network, which also indicates that these space debris networks are not scale-free (Newman, 2003).

Centrality: In the example relating to Figure 3.8 it was shown that vertices on a chain with low degree centrality could have a high betweenness or low closeness centrality. Such objects could be potential targets to cut chains of conjunctions and reduce the robustness of the networks. However, it is expected that if network theory was to be used to determine ADR criteria, then removing the hubs would be the most cost-effective way of reducing the future growth of the environment. This is because Case Study 2 indicated that a removal strategy based on degree centrality would be the most effective at reducing future collisions. It was 7.9 times more effective than a random removal strategy, and 1.6 times more effective than the second best performing targeted strategy, based on betweenness centrality. Removing vertices with the highest degree

centralities would act to remove the largest hubs and change the degree distribution. Not only would the high degree vertices be removed, but the degree of their neighbours would also be reduced. Indeed, if their neighbours had degree, $k = 1$, then they would also be completely removed from the network.

Complexity: The network degree for DAMAGE and SOCRATES networks is $\bar{K} \approx 3$. This means that on average, each vertex is connected to three others. However, the disassortativity and degree distributions show that there are a few objects that are involved in many more conjunctions, up to $k_{max} = 82$. In addition, the degree distribution of the networks indicates that the space debris environment may be a complex system.

As noted in Section 2.2.6, the definition of complexity is ambiguous in the literature. However, the degree distribution of SOCRATES network in 2006 and 2010 in Figure 3.23 shows how the space debris environment may have evolved into a complex system. This is based on the calculation of the exponents of the two distributions, which lie between $1.745 < \gamma_{2006} < 2.948$ and $1.797 < \gamma_{2010} < 2.420$. In addition, on the 2010 distribution, there is a 'fat tail' with a wide spread of high degree hubs up to a maximum degree of $k_{max} = 59$. The appearance of the larger hubs is supported by the increase in disassortative mixing seen in the 2010 network. Furthermore, the DAMAGE networks built from an increasing number of Monte Carlo runs in Section 3.1.3 show the formation of a giant component after the addition of only three MC runs. This indicates a robust network, but also the emergence of structure which is another characterisation of complexity according to Calderelli and Vespignani (2007).

Complexity in the space debris environment may influence future policy decisions and would reinforce the need for networks in addition to other techniques for modelling aspects of the debris environment and ADR strategies. This is because the nature of a complex system links to the benefits provided by representing debris objects as a network: namely, that individual objects do not act in isolation. However, it is important to note that the space debris environment does not need to be complex in order to be modelled as a network.

5.3 Assessing the use of network theory for determining ADR target criteria

The third aim of this thesis was to assess the use of network theory as a method for determining ADR target criteria.

5.3.1 Advantages

ADVANTAGE: Network theory is a well-established visualisation and analysis tool that can be used to conceptualise and analyse large datasets comprised of thousands of individual components and interactions. Network theory is applied here to datasets containing up to 8,421 vertices and 15,251 edges. Network theory shows the result of a debris-generating event and how the space debris environment has increased in robustness and complexity as it has evolved.

ADVANTAGE: Network theory is a useful tool for understanding the effects of debris-generating events because data are not analysed in isolation. This means that the role of objects in a sequence of conjunction events can be analysed. For example, the 1,875 fragments generated by the collision between Iridium-33 and Cosmos-2251 have gone on to be involved in conjunction events with other objects. When the objects are represented on a multi-relational network, it becomes clear if they are involved in other conjunctions or if they are the parent objects of further debris. Thus, the benefits of implementing mitigation policies to prevent further explosions or ADR before a collision, can be seen. If the removal of objects via ADR is considered as a number of small-scale changes to a space debris network, then it is possible to conceptualise the improvements to the system as a whole in terms of chains of events. This is the basis for remediation; it is hoped that by removing a few objects, the collision rate will decrease.

ADVANTAGE: Network theory provides an alternative and complimentary approach to the existing proposed methods of determining ADR target criteria:

- Alary (2010) only focuses on object mass, ignoring the influence of

collision probability on the creation of debris. Networks can be weighted on either the mass of objects, or collision probability, or both.

- Talent (2009) assumes the removal of only one type of object. Multi-relational networks could be used to examine the removal of various types of objects in a series of scenarios.

- The Alfano et al. (2009) method uses SOCRATES conjunctions and takes close approaches of orbiting objects into account. This is necessarily similar to the network theory approach using networks built from the SOCRATES dataset. Therefore the networks share the same uncertainties, such as age of TLE data, as the Alfano et al. (2009) method.

- The methods proposed by McKnight (2010), Kawamoto et al. (2009), and Bastida-Virgili and Krag (2009) take into account the technological constraints that will be placed on ADR. Network theory can also accommodate technological considerations using weighted, multi-relational networks to constrain the selection of targets. For example, targeting areas of high spatial density (Kawamoto et al., 2009; Bastida-Virgili and Krag, 2009) relates to the use of degree centrality. This is because in areas of high spatial density there are more likely to be objects that could collide with many others. These would be represented by hubs on a network.

- Finally, the Liou and Johnson (2009) method is based on the calculation of the risk that an object poses to the environment in terms of its collision probability and mass. However, objects with a high collision risk that are not identified at the start of the simulation year can be left in a simulation and then go on to cause collisions. This can be overcome using network theory. Measures such as degree centrality or the weighted equivalent, strength, can identify all high risk objects from the outset. A variety of scenarios could be conducted to examine the role that each object played in the environment in a given simulation year. If necessary, this might indicate that more objects needed to be removed in one year than another.

5.3.2 Disadvantages

DISADVANTAGE: No formal method exists to analyse networks that are initially weighted according to their vertices (Bullock, 2009). This is a significant problem if networks are going to be used to determine target criteria for ADR. Ideally, vertices would be weighted according to the representative object's mass as the mass affects the outcome of a collision; for example, a collision between two objects of 200 kg and 100 kg objects would result in a higher number of fragments than in a collision between two objects with mass 2 kg and 1 kg. The research undertaken in 'Case Study 1: Removals based on weighted measures' tried to overcome the problem of not having a method to weight vertices by multiplying weighted measures based on edge properties with the object's mass. However, this did not overcome a second problem with unweighted vertices: not all objects in the environment are suitable for removal. In both the uni-relational and multi-relational networks that were studied in this thesis, the vertices were treated as if they were all suitable targets. However, this is not the case. In multi-relational networks (Figure 3.7) the 'launch group' was represented as a vertex, but this type of vertex does not represent a physical object therefore it cannot be removed. Furthermore, in the SOCRATES datasets some objects are given "unknown status" which means there is no way of telling if the object is suitable for removal. If network theory is used to formulate removal criteria for ADR a better solution is needed. Weighting vertices would provide a more robust, more accurate description of the environment as a network.

DISADVANTAGE: Uncertainties in the DAMAGE and SOCRATES datasets are directly incorporated into networks and their analysis. There are three types of uncertainty in models: *epistemic*, *aleatory*, and *deep*. Epistemic uncertainty is due to a lack of knowledge about the system that is being modelled and can be reduced if more information is acquired (Ross, 2006). An example of epistemic uncertainty in DAMAGE forecasts is the number of fragments produced by a collision. Ground tests are used to model the number of fragments produced by hyper-velocity impacts (Hanada and Liou, 2008). The results of these tests are incorporated into forecasts to reduce the uncertainty relating to fragment

generation. An example of epistemic uncertainty in the SOCRATES datasets is the quality of the TLE data. Epistemic uncertainty could be reduced with the implementation of a more comprehensive SSA program used to provide better quality TLE data.

In addition to epistemic uncertainty, SOCRATES does not give information about debris-debris conjunctions. This is because SOCRATES only aims to provide a service to satellite operators so that they can manoeuvre their assets if a conjunction is predicted (Kelso and Alfano, 2005). However, this means that networks built using SOCRATES are limited to only representing conjunctions involving satellites. If these networks were used for developing target criteria for ADR then debris objects that only pose a threat to other debris objects would not be considered as targets.

Aleatory uncertainty is the result of inherent variability and is irreducible (Pollard et al., 2002; O'Hagan, 2006). Sources of aleatory uncertainty are modelled as probability distributions (Oberkampf et al., 2004). Examples of aleatory uncertainty are conjunction probability in SOCRATES and collision probability in DAMAGE. Deep uncertainty arises as a result of a lack of knowledge about how a system acts as a whole even if the behaviour of individual parts is understood i.e. as a result of complexity (Bankes, 2002; Lempert, 2002). Deep uncertainty means that the effects of any one intervention in the system cannot be predicted with complete accuracy, because the system is always responding and adapting to changes (Glouberman et al., 2003).

Forecasting is based on the extrapolation of current and historical trends to identify future characteristics of a system (Dortmans, 2005). Sources of uncertainties in forecasting the evolution of the space debris environment include future launch traffic, explosion and collision rates, break-up processes, and solar activity (Martin et al., 2004; Klinkrad, 2006). As a result of the uncertainties, the models suffer from cumulative prediction errors that are magnified the longer the simulation runs. Despite the uncertainties, forecasting is, and will remain, a powerful tool for characterising and predicting trends in the long-term evolution of the space debris environment. However, alternatives

should be considered to complement forecasting for the development of remediation policies. A proposed method concerns the use of *adaptive policies* and *backcasting* (Lovins, 1977; Robinson, 1982). Adaptive policies are designed to change as time progresses based on new information; whereas, non-adaptive policies are not designed to change. Backcasting is a 'scenario analysis approach' which involves studying several alternative strategies designed to reach a predetermined 'ideal' future, and then forming adaptive policies with the objective of reaching that future (Robinson, 2003; Quist and Vergragt, 2006; Dortmans, 2005). According to Höjer and Mattsson (2000), backcasting is mainly appropriate where current trends are leading towards an unfavourable future; therefore it could be used for the development of ADR target criteria. The successful application of backcasting would require the definition of what the international community deemed to be an 'ideal' future.

The Monte Carlo method is used for analysing uncertainty parameters where the goal is to determine how random variation, lack of knowledge, or error affects the sensitivity, performance, or reliability of the system that is being modelled (Wittwer, 2004). However, using an average of MC runs increases the apparent effectiveness of the individual ADR strategies as the full range of outcomes is ignored. A future requirement for reliably identifying specific objects from networks as target objects, using DAMAGE simulations as a data source, is a study that determines how many MC runs are necessary to accurately determine the outcome of ADR removals.

5.4 Other issues

In addition to the aims set out at the beginning of this thesis, it is also important to discuss the technological, financial, political, and legal challenges that face ADR.

5.4.1 Technology

Drag augmentation, momentum exchange tethers, electrodynamic tethers, and attached propulsion modules are four potential ADR technologies discussed in Section 1.1.5. In addition to the specific disadvantages related to physically interacting with debris objects that need to be overcome before those technologies can be successful, two general issues also remain: capability for multiple removals and response time.

The need for multiple removals is a problem addressed by one modelling study discussed in the literature review (Bastida-Virgili and Krag, 2009), but it has not been considered in the network studies in this thesis. Unless all parts of a launch system are de-orbited, an ADR technology will leave at least one object in orbit by virtue of its launch; therefore, there is a need to remove at least two objects per ADR mission. Bonnal and Bultel (2009) discussed the need for a system capable of removing more than one object, stating that a large, modern launcher is capable of de-orbiting ten to 15 debris objects from LEO. The use of an ADR technology that can achieve multiple removals is likely to guide the selection of removal criteria to be based on targeting objects within specific inclinations bands to limit the ΔV required.

The required response time of ADR technology will depend on the method chosen to identify target objects. If the targets are selected based on conjunction assessments that identify them as at imminent threats (i.e. being involved in a conjunction that has a high collision probability) then the technology needs to be flexible and responsive. Having a responsive ADR system in place requires the development of 'extreme performance vehicles' to replace current inflexible systems and funding (Larrimore, 2007; Neyland, 2009). A concept such as 'Rapid Access to Space' is a flexible system that could meet this demand. 'Rapid Access to Space' is an operational philosophy that is designed to reduce launch costs using small and capable systems that can perform efficient orbit manoeuvres and transfers (Neyland, 2009).

5.4.2 Finance

The cost estimates for ADR vary depending on the proposed technology and the size and orbit of the debris object to be removed. As the IAA (2005) paper points out, financing ADR requires "spending now for future rewards" which is similar to the need for spending on remediation of other problems, such as climate change. According to Bellido (2010) and Alary (2010), ADR and its associated costs are considered small compared to the cost of the continued growth of the debris population and its associated risks: the increased risk of damage or loss of a satellite, increased insurance premiums, or the loss of access to space (Bellido, 2010). The total value of assets in orbit in 2009 was $4.2 trillion (Helly, 2009). On average satellites cost $500 million to replace (Vance, 2009). In this context, even at the upper end of the scale of proposed costs stated in Section 1.2 ($100 million per object), ADR appears to be cost-effective. However, this needs to be proven using a thorough cost-benefit analysis if ADR is to be funded.

To be considered cost-effective an ADR mission will need to remove the most objects that would otherwise contribute to the growth of the future space debris population, at the least cost per object. Maximising cost-effectiveness requires starting an ADR program early because the predicted exponential growth rate of the population means that the cost-benefit ratio of ADR will increase in the future (Eichler and Bade, 1993; Liou and Johnson, 2009; McKnight, 2009; Hoyt, 2009). McKnight (2010) summarises the benefits of starting ADR as soon as possible as, "Pay me now or pay me more later". This is because, the later ADR starts, the more objects will have to be removed to have the same effectiveness, with direct implications on the cost-benefit ratio of remediation (IAA, 2010).

The question of who will pay for ADR is also unresolved. A number of suggestions have been made: salvage contracts (White, 2009), bounties (Carroll, 2009), and 'eco-taxes' (Bonnal and Bultel, 2009).

- Salvage contracts: White (2009) believes that a treaty similar to the International Convention on Maritime Salvage (IMO, 1989) could be

applied to Earth orbit. A salvage convention would provide legal certainty and financial incentives for capturing, servicing, recycling, or relocating debris (White, 2009; Wagenbach, 2010).

- Bounties: Carroll (2009) proposes using a "Bounty and Fee" system. The fees would be designed to act as an incentive to satellite operators to encourage them to make decisions that will increase the sustainability of the space debris environment such as choosing where to leave their satellites at EOL. The fees would be used to pay the bounties on objects that were determined to be necessary for removal.
- Eco-tax: Bonnal and Bultel (2009) propose levying an 'eco-tax' if satellite operators do not comply with international space debris regulations. This is a form of the "Polluter Pays Principle" (OECD, 1972) originally introduced as a way to tackle the pollution that has contributed to climate change (Bradley and Wein, 2009).

5.4.3 International cooperation

Ensuring sustainable access and use of Earth orbit is a major international issue as the benefits gained from the use of space systems are shared by all stakeholders –commercial, civilian, and military (Brachet, 2010). It is already recognised that international cooperation is required for mitigation to succeed and for improving space situational awareness, as outlined for example, the US National Space Policy (2010). It follows that it is important to ensure that there is international understanding, cooperation, and participation in remediation. International cooperation may take the form of internationally agreed goals at the national level, as bilateral or multi-lateral agreements, or sharing the organisation of ADR planning between space agencies (Mejía-Kaiser, 2009). The 1987 Montreal Protocol (and its subsequent amendments) was designed to implement actions that would stop the depletion of the ozone layer (Protocol, 1987). It is an example of the success of a multi-lateral international agreement that was applied to address a global problem suggesting that a similar agreement could be put in place for ADR.

Liou (2011) summarises the international requirements for ADR as the "four critical C's" –consensus, cooperation, collaboration, and [financial] contributions. Specifically, agreement and cooperation is needed to:

- Define ownership of debris objects and liability: Whilst states are responsible for all of their space objects, ownership and liability disagreements lead to complicated legal issues (Mejía-Kaiser, 2009). Determining the cause of debris production and proof of liability is difficult, as proof of a violation of standard care and conduct by the launching state is required (Kunstadter, 2009).

- Share space situational awareness: International cooperation can be used to provide extensive, accurate spacecraft position data to aid remediation (Moran, 2009). Weeden (2009) recommends that an international discussion on the problem of sharing space situational awareness data is initiated that does not involve forcing a state to reveal classified information.

- Make assurances that ADR technology will not be used as a space weapon: Removing objects from orbit without prior consent could be considered a belligerent act (Mejía-Kaiser, 2009). Without international cooperation there is a risk that some states may oppose ADR, perceiving it as a threat. In addition, there needs to be general international agreement and transparency on the technical merits of removing objects (Weeden, 2009).

Chapter 6

CONCLUSIONS

The overall aim of this thesis has been to apply network theory to datasets that represent the space debris environment with a view to developing target criteria for ADR. An important part of this has been using network and vertex measures to characterise the environment to understand its structure and show how debris-generating events impact on the environment as a whole. The adverse effects of fragmentation events are clearly shown in the changes between networks based on SOCRATES conjunction assessments in 2006 and 2010.

ADR will be considered effective if it leads to long-term stability of the environment i.e. resulting in a negative growth rate of objects large enough to cause catastrophic collisions (IAA, 2010). The ERF and NERF provide quantitative measures of the effectiveness of an ADR scenario in a simulation model (Lewis et al., 2009b). Nevertheless, difficulties in defining the success of an operational solution still remain, because changing the environment in any way through removal or addition of objects affects the future of the environment. This needs constant review using simulation modelling.

In Chapter 1 the 'best case scenario' future simulations carried out by Liou (2010a) showed that the debris population will increase in the future due to collisions even if launches are stopped. This underlines the need to prevent future collisions through the targeted removal of debris and the continued application of mitigation measures for spacecraft at their EOL. Using networks

to represent space debris reinforces these concepts because the approach has shown: how robust the space debris environment is with the existence of chains of conjunction events, the potential complexity of the environment, disassortative mixing which has lead to the formation of hubs, and the dependent nature of the interactions which mean that individual objects should not be treated in isolation.

Chapter 3 showed how well suited network theory is to representing space debris environment data, using both DAMAGE and SOCRATES datasets. The small uni-relational DAMAGE networks highlighted key topological features such as the importance of vertices with low degree and high betweenness centrality to the structure of the network and the maintenance of the giant component. The multi-relational DAMAGE networks indicated the potential of representing different types of objects and their heritage with different vertices and edges. SOCRATES datasets only represent conjunctions between payloads and other objects (including debris) and therefore each edge on the network is connected to at least one payload. It is expected that the networks would appear even more robust if debris vs. debris conjunctions were also represented. This is because there would be more objects involved in conjunctions, and thus there would be more vertices and more edges on the networks. This would increase the size of the giant component and likely reduce the network diameter.

The examples in Chapter indicate that network theory can be successfully applied to datasets that represent the space debris environment to determine its unique characteristics. The findings indicate that the networks have weaknesses that can be exploited through the development of effective target criteria. The SOCRATES networks in Chapter 3 indicated the high robustness and potential complexity of the space debris environment based on conjunctions between satellites and debris. However, the case studies in Chapter 4 did not conclusively find that network theory could be used to identify target objects for ADR. Although progress has been made with the application of network theory to the problem of determining target criteria for ADR there is certainly the capacity for further research. One idea for future work would be using network theory in reverse to the methods applied in this thesis. Instead of trying to identify

targets based on vertex measures, vertex measures of targets chosen by another method could be analysed. In this way, a question such as "How important are rocket bodies to the robustness of the network?" could be answered.

The space debris environment is a dynamic system that evolves over time. However, the networks in this thesis represent static situations that do not respond to the removal or addition of vertices. Thus, it would be more accurately represented by temporal networks based on a series of SOCRATES conjunction assessments or DAMAGE datasets constructed at each time step during a simulation. This way, the evolution of the space debris environment could be understood in terms of the development of hubs or the removal of target objects. As not all debris objects are possible targets for removal, this information needs to be incorporated into a network before reliable criteria can be established. Therefore, the networks would be multi-relational and weighted in a way that reflected the ability or inability for an object to be removed.

There are many problems associated with ADR that need to be solved before it can successfully take place, for example, the determination of target criteria and for the existing technical, political, financial, and legal issues. However, the research here shows that network theory could theoretically be used to create target criteria for ADR. This thesis shows that 'space debris networks' are robust and disassortative. Although there are limitations due to the uncertainties in the data used to create the networks, the findings suggest that careful development and application of target criteria would result in successful ADR.

Bibliography

Achacoso, T. B. and Yawamoto, W. S. (1992). *AY's Neuroanatomy of C.Elegans for Computation*, CRC Press, Boca Raton, USA.

AGI (2011). STK/Conjunction Analysis Tools (CAT), `http://www.agi.com/products/by-product-type/applications/stk/add-on-modules/stk-conjunction-analysis-tools/`.

Alary, D. (2010). A system view of large debris removal: technical and non-technical issues, *1st European Workshop on Active Debris Removal*, Paris, France.

Albert, R., Albert, I. and Nakarado, G. L. (2004). Structural vulnerability of the North American power grid, *Physical Review E* **69**: 025103 1–4.

Albert, R. and Barabàsi, A.-L. (2002). Statistical mechanics of complex networks, *Reviews of Modern Physics* **74**: 47–97.

Albert, R., Jeong, H. and Barabàsi, A.-L. (2000). Error and attack tolerance of complex networks, *Nature* **406**: 378–382.

Alby, F. and Bonnal, C. (2010). Welcome to the workshop, *1st European Workshop on Active Debris Removal*, Paris, France.

Alfano, S. (2006). Satellite collision probability enhancements, *Journal of Guidance, Control, and Dynamics* **29**(3): 588–592.

Alfano, S., Finkleman, D., Kelso, T. S., Vallado, D. and Oltrogge, D. L. (2009). Identifying threatening objects for removal and planning missions and

architecture to avoid collisions, *DARPA/NASA Orbital Debris Removal Conference*, Chantilly, VA, USA.

Ash, R. L., O'Donoghue, P. J., Chambers, E. J. and Raney, J. P. (1993). A methodology for selective removal of orbital debris, *Advances in Space Research* **13**(8): 243–247.

Bagler, G. (2009). Complex network view of performance and risks on airport networks, *in* Larauge, P B and Castille, M E (eds), *Airports: Performance, Risks, and Problems*, Nova Science, New York, USA.

Bankes, S. C. (2002). Tools and techniques for developing policies for complex and uncertain systems, *PNAS* **99**(3): 7263–7266.

Bar-Sever, Y. and Kuang, D. (2004). New empirically derived solar radiation pressure model for global positioning system satellites, *Technical report*, InterPlanetary Network.

Bar-Yam, Y. (1997). *Dynamics of Complex Systems*, Perseus Books, Reading, MA.

Barabàsi, A.-L. (2007). The architecture of complexity, *IEEE Control Systems Magazine* pp. 33–42.

Barabàsi, A.-L. and Albert, R. (1999). Emergence of scaling in random networks, *Science* **286**: 509–512.

Barabàsi, A.-L. and Bonabeau, E. (2003). Scale-free networks, *Scientific American* **288**(5): 50–59.

Barabàsi, A.-L., Ravasz, E. and Vicsek, T. (2001). Deterministic scale-free networks, *Physica A* **299**: 559–564.

Barthelémy, M. (2004). Betweenness centrality in large complex networks, *The European Physical Journal B* **38**(2): 163–168.

Bastida-Virgili, B. and Krag, H. (2009). Strategies for active removal in LEO, *5th European Conference on Space Debris*, Darmstadt, Germany.

Bellido, E. (2010). Orbit servicing solutions for space debris mitigation, *1st European Workshop on Active Debris Removal*, Paris, France.

Bendisch, J., Wegener, P. and Rex, D. (1997). The long-term evolution of debris orbits in view of spatial object accumulation, *2nd European Conference of Space Debris*, ESA, Darmstadt, Germany, p. 345.

Benson, T. (2011). Glenn Research Center, `http://www.grc.nasa.gov/WWW/k-12/airplane/airprop.html`.

Bischof, B., Kerstein, L. and Starke, J. (2002). Robotic geostationary orbit restorer (ROGER), *34th COSPAR Scientific Assembly*, Houston, USA.

Boccaletti, S., Latora, V., Moreno, Y., Chavez, M. and Hwang, D.-U. (2006). Complex networks: Structure and dynamics, *Physics Reports* **424**: 175–308.

Bonacich, P. (1987). Power and centrality: A family of measures, *American Journal of Sociology* **92**(5): 1170–1182.

Bonnal, C. and Bultel, P. (2009). High level requirements for an operational space debris deorbiter, *DARPA/NASA Orbital Debris Removal Conference*, Chantilly, VA, USA.

Borgatti, S. P. (2005). Centrality and network flow, *Social Networks* **27**: 55–71.

Brachet, G. (2010). Sustainability of space activites, *1st European Workshop on Active Debris Removal*, Paris, France.

Bradley, A. M. and Wein, L. M. (2009). Space debris: Assessing risk and responsibility, *Advances in Space Research* **43**(9): 1372–1390.

Brilliantov, N. V., Krapivsky, P., Schmidt, J. and Spahn, F. (2009). On the distribution of particle sizes in saturns rings, *European Planetary Science Congress*, Potsdam, Germany.

Brookes, C. J. (1994). Evaluation of odd zonal harmonics in the Earth's gravitational potential, *Proceedings of the Royal Society of London. Series A, Mathematical and Physical Sciences* **446**(1926): 149–168.

Bullock, S. (2009). Personal communication.

Calderelli, G. and Vespignani, A. (2007). Large scale structure and dynamics of complex networks, *in* G. Calderelli and A. Vespignani (eds), *Complex Systems and Interdisciplinary Science*, Vol. 2, World Scientific Publishing Co. Pte. Ltd., City of Singapore, Singapore, pp. 5–16.

Carley, K. M. (2009). Dynamic network analysis, *NRC workshop on Social Network Modeling and Analysis*, Carnegie Mellon University.

Carpenter, M. A. and Stajkovic, A. D. (2006). Social network theory and methods as tools for helping busness confront global terrorism: capturing the case and contingencies presented by dark social networks, *in* G. G. S. Suder (ed.), *Corporate Strategies Under International Terrorism and Uncertainty*, Edward Elgar Publishing Limited, Cheltenham, UK, pp. 7–19.

Carreras, B. A., Lynch, V. E., Sachtjen, M. L., Dobson, I. and Newman, D. E. (2001). Modeling blackout dynamics in power transmission networks with simple structure, *34th Hawaii International Conference on System Sciences*, Maui, Hawaii.

Carroll, J. (2009). Bounties for orbital debris threat reduction, *DARPA/NASA Orbital Debris Removal Conference*, Chantilly, VA, USA.

Carvahlo, R., Bono, F., Gutiérrez, E., Just, W. and Arrowsmith, D. (2009). Robustness of trans-European gas networks, *Physical Review E* **80**: 016106 1–9.

Chapman, P. K. (2010). Deploying SunSats, *Online Journal of Space Communication* **16**.

Chassin, D. P. and Posse, C. (2005). Evaluating North American electric grid reliability using the Barabsi-Albert network model, *Physica A* **355**: 667–677.

Christiansen, E. L., Hyde, J. L. and Bernhard, R. P. (2004). Space shuttle debris and meteoroid impacts, *Advances in Space Research* **34**: 1097–1103.

Christley, R. M., Pinchbeck, G. L., Bowers, R. G., Clancy, D., French, N. P., Bennett, R. and Turner, J. (2005). Infection in social networks: Using network analysis to identify high-risk individuals, *American Journal of Epidemiology* **162**(10): 1024–1031.

Clauset, A., Shazili, C. R. and Newman, M. E. J. (2009). Power-law distributions in empirical data, *SIAM Review* **51**: 661–703.

Cline, M. S., Smoot, M., Cerami, E., Kuchinsky, A., Landys, N., Workman, C., Christmas, R., Avila-Campilo, I., Creech, M., Gross, B., Hanspers, K., Isserlin, R., Kelley, R., Killcoyne, S., Lotia, S., Maere, S., Morris, J., Ono, K., Pavlovic, V., Pico, A. R., Vailya, A., Wang, P.-L., Adler, A., Conklin, B., Hood, L., Kuiper, M., Sander, C., Scwikowski, I., Schmulevich, B., Warner, G., Ideker, T. and Bader, G. (2007). Integration of biological networks and gene expression data using cytoscape, *Nature Protocols* **2**: 2366–2382.

Cohen, R., Erez, K., ben Avraham, D. and Havlin, S. (2000). Resilience of the internet to random breakdowns, *Physical Review Letters* **85**(21): 4626–4628.

Collier, J. (2004). Self-organization, individuation, and identity, *Revue Internationale de Philosophie* **228**: 151–172.

Collier, J. and Burch, M. (1998). Order from rhythmic entrainment and the origin of levels through dissipation, *Symmetry: Art and Science* **9**: 2–4.

Comellas, F. and Miralles, A. (2009). Modelling complex networks with self-similar outerplanar unclustered graphs, *Physica A* **388**(11): 2227–2233.

Corporation, G. (1988). Concept evaluation/test for the tumbling satellite retrieval kit, *Technical report*, Grumman Corporation, Space Systems Division.

Crucitti, P., Latora, V. and Marchiori, M. (2004). A topological analysis of the Italian electric power grid, *Physica A* **338**: 92–97.

CSSI (2011). Center for Space Standards and Innovation, `http://www.centerforspace.com/`.

DallAsta, L., Barrat, A., Barthelémy, M. and Vespignani, A. (2006). Vulnerability of weighted networks, *Journal of Statistical Mechanics* **4**: P04006.

Dekker, A. H. and Colbert, B. D. (2004). Network robustness and graph topology, *27th Australasian Computer Science Conference*, Dunedin, New Zealand.

Donath, T., Schnildkrecht, T., Brousse, P., Laycock, J., Michal, T. and Ameline, P. (2005). Proposal for a European space surveillance system, *4th European Conference on Space Debris*, Darmstadt, Germany, pp. 31–38.

Donato, D., Laura, L., Leonardi, S. and Millozzi, S. (2007). Modeling the webgraph: How far we are, *in* G. Calderelli and A. Vespignani (eds), *Large Scale Structures and Dynamics of Complex Networks*, Vol. 2, World Scientific Publishing Co. Pte. Ltd., City of Singapore, Singapore, pp. 133–161.

Dorogovtsev, S. N. and Mendes, J. F. F. (2002). Evolution of networks, *Advances in Physics* **51**(4): 1079–1187.

Dortmans, P. J. (2005). Forecasting, backcasting, migration landscapes and strategic planning maps, *Futures* **37**: 273–285.

Dybiec, B., Kleckowski, A. and Gilligan, C. A. (2004). Controlling disease spread on networks with incomplete knowledge, *Physical Review E* **70**: 066145 1–5.

Eichler, P. and Bade, A. (1993). Strategy for the economical removal of numerous larger debris objects from Earth orbits, *Acta Astronautica* **29**: 29–36.

Emmert, J. T., Picone, J. M., Lean, J. L. and Knowles, S. H. (2004). Global change in the thermosphere: Compelling evidence of a secular decrease in density, *Journal of Geophysical Research* **109**(A02301).

ESA (2005). Space debris: Assessing the risk, `http://www.esa.int/SPECIALS/ESOC/SEMZL0P256E_0.html`.

ESA (2007). Space debris spotlight, `http://www.{ESA}.int/{ESA}CP/SEMHDJXJD1E_FeatureWeek_0.html`.

ESA (2009a). Scanning and observing, `http://www.esa.int/esaMI/Space_Debris/SEMD31WPXPF_0.html`.

ESA (2009b). Space debris: Analysis and prediction, `http://www.esa.int/esaMI/Space_Debris/SEMXP0WPXPF_0.html`.

ESA (2010). Space situational awareness: What is SSA?, `http://www.esa.int/ESAMI/SSA/SEMYTICKP6G_0.html`.

Faloutsos, M., Faloutsos, P. and Faloutsos, C. (1999). On power-law relationships of internet topology, *Proceedings of ACM SIGCOMM* .

Finkleman, D., Alfano, S., Johnson, T., Kelso, T. S., Vallado, D. and Oltrogge, D. (2008). Space debris birth to death analysis from concern to consequences, *Advanced Maui Optical and Space Surveillance Technologies*, Maui, Hawaii.

Fox-Keller, E. (2005). Revisiting "scale-free" networks, *BioEssays* **27**: 1060–1068.

Freeman, L. C. (1977). A set of measures of centrality based on betweenness, *Sociometry* **40**(1): 35–41.

Furukawa, Y., Masui, H., Toyoda, K. and Cho, M. (2009). Preliminary study of development of space debris removal method using electrostatic force, *DARPA/NASA Orbital Debris Removal Conference*, Chantilly, VA, USA.

Gallos, L. K., Cohen, R., Argyrakis, P., Bunde, A. and Havlin, S. (2005). Stability and topology of scale-free networks under attack and defense strategies, *Physical Review Letters* **94**: 188701 1–4.

Gladman, B. J., Davis, D. R., Neese, C., Jedicke, R., Williams, G., Kavelaars, J. J., Petit, J.-M., Scholl, H., Holman, M., Warrington, B., Esquerdo, G. and Tricarico, P. (2009). On the asteroid belts orbital and size distribution, *Icarus* **202**: 104–118.

Glouberman, S., Campsie, P., Gemar, M. and Miller, G. (2003). A toolbox for improving health in cities: A discussion paper, *Technical report*, The Caledon Institute of Social Policy.

Goh, K.-I., Kahng, B. and Kim, D. (2001). Universal behavior of load distributions in scale-free networks, *Phys. Rev. Lett.* **87**(27): 278701 1–4.

Goldstein, J. (1999). Emergence as a construct: History and issues, *Emergence: Complexity and Organization* **1**: 49–72.

Gradie, J. and Tedesco, E. (1982). Compositional structure of the asteroid belt, *Science* **216**: 1405–1407.

Gross, J. L. and Yellen, J. (2005). *Graph theory and its applications*, Vol. 2nd of *Discrete Mathematics and its applications*, Chapman & Hall, CRC, Boca Raton, Florida.

Hanada, T. and Liou, J.-C. (2008). Comparison of fragments created by low- and hyper-velocity impacts, *Advances in Space Research* **41**(7): 1132–1137.

Helly, J. J. (2009). Requirements analysis framework for an operational orbital debris removal system, *DARPA/NASA Orbital Debris Removal Conference*, Chantilly, VA.

Hidalgo, C. A. (2008). Thinking outside the cube, *Physics World* **21**(12).

Hidalgo, C. A. and Rodriguez-Sickert, C. (2008a). The dynamics of a mobile phone network, *Physica A* **387**: 3017–3024.

Hidalgo, C. A. and Rodriguez-Sickert, C. (2008b). Persistence, topology and sociodemographics of a mobile phone network, *Physica A (forthcoming)* .

Hill, N. M. and Stevens, A. (2008). Measurement of satellite impact fragments, *Orbital Debris Quarterly News* **12**(1): 9–10.

Höjer, M. and Mattsson, L.-G. (2000). Determinism and backcasting in future studies, *Futures* **32**(7): 613–634.

Holme, P., Kim, B. J., Yoon, C. N. and Han, S. K. (2002). Attack vulnerability of complex networks, *Physical Review E* **65**(5): 056109 1–14.

Hoyt, R. (2009). Rustler: Architecture and technologies for low-cost remediation of the LEO large debris population, *DARPA/NASA Orbital Debris Removal Conference*, Chantilly, VA, USA.

Hoyt, R. and Forward, R. (2000). The terminator tether: Autonomous deorbit of LEO spacecraft for space debris mitigation, *38th Aerospace Sciences Meeting & Exhibit*, Reno, Nevada.

Hunt, J. (2010a). Brief introduction to TLEs and satellite IDs, `http://www.satobs.org/element.html`.

Hunt, J. (2010b). Tracking programs and TLE resources, `http://www.satobs.org/tletools.html`.

Hwang, W., Cho, Y.-R., Zhang, A. and Ramanathan, M. (2006). Bridging centrality: Identifying bridging nodes in scale-free networks, *12th International Conference on Knowledge Discovery and Data Mining*, Philadelphia, USA.

IAA (2005). Position paper on space debris mitigation: Implementing zero debris creation zones, *Technical report*, International Academy of Astronautics.

IAA (2008). Space debris environment remediation, *Technical Report 0.2*, International Academy of Astronautics.

IAA (2010). Space debris environment remediation, *Technical Report 0.4*, International Academy of Astronautics.

IADC (1998). Space debris mitigation, *35th Session of the Scientific and Technical Subcommittee on Peaceful Uses of Outer Space*, Vienna, Austria.

IADC (2002). Inter-agency space debris coordination committee space debris and mitigation guidelines.

IADC (2007). Inter-agency space debris coordination committee space debris and mitigation guidelines, *Technical report*, IADC.

Iess, L., Bruno, C., Ulivieri, C., Ponzi, U., Parisse, M., Laneve, G., Vannaroni, G., Dobrowolny, M., de Venuto, F., Bertotti, B. and Anselmo, L. (2002). Satellite de-orbiting by means of electrodynamic tethers part i: general concepts and requirements, *Acta Astronautica* **50**(7): 399–406.

IMO (1989). International convention on salvage, `http://www.jus.uio.no/lm/imo.salvage.convention.1989/doc.html`.

Ivezic, Z., Tabachnik, S., Rafikoz, R. Z., Lupton, R. H., Quinn, T., Hammergren, M., Eyer, L., Chu, J., Armstrong, J. C., Fan, X., Finlator, K., Geballe, T. R., Gunn, J. E., Hennessy, G. S., Knapp, G. R., Leggett, S. K., Munn, J. A., Pier, J. R., Rockosi, C. M., Schneider, D. P., Strauss, M. A., Yanny, B., Brinkmann, J., Csabai, I., Hindsley, R. B., Kent, S., Lamb, D. Q., Margon, B., McKay, T. A., Smith, A., Waddell, P. and York, D. G. (2001). Solar system objects observed in the Sloan digital sky survey commissioning data, *The Astronomical Journal* **122**: 2749–2784.

Izquierdo, J. G., Rozemeijer, H. and Münchelberg, S. (2000). The tether system experiment - preparing for ESA's first tether mission, *Technical report*, European Space Agency.

Jacchia, L. G. (1971). Revised static models of the thermosphere and exosphere with empirical temperature profiles, *Technical Report 332*, Smithsonian Astrophysics Observatory.

Janson, S., Knuth, D. E., Lucsak, T. and Pittel, B. (1993). The birth of the giant component, *Random Structures Algorithms* **4**(3): 231–358.

Jehn, R., Viñals-Larruga, S. and Klinkrad, H. (1993). DISCOS - the European space debris database, *44th International Astronautical Congress*, Graz, Austria.

Jing, Z., Lin, T., Hong, Y., Jian-Hua, L., Zhi-Wei, C. and Yi-Xue, K. L. (2007). The effects of degree correlation on network topologies and robustness, *Chinese Physics* **16**(12): 3571.

Johnson, N. L. (2011). USA space debris environment, operations, and policy updates, *48th Session of the Scientific and Technical Subcommittee UNCOPUOS*, Vienna, Austria.

Johnson, N. L., Krisko, P. H., Liou, J.-C. and Anz-Meador, P. D. (2001). NASAs new breakup model of EVOLVE 4.0, *Advances in Space Research* **28**(9): 1377–1384.

Johnson, N. L., Stansbery, E., Liou, J.-C., Horstman, M., Stokely, C. and Whitlock, D. (2008). The characteristic consequences of the break-up of the Fengyun-1C spacecraft, *58th International Astronautical Federation Congress*, Hyderabad, India.

Kaplan, M. H. (2009). Large debris momentum removal methods and capture concepts, *DARPA/NASA Orbital Debris Removal Conference*, Chantilly, VA, USA.

Kawamoto, S., Makida, T., Sasaki, F., Okawa, Y. and Nishida, S.-I. (2006). Precise numerical simulations of electrodynamic tethers for an active debris removal system, *Acta Astronautica* **59**: 139–148.

Kawamoto, S., Ohkawa, Y., Nishida, S., Kitamura, S., Kibe, S., Hanada, T. and Mine, M. (2009). Strategies and technologies for cost effective removal of large sized debris, *DARPA/NASA Orbital Debris Removal Conference*, Chantilly, VA, USA.

Kawamoto, S., Ohkawa, Y., Terui, F., Nishida, S., Kitamura, S., Kibe, S., Hanada, T. and Mine, M. (2010). Studies on active debris removal in Japan, *1st European Workshop on Active Debris Removal*, Paris, France.

Keating, G. M., Tolson, R. H. and Bradford, M. S. (2000). Evidence of long term global decline in the Earth's thermospheric densities apparently

related to anthropogenic effects, *Geophysical Research Letters* **27**(10): 1523–1526.

Kelso, T. S. (2004). Space surveillance, `http://celestrak.com/columns/v04n01/`.

Kelso, T. S. (2006). Frequently asked questions: Two-line element set format, `http://celestrak.com/columns/v04n03/`.

Kelso, T. S. (2007). Validation of SGP4 and IS-GPS-200D against GPS precision ephemerides, *17th AAS/AIAA Space Flight Mechanics Conference*, Sedona, Arizona.

Kelso, T. S. (2009a). Iridium 33/Cosmos 2251 collision, `http://celestrak.com/events/collision/`.

Kelso, T. S. (2009b). SOCRATES, `http://celestrak.com/SOCRATES/`.

Kelso, T. S. (2010). Chinese ASAT test, `http://celestrak.com/events/asat.asp`.

Kelso, T. S. and Alfano, S. (2005). Satellite orbital conjunction reports assessing threatening encounters in space (SOCRATES), *AAS/AIAA Space Flight Mechanics Conference*, Copper Mountain, Colorado.

Kessler, D. J. (1991). Collisional cascading: the limits of populations growth in Low Earth Orbit, *Advances in Space Research* **11**(12): 63–65.

Kessler, D. J. (2000). Critical density of spacecraft in Low Earth Orbit: Using fragmentation data to evaluate the stability of the ortbial debris environment, *Technical report*, Lockheed Martin.

Kessler, D. J. and Anz-Meador, P. D. (2001). Critical number of spacecraft in Low Earth Orbit: Using satellite fragmentation data to evaluate the stability of the orbital debris environment, *3rd European Conference on Space Debris*, Vol. SP-473, ESA, Darmstadt, Germany, pp. 265–272.

Kessler, D. J. and Cour-Palais, B. G. (1978). Collision frequency of artifical satellites: the creation of a debris belt, *Journal of Geophysical Research* **83**(A6): 2637–2646.

Kinard, W. H. (2007). Long duration exposure facility archive system, `http://setas-www.larc.nasa.gov/LDEF/index.html`.

Klinkrad, H. (1991). DISCOS - ESA's database and information system characterising objects in space, *Advances in Space Research* **11**(12): 43–52.

Klinkrad, H. (2006). *Space Debris: Models and Risk Analysis*, Springer-Praxis books in Aeronautical Engineering, 1st edn, Praxis Publishing Ltd, Chichester, UK.

Klinkrad, H. (2009). Meteoroid and debris protection, *in* Musgrave, G, Larsen, A and Sgobba, T (eds), *Safety Design for Space Systems*, Butterworth-Heinemann, Oxford, UK, pp. 319–332.

Klinkrad, H. and Johnson, N. L. (2009). Space debris environment remediation, *DARPA/NASA Orbital Debris Removal Conference*, Chantilly, VA, USA.

Knipp, D. (2005). The neutral upper atmosphere and its influence on basic orbital dynamics at the edge of space, *Space Waether*, National Center for Atmospheric Research, Boulder, Colorado.

Knowles, S. H., Picone, J. M., Thonnard, S. E. and Nicholas, A. C. (2001). The effect of atmospheroc drag on satellite orbits during the Bastille Day event, *Solar Physics* **204**: 387–397.

Krisko, P. H. (2004). Evolve historical and projected orbital debris test environments, *Advances in Space Research* **34**: 975–980.

Krisko, P. H., Johnson, N. L. and Opiela, J. N. (2001). Evolve 4.0 orbital debris mitigation studies, *Advances in Space Research* **28**(9): 1385–1390.

Kunstadter, C. (2009). Orbital debris and space insurance, *DARPA/NASA Orbital Debris Removal Conference*, Chantilly, VA, USA.

Lappas, V., Adeli, N., Visagie, L., Theodorou, T., Fernandez, J., le Couls, O., Guenat, H. and Perren, M. (2010). Cubesail: A 3D cubesat solar sailing/deorbiting demonstration mission, *1st European Workshop on Active Debris Removal*, Paris, France.

Larrimore, S. C. (2007). Operationally responsive space: A new paradigm or another false start?, *Technical report*, Maxwell Air Force Base.

Latora, V. and Marchiori, M. (2005). Vulnerability and protection of infrastructure networks, *Physical Review E* **71**: 015103 1–4.

Lempert, R. J. (2002). A new decision science for complex systems, *PNAS* **99**(3): 7309–7313.

Lewis, H. G., Newland, R. J., Swinerd, G. G. and Saunders, A. (2010). A new analysis of debris mitigation and removal using networks, *Acta Astronautica* **66**(1-2): 257–268.

Lewis, H. G., Saunders, A., Swinerd, G. G. and Newland, R. J. (2011). Effect of thermospheric contraction on remediation of the near-earth space debris environment, *Journal of Geophysical Research* **116**(A00H08).

Lewis, H. G., Swinerd, G. G., Ellis, C. S. and Martin, C. E. (2005). Response of the space debris environment to greenhouse cooling, *4th European Conference on Space Debris*, Darmstadt, Germany.

Lewis, H. G., Swinerd, G. G., Martin, C. E. and Campbell, W. S. (2004). The stability of disposal orbits at super-synchronous altitudes, *Acta Astronautica* **55**(3-9): 299–310.

Lewis, H. G., Swinerd, G. G. and Newland, R. J. (2009a). The space debris environment: Future evolution, *European Air and Space Conference*, Manchester, UK.

Lewis, H. G., Swinerd, G. G., Newland, R. J. and Saunders, A. (2009b). Active removal study for on-orbit debris using DAMAGE, *5th European Conference on Space Debris*, Darmstadt, Germany.

Lewis, H. G., Swinerd, G. G., Newland, R. J. and Saunders, A. (2009c). The fast debris evolution model, *Advances in Space Research* **34**(5): 568–578.

Lewis, H. G., Swinerd, G. G., Williams, N. and Gittins, G. (2001). DAMAGE: a dedicated GEO debris model framework, *Proceedings of the 3rd European Conference on Space Debris*, European Space Agency, Noordwijk, Netherlands, pp. 373–378.

Li, L., Alderson, D., Tanaka, R., Doyle, J. V. and Willinger, W. (2005). Towards a theory of scale-free graphs: Definition, properties, and implications (extended version), *Technical report*, California Institute of Technology.

Liljeros, F., Edling, C. R., Amaral, L. A. N., Stanley, H. E. and Aberg, Y. (2001). The web of human sexual contacts, *Nature* **411**: 907–908.

Liou, J.-C. (2006). Collision activities in the future orbital debris environment, *Advances in Space Research* **38**: 2102–2106.

Liou, J.-C. (2008). A statistical analysis on the future debris environment, *Acta Astronautica* **62**(2-3): 264–271.

Liou, J.-C. (2009). NASA's long-term debris environment and active debris removal modeling activities, *DARPA/NASA Orbital Debris Removal Conference*, Chantilly, VA, USA.

Liou, J.-C. (2010a). The top 10 questions for active debris removal, *1st European Workshop on Active Debris Removal*, Paris, France.

Liou, J.-C. (2010b). An updated assessment of the orbital debris environment in LEO, *Orbital Debris Quarterly News* **14**(1): 7–8.

Liou, J.-C. (2011). Active debris removal - a grand engineering challenge for the twenty-first century, *submitted to the American Astronomical Society 2011* .

Liou, J.-C., Hall, D. T., Krisko, P. H. and Opiela, J. N. (2004). LEGEND- a three-dimensional LEO-to-GEO debris evolutionary model, *Advances in Space Research* **34**: 981–986.

Liou, J.-C. and Johnson, N. L. (2005). A LEO satellite postmission disposal study using LEGEND, *Acta Astronautica* **57**(2-8): 324–329.

Liou, J.-C. and Johnson, N. L. (2006). Risks in space from orbiting debris, *Science* **311**: 340 – 341.

Liou, J.-C. and Johnson, N. L. (2008). Instability of the present LEO satellite populations, *Advances in Space Research* **41**(7): 1046–1053.

Liou, J.-C. and Johnson, N. L. (2009). A sensitivity study of the effectiveness of active debris removal, *Acta Astronautica* **64**(2-3): 236–243.

Liou, J.-C., Johnson, N. L. and Hill, N. M. (2010). Controlling the growth of future LEO debris populations with active debris removal, *Acta Astronautica* **66**: 648–653.

Liou, J.-C., Kessler, D. J., Matney, M. J. and Stansbery, E. G. (2003). A new approach to evaluate collision probailiites among asteroids, comets and Kuiper Belt objects, *Proceesings of the 34th Lunar and Planetary Science Conference*, Vol. 34, League City, Texas, p. 1828.

Lovins, A. B. (1977). Cost-risk-benefit assessments in energy policy, *Geo Wash. L. Rev.* **911**(5): 911.

Maessen, D. C., van Breukelen, E. D., Zandbergen, B. T. C. and Bergsma, O. K. (2007). Development of a generic inflatable de-orbit device for cubesats, *58th International Astronautical Congress*, Hyderabad, India.

Martin, C., Walker, R. and Klinkrad, H. (2004). The sensitivity of the ESA DELTA model, *Advances in Space Research* **34**: 969–974.

Matney, M., Settecerri, T., Johnson, N. L. and Stansbery, E. (1997). Characterization of the breakup of the Pegasus rocket body 1994-029b, *Second European Conference on Space Debris*, Vol. ESA-SP 393, ESA, Darmstadt, Germany, pp. 289–292.

McKnight, D. (2009). Removing orbital debris without going into orbit, *DARPA/NASA Orbital Debris Removal Conference*, Chantilly, VA, USA.

McKnight, D. (2010). Pay me now or pay me more later: start the development of active debris removal now, *Advanced Maui Optical and Space Surveillance Technologies Conference*, Maui, Hawaii.

Mejía-Kaiser, M. (2009). Removal of orbital debris: Legal and policy aspects, *DARPA/NASA Orbital Debris Removal Conference*, Chantilly, VA, USA.

Mitra, B., Peruani, F., Ghose, S. and Ganguly, N. (2007). Analyzing the vulnerability of superpeer networks against attack, *Conference on Computer and Communications Security*, Alexandria, Virginia, USA, pp. 225–235.

Molloy, M. and Reed, B. (1998). The size of the giant component of a random graph with a given degree sequence, *Combinatorics, Probability and Computing* **7**(3): 295–305.

Moran, P. (2009). Space debris management: System of systems perspective, *DARPA/NASA Orbital Debris Removal Conference*, Chantilly, VA, USA.

Moreira, A. A., Andrade, J. S., Hermann, H. J. and Indekeu, J. O. (2009). How to make a fragile network robust and vice versa, *Phys. Rev. Lett.* **102**(1): 018701 1–4.

Motter, A. E. and Lai, Y.-C. (2002). Cascade-based attacks on complex networks, *Physical Review E* **66**: 065102 1–4.

Narumi, T., Hanada, T. and Kawamoto, S. (2008). Space debris environmental evolutionary model in Low Earth Orbit, *Space Technology Japan* **7**(0): 11–17.

NASA (1995). NASA safety standard: Guidelines and assessment procedures for limiting orbital debris, *Technical report*, NASA Office of Safety and Mission Assurance.

NASA (2007). USA space debris environment and policy updates, *44th Session of the Scientific and Technical Subcommittee UNCOPUOS*.

NASA (2008). NASA handbook for limiting orbital debris, *Technical report*, National Aeronautics and Space Administration.

NASA (2009a). Orbital debris education package, *Technical report*, NASA Orbital Debris Program Office.

NASA (2009b). Orbital debris evolutionary models, `http://orbitaldebris.jsc.nasa.gov/model/evolmodel.html`.

NASA (2009c). Orbital debris frequently asked questions, `http://orbitaldebris.jsc.nasa.gov/faqs.html`.

NASA (2009d). Orbital debris modeling, `http://orbitaldebris.jsc.nasa.gov/model/engrmodel.html`.

NASA (2010). NASA science news: Solar s'mores, `http://science.nasa.gov/science-news/science-at-nasa/2000/ast30may_1m/`.

Nazarenko, A. I. and Menshikov, I. L. (2001). Engineering model of the space debris environment, *3rd European Conference on Space Debris*, Darmstadt, Germany, pp. 293–298.

Newland, R. J., Lewis, H. G. and Swinerd, G. G. (2009). Supporting the development of active debris removal using weighted networks, *5th European Conference on Space Debris*, Darmstadt, Germany.

Newman, L. K. (2010). The NASA robotic conjunction assessment process: Overview and operational experiences, *Acta Astronautica* **66**(7-8): 1253–1261.

Newman, M. E. J. (2001). Scientific collaboration networks II: Shortest paths, weighted networks, and centrality, *Phys. Rev. E* **64**(016132).

Newman, M. E. J. (2002a). Assortative mixing in networks, *Physical Review Letters* **89**(20): 208701 1–4.

Newman, M. E. J. (2002b). The structure and function of networks, *Comput. Phys. Commun.* **147**: 40–45.

Newman, M. E. J. (2003). The structure and function of complex networks, *SIAM Review* **45**(2): 167–256.

Newman, M. E. J. (2004). Analysis of weighted networks, *Physical Review E* **70**(5): 036131.

Newman, M. E. J. (2008). *The Mathematics of Networks*, The New Palgrave Encyclopedia of Economics, 2nd edn, Palgrave Macmillan, Basingstoke, UK.

Newman, M. E. J. and Park, J. (2003). Why social networks are different from other types of networks, *Physical Review E* **68**: 036122 1–8.

Neyland, D. (2009). Tactical technology office overview for the the first international conference on orbital debris removal, *DARPA/NASA Orbital Debris Removal Conference*, Chantilly, VA, USA.

Nishida, S.-I., Kawamoto, S., Okawa, Y., Terui, F. and Kitamura, S. (2009). Space debris removal system using a small satellite, *Acta Astronautica* **65**: 95–102.

Noca, M., Wiesendanger, R. and Sanders, B. (2010). New technologies and innovations for space debris clean-up, *1st European Workshop on Active Debris Removal*, Paris, France.

Nock, K. T., Aaron, K. M. and Medlock, K. G. (2009). Comparison of the performance of de-orbit methods in the LEO operational environment, *DARPA/NASA Orbital Debris Removal Conference*, Chantilly, VA, USA.

Oberkampf, W. L., Helton, J. C., Joslyn, C. A., Wojtkiewicz, S. F. and Ferson, S. (2004). Challenge problems: Uncertainty in system response given uncertain parameters, *Reliability Engineering and System Safety* **85**(1-3): 11–19.

ODPO (2007). Four satellite breakups in February add to debris population, *Orbital Debris Quarterly News* **11**(2): 3.

ODPO (2009a). Current debris environment in Low Earth Orbit, *Orbital Debris Quarterly News* **13**(3): 7.

ODPO (2009b). A review of different solar cycle 24 predictions and other long-term projections, *Orbital Debris Quarterly News* **13**(1): 7–8.

ODPO (2009c). Satellite collision leaves significant debris clouds, *Orbital Debris Quarterly News* **13**(2): 1–2.

ODPO (2010a). Chinese debris reaches new milestone, *Orbital Debris Quarterly News* **14**(4): 3.

ODPO (2010b). Top ten satellite breakups, *Orbital Debris Quarterly News* **14**(3): 2–3.

ODPO (2011a). Monthly number of objects in Earth orbit by object type, *Orbital Debris Quarterly News* **15**(1): 10.

ODPO (2011b). An update on LEO environment remediation with active debris removal, *Orbital Debris Quarterly News* **15**(2): 4–6.

OECD (1972). Guiding principles concerning international economics aspects of environmental policies.

O'Hagan, A. (2006). *Uncertain judgements: eliciting experts' probabilities*, John Wiley and Sons, Chichester, England.

Oswald, M., Wegener, P., Stabroth, S., Wiedemann, C., Rosebrock, J., Martin, C., Klinkrad, H. and Vörsmann, P (2005). The MASTER 2005 model, *4th European Conference on Space Debris*, Darmstadt, Germany.

Pardini, C. and Anselmo, L. (2009). USA-193 decay predictions using public domain trajectory data and assessment of the post-intercept orbital debris cloud, *Acta Astronautica* **64**(7-8): 787–795.

Pardini, C., Hanada, T. and Krisko, P. H. (2009). Benefits and risks of using electrodynamic tethers to de-orbit spacecraft, *Acta Astronautica* **64**(5-6): 571–588.

Pastor-Satorras, R., Vázquez, A. and Vespignani, A. (2001). Dynamical and correlation properties of the internet, *Phys. Rev. Lett.* **87**: 258701 1–4.

Pearson, J., Carroll, J., Levin, E. and Oldson, J. (2009). EDDE electrodynamic debris eliminator for active debris removal, *DARPA/NASA Orbital Debris Removal Conference*, Chantilly, VA, USA.

Phipps, C. R. and Campbell, J. W. (2009). A review of the ORION concept for space debris mitigation, *DARPA/NASA Orbital Debris Removal Conference*, Chantilly, VA, USA.

Picone, J. M., Emmert, J. T. and Lean, J. L. (2005). Thermospheric densities derived from spacecraft orbits: Accurate processing of Two Line Element sets, *Journal of Geophysical Research* **110**: A03301 1–19.

Pollard, S. J., Yearsley, R., Reynard, N., Duarte-Davidson, I. C., R, M. and Duerden, S. L. (2002). Current directions in the practice of environmental risk assessment in the United Kingdom, *Environment Science Technology* **36**: 530–538.

POST (2010). Space debris, *Technical Report 355*, Parliamentary Office for Science and Technology, UK.

Prigogine, I. and Stengers, I. (1984). *Order Out of Chaos*, Bantam, Toronto, Canada.

Protocol, T. M. (1987). The 1987 Montreal Protocol on substances that deplete the ozone layer, `http://ozone.unep.org/Ratification_status/montreal_protocol.shtml`.

Quist, J. and Vergragt, P. (2006). Past and future of backcasting: The shift to stakeholder participation and a proposal for a methodological framework, *Futures* **38**(9): 1027–1045.

Ramohalli, K. N. R. (1989). Autonomous space processor for orbital debris, *Proceedings of the Summer Design Conference NASA/Univeristy Space Research Association*, Huntsville, USA.

Reis, B. Y., Kohane, I. S. and Mandl, K. D. (2007). An epidemiological network model for disease outbreak detection, *PLoS Medicine* **4**(6): 1019–1031.

Reynolds, R. C. and Eichler, P. (1995). A comparison of debris environment projections using the EVOLVE and CHAIN models, *Advances in Space Research* **16**(11): 127–135.

Robinson, J. (1982). Energy backcasting: A proposed method of policy analysis, *Energy Policy* .

Robinson, J. (2003). Future subjunctive: backcasting as social learning, *Futures* **35**(8): 839–856.

Rosato, V., Bologna, S. and Tiriticco, F. (2007). Topological properties of high-voltage electrical transmission networks, *Electrical Power Systems Research* **77**(2): 99–105.

Ross, T. J. (2006). Engineering decisions involving aleatoric and epistemic uncertainty, *2nd International Forum on Engineering Decision Making*, Lake Louise, Canada.

Rossi, A., Anselmo, L., Pardini, C., Farinella, P. and Cordelli, A. (1997). Interaction of the satellite constellations with the Low Earth Orbit debris environment, *Proceedings of Mission Design and Implementation of satellite constellations workshop*, Toulouse, France, p. 327.

Rossi, A., Cordelli, A., Pardini, C., Anselmo, L. and Farinella, P. (1995). Modelling the space debris evolution: Two new computer codes, *AAS/AIAA Spaceflight Mechanics* **89**: 1217–1231.

Rosvall, M. (2006). *Information Horizons in a Complex World*, PhD thesis, Umeå University.

Ruault, J. M., Desjean, M. C., Bonnal, C. and Bultel, P. (2010). Active debris removal (ADR): From identification of problematics to in-flight demonstration preparation, *1st European Workshop on Active Debris Removal*, Paris, France.

Santerre, B., Bonneford, T. and Dupuy, C. (2008). The innovative deorbiting aerobrake systems "IDEAS" for small satellites: The use of gossamer technology for a cleaner space, *Proceedings of 'The 4S Symposium - Small Satellites Systems and Services'*, Rhodes, Greece.

Saunders, A., Lewis, H. and Swinerd, G. (2011). Further evidence of long-term thermospheric density change using a new method of satellite ballistic coefficient estimation, *Journal of Geophysical Research* **116**(A00H10).

Schneider, C. M., Moreira, A. A., Andrade Jr., J. S., Havlin, S. and Herrmann, H. J. (2009). Onion-like network topology enhances robustness against malicious attacks, *ETH Zurich, Universidade Federal do Cear, Bar-Ilan University*, pp. 1–4.

Scott, D. M., Novak, D., Aultman-Hall, L. and Guo, F. (2005). Network robustness index: A new method of identifying critical links and evaluating performance of transportation networks, *Technical report*, Centre for Spatial Analysis, McMaster University.

SDA. (2010). Space Data Center, `http://www.space-data.org/sda/space-data-center/`.

Shannon, P., Markiel, A., Ozier, O., Baliga, N. S., Wang, J. T., Ramage, D., Amin, N., Schwikowski, B. and Ideker, T. (2003). Cytoscape: a software environment for integrated models of biomolecular interaction networks, *Genome Research* **13**: 2498–2504.

Shargel, B., Sayama, H., Epstain, I. R. and Bar-Yam, Y. (2003). Optimization of robustness and connectivity in complex networks, *Phys. Rev. Lett.* **90**(6): 068701–1 – 068701–4.

Shepelyansky, D. L., Pikovsky, A. S., Schmidt, J. and Spahn, F. (2009). Synchronization mechanism of sharp edges in rings of Saturn, *Monthly Notices of the Royal Astronomical Society* **395**(4): 1934–1940.

Sheriff, R. E. and Hu, Y. F. (2001). *Mobile Satellite Communication Networks*, John Wiley & Sons, Chichester, UK.

Spacetrack (2009). Space Track: The source for space surveillance data, `http://www.space-track.org/perl/login.pl`.

Stansbery, E. G. and Foster Jr., L. (2004). Monitoring the Low Earth Orbit debris environment over an 11-year solar cycle, *Advances in Space Research* **34**(5): 878–883.

Stansbery, G., Matney, M., Liou, J.-C. and Whitlock, D. (2008). A comparison of catastrophic on-orbit collisions, *Proceedings of the Advanced Maui Optical and Space Surveillance Technologies Conference*, The Maui Economic Development Board, Maui, Hawaii, p. E50.

Stark, J. P. W., Swinerd, G. S. and Fortescue, P. W. (2003). *Spacecraft Systems Engineering*, 3rd edn, John Wiley & Sons, chapter 4, pp. 100–115.

Starke, J., Bischof, B., Foth, W.-P. and Günther, H.-J. (2009). ROGER: A potential orbital space debris removal system, *DARPA/NASA Orbital Debris Removal Conference*, Chantilly, VA, USA.

Stokely, C. L., Stansbery, E. G. and Goldstein, R. M. (2009). Debris flux comparisons from the Goldstone radar, Haystack radar and the HAX radar prior, during, and after the last solar maximum, *Advances in Space Research* **44**: 364–370.

Su, S.-Y. (1993). On runaway conditions of orbital debris environment, *Advances in Space Research* **13**(8): 221–224.

Talent, D. L. (1990). Analytic model for orbital debris environmental management, *NAIAA/NASA/DOD Orbital Debris Conference: Technical Issues and Future Directions*, Baltimore, USA.

Talent, D. L. (1992). Analytic model for orbital debris environmental management, *Journal of Spacecraft and Rockets* **29**(4): 508–513.

Talent, D. L. (2009). A prioritization methodology for orbital debris removal, *DARPA/NASA Orbital Debris Removal Conference*, Chantilly, VA, USA.

Terui, F. (2010). 3-D shape model based visual motion estimation for failed satellite, *1st European Workshop on Active Debris Removal*, Paris, France.

UCS (2009). Historical growth of space debris, *Technical report*, Union of Concerned Scientists.

UNCOPUOS (2001). National research on space debris, safety of space objects with nuclear power sources on board and problems relating to their collision with space debris, *Technical report*, Committee on the Peaceful Uses of Outer Space.

UNCOPUOS (2007). Annex IV: Report of the scientific and technical subcommittee on its forty-fourth session, held in Vienna from 12 to 23 February 2007, *Technical report*, Committee on the Peaceful Uses of Outer Space.

US National Space Policy (2010). National Space Policy of the United States of America, `http://www.whitehouse.gov/sites/default/files/national_space_policy_6-28-10.pdfl`.

Vallado, D., Crawford, P., Hujsack, R. and Kelso, T. S. (2006). Revisiting spacetrack report #3, *AIAA/AAS Astrodynamics Specialist Conference*, Keystone, Colorado.

Vallado, D. and Finkleman, D. (2008). A critical assessment of satellite drag and atmospheric density modeling, *AIAA/AAS Astrodynamics Specialist Conference*, Honolulu, Hawaii.

Vance, L. (2009). First order value analysis for orbital debris removal, *DARPA/NASA Orbital Debris Removal Conference*, Chantilly, VA, USA.

Wagenbach (2010). RetroSpace: A profitable end-to-end system for active debris removal, *1st European Workshop on Active Debris Removal*, Paris, France.

Walker, R., Crowther, R., Marsh, V. and Stokes, P. H. (1997). Satellites constellations and their long term impact on the derbis environment in Low Earth Orbit, *2nd European Conference on Space Debris*, Darmstadt, Germany, p. 359.

Walker, R. and Martin, C. (2004). Cost-effective and robust mitigation of space debris in Low Earth Orbit, *Advances in Space Research* **34**(5): 1233–1240.

Walker, R., Martin, C. E., Stokes, P. H., Wilkinson, J. E. and Klinkrad, H. (2001). Analysis of the effectiveness of space debris mitigation measures using the DELTA model, *Advances in Space Research* **28**(9): 1437–1445.

Walker, R., Stokes, P. H. and Wilkinson, J. E. (2000). Long-term collision risk prediction for Low Earth Orbit satellite constellations, *Acta Astronautica* **47**(2-9): 707–717.

Wang, J.-W. and Rong, L.-L. (2009). Cascade-based attack vulnerability on the US power grid, *Safety Science* **47**: 1332–1336.

Wang, X. F. and Chen, G. (2003). Complex networks: Small-world, scale-free and beyond, *IEEE Circuits and Systems Magazine* **3**(1): 6–20.

Weeden, B. (2009). Active debris removal: An opportunity for leadership and cooperation, *DARPA/NASA Orbital Debris Removal Conference*, Chantilly, VA, USA.

Weiss, M. A. (1997). *Data structures and algorithm analysis in C*, 2nd edn, Addison Wesley, Reading, Massachusetts.

White, W. (2009). Space debris: Laws, regulations, international guidelines, and incentives for remediation, *DARPA/NASA Orbital Debris Removal Conference*, Chantilly, VA, USA.

Wiedemann, C., Krag, H., Bendisch, J. and Sdunnus, H. (2004a). Analysing cost of space debris mitigation methods, *Advances in Space Research* **34**: 1241–1245.

Wiedemann, C., Oswald, M., Bendisch, J., Sdunnus, H. and Vörsmann, P. (2004b). Cost and benefit analysis of space debris mitigation measures, *Acta Astronautica* **55**: 311–324.

Wittwer, J. W. (2004). Monte Carlo simulation basics, `http://www.vertex42.com/ExcelArticles/mc/MonteCarloSimulation.html`.

Wright, D. (2007). Space debris, *Physics Today* **October 2007**: 35–40.

Xu, L. Y., Horstman, M., Krisko, P. H., Liou, J.-C., Matney, M. J., Stansbery, E. G., Stokely, C. and Whitlock, D. (2009). Modeling of LEO orbital debris populations for ORDEM2008, *Advances in Space Research* **43**(5): 769–782.

Yoshida, H. and Araki, M. (1994). Social impact of space debris: study of economic and political issues, *Acta Astronautica* **34**: 345–355.

Zebker, H. A., Marouf, E. A. and Tyler, G. L. (1985). Saturn's rings: Particle size distributions for thin layer models, *Icarus* **64**: 531.

Zhou, T., Liu, J.-G. and Wang, B.-H. (2005). Comment on scientific collaboration networks II: Shortest paths, weighted networks, and centrality, *arXiv Physics and Society* **0511084**.

Appendix A

Appendix

A.1 Initial code

Written by Dr F M Bélanger and R J Newland

A.1.1 rjnNetworkAnalysis

```
#include "BFS_FIFOQueue.cpp"
#include <stdio.h>
#include <stdlib.h>
#include <string.h>
#include <math.h>
#include <iostream>
#include <algorithm>
#include <vector>
#include <time.h>
using namespace std;

//check diameter again

#define FILENAME "SOCRATES 291009 NAMES.csv" //input file
```

```
#define OUTPUT "SOCRATES 291009 NAMES output.csv" //output file

void BFS(int,int,float*,int,int*);

//qsort function
int compare(const void* a,const void* b)
//sort integers in list to define unique number of vertices
{
int* arg1= (int*)a;
int* arg2 = (int*)b;
if (*arg1 == *arg2) //if two numbers are the same, don't count
return 0;
else
if (*arg1 < *arg2) //if the two numbers are different,
there is another unique vertex
return -1;
else
return 1;
}

//the main function
int main()
{
FILE *input;
FILE *output;

time_t seconds; //Start time
seconds = time(NULL);
printf("%ld hours since 1st January 1970\n", seconds/3600);

int index = 0;
int a,b,i,j,k,n;
char temp[100]; //temporary values for reading the input file
```

```
 //if this was a n int, could I keep the original objects values?
int e = 0; //number of edges
int v = 0; //number of unique vertices
int vindex = 0; //for counting unique number of vertices
int sort = 0; //for counting unique number of vertices
int unique = 1;
//unique numbers in array = number of vertices in network
float beta = 0; //beta index
float gamma = 0; //gamma index
int p = 0;
//p is the number of sub-graphs in the network and should be calculated
int mycount; //counting for distributions
int mycountNN; //counting for distributions
float sumdij =0; //sum of shortest paths
float Degree = 0;
float Strength = 0;
float Assortativity =0; //Nearest neighbour degree
float Affinity =0;
int maxDegree = 0; //maximum degree of the network
float Clustering = 0;
int maxShortestPath = 0; //longest shortest path
float averageShortestPath =0; //average shortest path
float Closeness = 0;

//variables for PCC
int indexa = 0; //index of COSPAR/vertex id 1
int indexb = 0; //index of COSPAR/vertex id 2
int indexX = 0; //index of degree of vertex 1
int indexY = 0; //index of degree of vertex 2
int X = 0; //Degree of vertex 1
int Y = 0; //Degree of vertex 2
double sumX = 0; //Sum degrees in column 1
double sumY = 0; //Sum degrees in column 2
```

```
double Xbar = 0; //Average degree for column 1
double Ybar = 0; //Average degree for column 1
double Nu = 0; //numerator of PCC equation
double De1 = 0; //1st part of denominator of PCC equation
double De2 = 0; //2nd part of denominator of PCC equation
double De = 0; //Denominator of PCC equation
float r = 0; //Pearson's Correlation Coefficient

//matrices
char *result; //values from input file
int *sortArray=0;
float  *wAdjMatrix=0;
float  *adjMatrix=0;
float *degMatrix=0;
float *strMatrix=0;
float* affMatrix = 0;
float* NNMatrix = 0;
int* countNNMatrix = 0; //for calculating distribution
int* countMatrix = 0; //for calculating distribution
float* varMatrix = 0;
//for calculating distribution (number of unique varibles)
float* distributionMatrix = 0; //for calculating distribution
float* distributionNNMatrix = 0; //for calculating distribution
int* aMatrix = 0; //for PCC
int* bMatrix = 0; //for PCC
int* XMatrix = 0; //for PCC
int* YMatrix = 0; //for PCC
float *eiMatrix=0; //for clustering: ei is the number of triangles
float *ciMatrix=0; //clustering coefficients
int *pathMatrix=0;
//the shortest path matrix contains all distance dij values
int *sumShortestPathMatrix=0; //sum of rows in pathMatrix
float *closenessMatrix=0;
```

```
float *siEigenMatrix = 0; //eigenvector centrality (initial matrix)

//if the program cannot read the file, print an error message
input=fopen(FILENAME,"r");
if (input==NULL)
{
fprintf(stderr,"Cannot open file%s\n",FILENAME);
return(1);
}

//if the program can read the file, tokenise the string of values
to give individual numbers
while (fscanf(input, "%s", &temp) == 1)
//while there are values in the dataset
{
result = strtok(temp,","); //the values are separated by ","
if (result)
{
a = atoi(result); //integer in column 1
index++;
}
result = strtok(NULL,",");
//NULL tells the program to keep reading from the same string
if (result)
{
b = atoi(result); //integer in column 2
index++;
}
}

//define the unique number of vertices
sortArray = (int *)malloc(index * sizeof(int));
memset(sortArray, 0, index * sizeof(int));
```

```
rewind(input); //rewind to the beginning of the file

while (fscanf(input, "%s", &temp) == 1)
{
result = strtok(temp,",");
if (result)
//if there is a number in the column, add one to the index
{
sortArray[vindex] = atoi(result);
vindex++;
}
result = strtok(NULL,",");
//if there is a number in the next column, add  one to the index
if (result)
{
sortArray[vindex] = atoi(result);
vindex++;
}
//printf("index %d\n",vindex);
}

qsort(sortArray,index,sizeof(int),compare);
//sort array sortArray using the qsort function above

for(i=0;i<index;i++)
{
if (sortArray[i]!=sort)
{
sort=sortArray[i];
unique++;
//when the value above is not the same as  below, increase the index
}
```

```
}

e=(index/2); //the number of edges
printf("Number of edges = %d\n", e);
v=unique; //the number of vertices
printf("Number of vertices = %d\n\n", v);

//allocate memory based on order of network
wAdjMatrix = (float *)malloc(v * v * sizeof(float));
memset(wAdjMatrix, 0, v * v * sizeof(float));

adjMatrix = (float *)malloc(v * v * sizeof(float));
memset(adjMatrix, 0, v * v * sizeof(float));

degMatrix = (float *)malloc(v * sizeof(float));
memset(degMatrix, 0, v * sizeof(float));

strMatrix = (float *)malloc(v * sizeof(float));
memset(strMatrix, 0, v * sizeof(float));

NNMatrix = (float*)malloc(v * sizeof(float));
memset(NNMatrix, 0, v * sizeof(float));

affMatrix = (float*)malloc(v * sizeof(float));
memset(affMatrix, 0, v * sizeof(float));

aMatrix = (int*)malloc(e * sizeof(int));
memset(aMatrix, 0, e * sizeof(int));

bMatrix = (int*)malloc(e * sizeof(int));
memset(bMatrix, 0, e * sizeof(int));

XMatrix = (int*)malloc(e * sizeof(int));
```

```
memset(XMatrix, 0, e * sizeof(int));

YMatrix = (int*)malloc(e * sizeof(int));
memset(YMatrix, 0, e * sizeof(int));

eiMatrix = (float *)malloc(v * sizeof(float));
memset(eiMatrix, 0, v * sizeof(float));

ciMatrix = (float *)malloc(v * sizeof(float));
memset(ciMatrix, 0, v * sizeof(float));

pathMatrix = (int *)malloc(v * v * sizeof(int));
//no memset, all values are set to -2 below

sumShortestPathMatrix = (int *)malloc(v * sizeof(int));
memset(sumShortestPathMatrix, 0, v * sizeof(int));

closenessMatrix = (float *)malloc(v * sizeof(float));
memset(closenessMatrix, 0, v * sizeof(float));

siEigenMatrix = (float *)malloc(v * v* sizeof(float));
memset(siEigenMatrix, 0, v * v* sizeof(float));



//Indices and Measures
//beta and gamma indices
beta = e/(v*1.0);
//beta measures connectivity by the ratio of edges to vertices, can be greater than one.
//complex networks have a high beta.
gamma = e/(0.5*v*(v-1));
//gamma measures the connectivity of the network (ratio of edges to all possible edges)
printf("Indices (beta and gamma) \n %f\n %f\n", beta, gamma);
```

```
//Giant Component
//see Fernando Peruani's email and Eq.4 in paper
//Percolation Threshold
//if f is the fraction of v removed, fc is the critical
fraction of v that need to be removed to breakdown the GC

//Adjacency Matrix
rewind(input);

a = 0; //reset values
b = 0;

while (fscanf(input, "%s", &temp) == 1) //read the input file
{
result = strtok(temp,",");
if (result)
{
a = atoi(result);
}
result = strtok(NULL,",");
//NULL tells the computer not to move to the next line
if (result)
{
b = atoi(result);
}
result = strtok(NULL,","); //matrix is being filled
if (result)
{
wAdjMatrix[a*v+b]=atof(result); //fill the matrix symmetrically
wAdjMatrix[b*v+a]=atof(result); //fill the matrix symmetrically
}
}
```

```
rewind(input);

a = 0; //reset values
b = 0;

while (fscanf(input, "%s", &temp) == 1) //read the input file
{
result = strtok(temp,",");
if (result)
{
a = atoi(result);
}
result = strtok(NULL,",");
//NULL tells the computer not to move to the next line
if (result)
{
b = atoi(result);
}
result = strtok(NULL,",");
if (result)
{
adjMatrix[a*v+b]=1; //fill the matrix symmetrically
adjMatrix[b*v+a]=1; //fill the matrix symmetrically
}
}
fclose(input); //close the data file


//Degree, Strength, Nearest Neighbour Degree and Affinity
for(i=0; i<v; i++)
{
for(j=0; j<v; j++)
{
```

```
if(wAdjMatrix[i*v+j]>0.00000)
//if there is a non-zero value in the Adjacency Matrix...
degMatrix[i]++; //add one to the degree
strMatrix[i]+=wAdjMatrix[i*v+j]; //add the weighted values
}
}

for(i=0; i<v;i++)
{
for(j=0;j<v;j++)
{
if(wAdjMatrix[i*v+j]>0.00000)
NNMatrix[i]+=degMatrix[j]; //assortativity
affMatrix[i]+=wAdjMatrix[i*v+j]*degMatrix[j]; //affinity
}
}

for(i=0;i<v;i++)
{
NNMatrix[i]/=(double)degMatrix[i]; //nearest neighbour degree
affMatrix[i]/=strMatrix[i]; //affinity
Assortativity +=(NNMatrix[i]/v);
//average network nearest neighbour degree
Affinity +=(affMatrix[i]/v); //average network affinity
}

for(j=0; j<v; j++)
{
// printf("%f\t", degMatrix[j]);
// printf("%f\n", strMatrix[j]);
Degree += (degMatrix[j]/v); //average network degree
Strength += (strMatrix[j]/v); //average network strength
// printf("%f\t", NNMatrix[j]);
```

```
// printf("%f\n", affMatrix[j]);
}
printf("Network Degree = %f\n", Degree);
printf("Network Strength = %f\n", Strength);
printf("Network Assortativity = %f\n", Assortativity);
printf("Network Affinity = %f\n", Affinity);


//Distributions
maxDegree = *max_element(degMatrix, degMatrix+v);
//first, calculate the largest degree in the degree matrix
printf("Maximum Degree = %d\n", maxDegree);
//use maxDegree to allocate the size of the two matrices

countMatrix = (int*)malloc((maxDegree+1)  * sizeof(int));
memset(countMatrix, 0, (maxDegree+1) * sizeof(int));

distributionMatrix = (float*)malloc((maxDegree+1)*sizeof(float));
memset(distributionMatrix, 0, (maxDegree+1) * sizeof(float));

varMatrix = (float*)malloc(v*sizeof(float));
memset(varMatrix, 0, v*sizeof(float));

countNNMatrix = (int*)malloc((v+1) * sizeof(int));
memset(countNNMatrix, 0, (v+1) * sizeof(int));

distributionNNMatrix = (float*)malloc((v+1)  * sizeof(float));
memset(distributionNNMatrix, 0, (v+1) * sizeof(float));


//Degree Distribution
n = 0; //reset n to 0
printf("Degree Distribution\n");
```

```
for (i=0; i<(maxDegree+1); i++)
//count the occurence of each value in the degree matrix
{
mycount = (int) count (degMatrix, degMatrix+v, n++);
countMatrix[i]+= mycount;
printf("%d\n", countMatrix[i]);
}

for (i=0; i<(maxDegree+1); i++)
{ //the probability of a degree being chosen at random
distributionMatrix[i]=countMatrix[i]/(v*0.01);
//divided by the number of vertices in the network
printf("%f\n", distributionMatrix[i]);
}
printf("\n");


//NNDegree Distribution
n = 0;
printf("NNDegree Distribution\n");
for(i=0; i<v;i++) //for every value in the NNMatrix
{
if(NNMatrix[i]!=NNMatrix[i-1])
//if the value is not the same as the value(s) before
varMatrix[i]= NNMatrix[i]; //assign a new variable value
}

for (i=0;i<v;i++) //count the occurences of one the variables...
{ //...in the NNMatrix
if (varMatrix[i]!=0)
mycountNN = (float) count (NNMatrix, NNMatrix+v, varMatrix[i]);
countNNMatrix[i]=mycountNN;
printf("%d\n", countNNMatrix[i]);
```

```
}

for(i=0; i<v; i++)
{
distributionNNMatrix[i]=countNNMatrix[i]/(v*0.01);
//the probability of a NNdegree being found at random
printf("%f\n", distributionNNMatrix[i]);
//divided by the number of vertices in the network
}


//Pearson's Correlation Coefficient (what about zero variance?)
input=fopen(FILENAME,"r");
if (input==NULL)
{
fprintf(stderr,"Cannot open file%s\n",FILENAME);
return(1);
}
while (fscanf(input, "%s", &temp) == 1) //scan the file
{
result = strtok(temp,","); //each result is separated by a ,
if (result) //if there is a result
{
a = atoi(result); //a is object 1
aMatrix[indexa]=a;
indexa++;
XMatrix[indexX]=degMatrix[a]; //X is the degree of object 1
indexX++;
}
result = strtok(NULL,",");
if (result)
{
b = atoi(result); //b is object 2
```

```
bMatrix[indexb] = b;
indexb++;
YMatrix[indexY] = degMatrix[b]; //Y is the degree of object 2
indexY++;
}
}
fclose(input);

for (i=0;i<e;i++)
{
sumX += XMatrix[i];
sumY += YMatrix[i];
}
Xbar = sumX/e; //calculate Xbar and Ybar
Ybar = sumY/e;

for (i=0;i<e;i++)
{
Nu += ((XMatrix[i])-Xbar)*((YMatrix[i])-Ybar); //the numerator
De1 += (XMatrix[i]-Xbar)*(XMatrix[i]-Xbar); //denominator part
De2 += pow ((YMatrix[i]-Ybar),2); //denominator part
}

De = sqrt (De1*De2); //denominator
r = Nu/De; //r
printf("Pearson's Correlation Coefficient, r = %f\n", r);


//Clustering
for (i=0;i<v;i++) //i, j and k in the adjacency matrix
{
if (degMatrix[i] != 1)
{
```

```
for (j = 0; j < v; ++j)
{
for (k = j; k < v; ++k)
{
if (j != k)
eiMatrix[i] += adjMatrix[i * v + j] * adjMatrix[j * v + k] *
adjMatrix[k * v + i];
}
//hack: need a way of taking a value of 1 if non-0 value
}
//in wAdjMatrix rather than creating an unweighted adjMatrix 0610
}
}

for (i=0;i<v;i++)
{
if (degMatrix[i] > 1)
ciMatrix[i]=(eiMatrix[i]*(2.0))/(degMatrix[i]*(degMatrix[i]-1));
else
{
ciMatrix[i] = 0.0;
//if  degree is 1 then the vertex will not be in a triangle
}
}

for(i=0; i<v;i++)
{
Clustering += ciMatrix[i]/v; //average network clustering
// printf("%f\t", eiMatrix[i]);
// printf("%f\n", ciMatrix[i]);
}
printf("Network Clustering = %f\n", Clustering);
```

```
// Shortest path matrix (using a call to BFS)
for (i = 0; i < v * v; ++i)
{
pathMatrix[i] = -2; //set initial values to -2
}

for (i = 0; i < v; i++)
{
for (j = i; j < v; j++)
{
if (pathMatrix[i * v + j] == -2)
{
//printf("Doing BFS for start %d -- end %d\n", i, j);
BFS(i, j, wAdjMatrix, v, pathMatrix);
//printf("End BFS for start %d -- end %d\n", i, j);
}
}
printf("All paths from %d found.\n", i);
}
printf("\n");

/* printf("Shortest Path matrix\n");
for (i = 0; i < v; i++)
{
for (j = 0; j < v; j++)
{
printf("%d\t", pathMatrix[i * v + j]);
}
printf("\n");
}
printf("\n");*/
```

```
int maxElementInRow = 0;

for(i=0; i<v; i++)
{
for(j=0; j<v; j++)
{
maxElementInRow = *max_element(pathMatrix, pathMatrix+(i*v+j));
if (maxElementInRow > maxShortestPath)
maxShortestPath=maxElementInRow;
else
maxShortestPath=maxShortestPath;
}
}
printf("Maximum Shortest Path (diameter)= %d\n", maxShortestPath);




for(i=0; i<v; i++)
{
for(j=0; j<v; j++)
{
sumShortestPathMatrix[i]+=pathMatrix[i*v+j];
//sum values in the pathMatrix value
}
}

for(i=0; i<v; i++)
{
sumdij += sumShortestPathMatrix[i];
//the average shortest path is the geodesic distance
}
//if average shortest path =1, network is fully connected
```

```
averageShortestPath = sumdij/(v*(v-1));
//this measure tells us about small world networks
printf("Average Shortest Path (geodesic)=%f\n",
averageShortestPath);


//Closeness
for(i=0; i<v; i++)
{
closenessMatrix[i]=((v-1.0)/(sumShortestPathMatrix[i]));
//http://research.microsoft.com/en-us/people/weic/faw08_centrality.pdf
//printf("%f\n", closenessMatrix[i]);
Closeness += (closenessMatrix[i]/v); //average network closeness
}
printf("Network Closeness = %f\n",Closeness);
printf("\n");


//Eigenvector centrality //work in progress
printf("Eigenvector centrality - siEigenMatrix\n\n");

for (i = 0; i < v; i++)
{
for (j = 0; j < v; j++)
{
siEigenMatrix[i*v+j]=adjMatrix[i*v+j]/degMatrix[j];
siEigenMatrix[j*v+i]=adjMatrix[i*v+j]/degMatrix[j];
//printf("%f", siEigenMatrix[i*v+j]);
}
//printf("\n");
}
printf("\n");
```

```
//first: the siEigenMatrix must be primitive and irreducible
//use a recursive function (which needs defining outside main() ?)
//Return results
//http://cis.stvincent.edu/html/tutorials/swd/recur/recur.html

time_t seconds2;
seconds2 = time(NULL);
printf("%ld hours since 1st January 1970\n", seconds2/3600);

//Open the output data file for writing
output = fopen(OUTPUT, "w");
fprintf (output, "NODE ID, Degree, Strength, Nearest Neighbour,
Affinity, Clustering, Closeness\n");
for (i=0;i<v;i++)
{
fprintf(output, "%d, %f, %f, %f, %f, %f, %f\n", i,
 degMatrix[i], strMatrix[i], NNMatrix[i], affMatrix[i],
ciMatrix[i], closenessMatrix[i]);
}
fprintf(output, "\n");

//Start time
fprintf(output, "Start, %ld", seconds/3600);
fprintf(output, "\n");

//End time
fprintf(output, "End, %ld", seconds2/3600);
fprintf(output, "\n");

//Vertices
fprintf(output, "Vertices, %d", v);
fprintf(output, "\n");
```

```
//Edges
fprintf(output, "Edges, %d", e);
fprintf(output, "\n");

//Beta
fprintf(output, "Beta Index, %f", beta);
fprintf(output, "\n");

//Gamma
fprintf(output, "Gamma Index, %f", gamma);
fprintf(output, "\n");

//Maximum Shortest Path Length (diameter)
fprintf(output, "Diameter, %d", maxShortestPath);
fprintf(output, "\n");

//Average Shortest Path Length (geodesic)
fprintf(output, "Geodesic, %f", averageShortestPath);
fprintf(output, "\n");

//Maximum Degree
fprintf(output, "Maximum Degree, %d", maxDegree);
fprintf(output, "\n");

//Network Degree
fprintf(output, "Degree, %f", Degree);
fprintf(output, "\n");

//Network Strength
fprintf(output, "Strength, %f", Strength);
fprintf(output, "\n");

//Network Assortativity
```

```
fprintf(output, "Nearest Neighbour, %f", Assortativity);
fprintf(output, "\n");

//Network Affinity
fprintf(output, "Affinity, %f", Affinity);
fprintf(output, "\n");

//PCC
fprintf(output, "PCC, %f", r);
fprintf(output, "\n");

//Clustering
fprintf(output, "Clustering, %f", Clustering);
fprintf(output, "\n");

//Closeness
fprintf(output, "Closeness, %f", Closeness);
fprintf(output, "\n\n");

//Degree Distribution
fprintf(output, "Degree Distribution\n");
for(i=0;i<maxDegree+1;i++)
{
fprintf(output, "%d, %f\n", i, distributionMatrix[i]);
}
fprintf(output, "\n");

//NNDegree distribution
fprintf(output, "NN Degree Distribution\n");
for(i=0;i<v;i++)
{
fprintf(output, "%f, %f\n", NNMatrix[i], distributionNNMatrix[i]);
}
```

```
fclose (output);


//free memory
free(sortArray);
free(adjMatrix); //free(wAdjMatrix);
free(degMatrix);
free(strMatrix);
free(countMatrix);
free(countNNMatrix);
free(distributionMatrix);
free(distributionNNMatrix);
free(varMatrix);
free(NNMatrix);
free(aMatrix);
free(bMatrix);
free(XMatrix);
free(YMatrix);
free(affMatrix);
free(eiMatrix);
free(ciMatrix);
//free(pathMatrix);
free(sumShortestPathMatrix);
free(closenessMatrix);
free(siEigenMatrix);

system("PAUSE");
return 0;
}

//BFS
void BFS(int startVertex, int endVertex, float* wAdjMatrix, int n,
```

```
int* pathMatrix)
{
int i; //Loop counter
BFS_FIFOQueue<int> childQueue; //Queue for the children
BFS_FIFOQueue<int> pathLength; //Queue for the geodesic distance
(shortest path length)
int targetQueued=0; //Flag the target when it has been found
int foundTarget=0; //Break control variable
int currentVertex = -1; //Current vertex
int currentLength = -1; //Current path length
int shortestPath= -1; //Return variable
int currentIndex = 0;
//Shortcut variable to reduce number of computations

int *visited=0;
visited = (int *)malloc(n* sizeof(int));
memset(visited, 0, n * sizeof(int));

if (startVertex == endVertex) //is the starting vertex the target?
{
pathMatrix[startVertex * n + startVertex] = 0;
}
else //if it isn't, queue the starting vertex and the path length
{
childQueue.queue(startVertex);
//nameOfQueue.queue(whatToPutInTheQueue)
//printf("Queueing %d\n", startVertex);
pathLength.queue(0); //nameOfQueue.queue(whatToPutInTheQueue)
visited[startVertex] = 1;
//put a 1 in the visited Matrix so we know we have been there
}

//BFS for the whole network until the target vertex is found
```

```
or all vertices are traversed
while(!childQueue.isEmpty())
{
currentVertex = childQueue.unqueue(); //unqueue the current parent
//printf("Unqueued %d\n", currentVertex);
currentLength = pathLength.unqueue();
//unqueue the current path length
currentIndex = n* currentVertex;

for (i=0;i<n;i++) //loop through the wAdjMatrix for this vertex
{
//printf("Checking node %d\n", i);
if (wAdjMatrix[currentIndex++] > 0.0)
//If the current vertex has a child at the currentIndex ...
{
//printf("Link found between %d and %d\n", currentVertex, i);
//printf("Target = %d, TQ = %d, i = %d\n",
endVertex, targetQueued, i);
if(i == endVertex && !targetQueued)
//Check: is this the target? if so, flag for later use.
{
//printf("Target %d found.\n", endVertex);
targetQueued =1;
pathMatrix[startVertex * n + i] = currentLength + 1;
pathMatrix[i * n + startVertex] = currentLength + 1;
}

if (pathMatrix[currentVertex * n + i] == -2)
//Check: have we previously stored the path? If not, store.
{
//printf("Speed hack. Link %d and %d = 1\n", currentVertex, i);
pathMatrix[currentVertex * n + i] = 1;
pathMatrix[i * n + currentVertex] = 1;
```

```
}

if(!foundTarget && !visited[i])
//Check: has target vertex been found? if not, query children.
{
//printf("queueing %d\n", i);
visited[i]=1;
childQueue.queue(i);
pathLength.queue(currentLength+1);

if(pathMatrix[startVertex * n + i] == -2)
//Anything that is queued is the shortest path
{
pathMatrix[startVertex * n + i] = currentLength + 1;
pathMatrix[i * n + startVertex] = currentLength + 1;
}
}
}
}

if(targetQueued == 1)
//Is the target as a child of the current child?
{
//If so, set the break control to prevent further queuing
foundTarget = 1;
}
} //Continue to clear the queue

free(visited);
}
```

A.1.2 BFS_FIFOQueue.cpp

```
template <typename T> class BFS_FIFOQueue
{
private:
template <typename S> class Vertex
{
private:
Vertex<S>* next; // Next element
Vertex<S>* previous; // Previous element
S value; // Current value at this point

public:
Vertex(S theValue, Vertex<S>* ptrPrev, Vertex<S>* ptrNext)
{
value = theValue;
previous = ptrPrev;
next = ptrNext;
}

S getValue()
{
return value;
}

void setPrevious(Vertex<S>* newPrev)
{
previous = newPrev;
}

void setNext(Vertex<S>* newNext)
{
next = newNext;
```

```
}

Vertex<S>* getNext()
{
return next;
}

Vertex<S>* getPrevious()
{
return previous;
}
};
int length;  // Number of elements
Vertex<T>* first; // First element in the queue
Vertex<T>* last; // Last element in the queue

int privateQueue(T);
// Private method to queue up nodes.
//Set private to protect data integrity

public:
BFS_FIFOQueue(); // Default constructor
~BFS_FIFOQueue(); // Default destructor
int getLength(); // Get number of elements in queue
T getFirst(); // Get the first element
T getLast(); // Get the last element
int queue(T); // Queue an element
T unqueue(); // Unqueue the first element
int isEmpty(); // Check if the queue is empty or not
};
```